

SUPPLEMENTAL METHODS

Cell lines and culture conditions

For our study, we used 11 GCB-DLBCL cell lines (DB, HT, OCI-Ly7, OCI-Ly8, OCI-Ly18, OCI-Ly19, Pfeiffer, SUDHL-4, SUDHL-6, SUDHL-7, and SUDHL-10) and 3 ABC-DLBCL cell lines (HBL-1, TMD8, and U2932). Basic characteristics of DLBCL cell lines used in the study are summarized below. All cell lines were cultured at 37°C with 5% CO₂ in RPMI media with L-glutamine (Gibco, catalog# 11875-119) supplemented with: fetal bovine serum (FBS, final concentration 10%; Atlanta Biologicals, catalog#: S11550), HEPES buffer (final concentration 20 mM; Gibco, catalog# 15630-080), sodium pyruvate (final concentration 1 mM; Gibco, catalog# 11360-070), gentamicin (final concentration 10 µg/ml; Gibco, catalog#: 15720-060), and penicillin/streptomycin (final concentration 100 U/mL and 100 µg/mL, respectively; Corning, catalog# 30-002-CI). Cell lines were validated by STR DNA fingerprinting by the MD Anderson Characterized Cell Line Core (CCLC) using the Promega 16 High Sensitivity STR Kit (Catalog # DC2100). The STR profiles matched known DNA fingerprints or were unique, based on comparison to 2556 known profiles of cell lines, including 2455 from online databases (see table below). The line designated as SUDHL-7 was matched to the SUDHL-8 cell line, but since confusion between these two names has been documented previously (https://www.dsmz.de/fileadmin/Bereiche/HumanandAnimalCellLines/False_LL_Cell_Lines.pdf), we continued to use the name SUDHL-7. All cell lines were periodically tested for Mycoplasma contamination using a Mycoplasma PCR detection kit (Applied Biological Materials, catalog#: G238)

Basic characteristics of DLBCL cell lines used, including Neon electroporation conditions.

Cell line	Cell line type	Ig Heavy isotype	Ig light isotype	Electroporation condition
DB	GCB-DLBCL	G	L	1700 V, 20 ms, 1 Pulse, R buffer
HBL-1	ABC-DLBCL	M	K	1200 V, 20 ms, 2 Pulses, R buffer
HT	GCB-DLBCL	not expressed	not expressed	1300 V, 30 ms, 1 Pulse, T buffer
OCI-Ly7	GCB-DLBCL	M	K	1700 V, 20 ms, 1 Pulse, R buffer
OCI-Ly8	GCB-DLBCL	M	L	1400 V, 10 ms, 3 Pulses, R buffer
OCI-Ly18	GCB-DLBCL	M	not expressed	1600 V, 20 ms, 2 Pulses, T buffer
OCI-Ly19	GCB-DLBCL	M	K	1500 V, 10 ms, 3 Pulses, R buffer
Pfeiffer	GCB-DLBCL	G	K	1150 V, 30 ms, 2 Pulses, T buffer
SUDHL-4	GCB-DLBCL	G4	K	1400 V, 20 ms, 2 Pulses, R buffer
SUDHL-6	GCB-DLBCL	M	K	1700 V, 20 ms, 1 Pulse, R buffer
SUDHL-7	GCB-DLBCL	G	K	1400 V, 20 ms, 2 Pulses, R buffer
SUDHL-10	GCB-DLBCL	G	L	1700 V, 20 ms, 1 Pulse, R buffer
TMD8	ABC-DLBCL	M	K	1700 V, 20 ms, 2 Pulses, T buffer
U2932	ABC-DLBCL	M	K	1400 V, 20 ms, 1 Pulse, R buffer

Results of cell line fingerprinting using STR.

Source	Sample Name	AMEL	CSF1PO	D13S317	D16S539	D5S818	D7S820	TH01	TPOX	vWA	Comments
Present study Public database: ATCC	DB	X,Y	10,11	9,11,12	11	11	11	6,8	8	15,16	
	DB	X,Y	10,11	11,12	11	11	11	6,8	8	15,16	MATCH
Present study	HBL1	X	10,11	8,9	9,11	10,11	11,12	6,9	8,9	16,17	Unique profile
Present study Public database: Sanger	HT	X,Y	10	14	11,14	11,13	8,10	6,7	11	17,18	
	HT	X,Y	10	13,14	11,13	11,13	8,10	6,7	11	17,18	MATCH
Present study DSMZ, ATCC, JCRB, RIKEN online search database	OCI-LY7	X,Y	12,13	11,12	12,13	11,12	10	6,9.3	8,12	15,18	
	OCI-LY7	X,Y	12,13	11,12	12,13	11,12	10	6,9.3	8,12	15,18	MATCH
Present study	OCI-LY8	X	11,12	11	9,11	10,13	11,12	6,9.3	9,11	17,19	Unique profile

Present study	OCI-LY18	X	10,12	10,12	11,13	11,12	10,12	6,9	8,11	15,19	
DSMZ, ATCC, JCRB, RIKEN online search database	OCI-LY18	X	10,12	10,12	11,13	11,12	10,12	6,9	8,11	15,19	MATCH
Present study	OCI-LY19	X	10,11	11,12	11,12	11,14	9,12	7,9.3	8,9	16,17	
MD Anderson CCLC database	OCI-LY19	X	10,11	11,12	11,12	11,13,14	9,12	7,9.3	8,9	16,17	MATCH
Present study	Pfeiffer	X,Y	10,11	11,12	12	10,13	8,12	9,9.3	9	17,18	
DSMZ, ATCC, JCRB, RIKEN online search database	Pfeiffer	X,Y	10,11	11,12	12	10,13	8,12	9,9.3	9	17,18	MATCH
Present study	SUDHL4	X,Y	12	11,12	11,13	11,12	8,11	6,9.3	9,11	18,19	
DSMZ, ATCC, JCRB, RIKEN online search database	SUDHL4	X,Y	12	11,12	11,13	11,12	8,11	6,9.3	9,11	18,19	MATCH
Present study	SUDHL-6	X	10	12,14	11,12	12	10	6,9.3	11,12	14,17	
MD Anderson CCLC database	SUDHL6	X	10	12,14	11,12	12	10	6,9.3	11,12	14,17	MATCH
Present study	SUDHL7	X	11,12	11	12	11,13	8	6,9	8	15,19	
Public database: DSMZ	SUDHL8	X	11,12	11,13	12	11,13	8	6,9	8	15,19	MATCH SUDHL8
Present study	SUDHL10	X,Y	10,13	10,11	10,11	11,12	8,11	8,9.3	8	17	
DSMZ, ATCC, JCRB, RIKEN online search database	SUDHL-10	X,Y	10,13	10,11	10,11	11,12	8,11	8,9.3	8	17	MATCH
Present study	TMD8	X,Y	11,12	9,11	9,11	12,13	8,10	6,7	11	14,18	
MD Anderson CCLC database	TMD8	X,Y	11,12	9,11	9,11	12,13	8,10	6,7	11	14,18	MATCH
Present study	U2932	X	10,12	11	12	12,13	9,13	9.3	11,12	14,17	
Public database: DSMZ	U2932	X	10,12	11	12	12	9,13	9.3	11,12	14,17	MATCH

Sequencing of immunoglobulin hypervariable regions (HVRs)

Sequences of immunoglobulin (Ig) heavy and light chain hypervariable regions (H-HVR and L-HVR, respectively) of cell lines were generally obtained by a two-step process. Individual HVRs were first amplified and sequenced from cDNA by an RT-PCR based method, most often using degenerate consensus primers.¹ For SUDHL-4, heavy and light chain HVRs were identified by a 5' RACE-based method,² including a reverse primer designed for identification of the light chain HVR (see table below). The most probable V, D (for H-HVR), and J segments were predicted using the IMGT/V-QUEST online tool^{3,4} (http://www.imgt.org/IMGT_vquest/share/textes/). In the second step, we used PCR with Advantage HD DNA polymerase (Clontech) to amplify the recombinant genomic location coding for the HVR, both as validation and to identify upstream and intronic regions to be used as homology arms. For this, primers were designed for each cell line separately; the forward primers began approximately 500 bp upstream of the start of translation of the predicted V region, according to Ensembl, and the reverse primers were designed downstream of predicted J segments or at the 3' end of the enhancer region. The genomic region was amplified as one long PCR product and sequenced from the ends and middle, except for the OCI-Ly7 heavy and light chain HVRs and the OCI-Ly19 light chain HVR; for these, the final sequence was determined from separately amplified overlapping parts, upstream (from approximately 500 bp upstream of the V to the cell line-specific J reverse primer) and downstream (from the cell line-specific forward primer in the middle of the V to the appropriate primer downstream of the J). For HBL-1, genomic sequences surrounding the kappa light chain HVR were identified from next-generation RNA sequencing data generated by the MD Anderson DNA Analysis Core Facility. Primers used for the PCR amplification of HVRs from genomic DNA and for their sequencing are listed in table below. All oligonucleotide primers (oligos) were ordered from Integrated DNA Technologies. All identified genomic sequences of HVRs used in our study are listed in the Sequences section below.

Oligonucleotide sequences used for PCR amplification of genomic loci of recombined heavy and light hypervariable regions.

Name	5' to 3' sequence	Cell lines	Comment
IgH HVR forward oligos			
HBL1_V4-34-upst_01_F	AGTACACATTGCATGGATCC	HBL1	
V3-53_upst_01_F	CAGACTTCACTAGGCATAGTCC	HT	
Ly7_V1-69_upst_02_F	TGCTGGACACTCATGTAGG	OCI-Ly7	upstream part
Ly7_V1-69_03_F	CTGCAAGACTTCTAGAGACACC	OCI-Ly7	downstream part
IGHV4-59_upstr_01_F	ATATTTTCAATCAGAAGTGTTAGAGG	SUDHL-4	
U2932_V4-39_upst_02_F	GTCCTGTCATTATTACATTCAGC	U2932	
TMD8_V3-48_upst_02_F	ATCCCAGACATGAGCTCC	TMD8, OCI-Ly19, SUDHL-6	
IgH HVR reverse oligos			
M-enh_02_R	GCTCAGTTACTCCATCAGACG	HBL1, HT, OCI-Ly19, U2932, TMD8	
IGH-J-region_02_R	AATGGCAGAATGTCCATCC	SUDHL4, SUDHL-6, OCI-Ly7 (downstream part)	
OCI-Ly7_J_R	CCTGAGGAGACGGTGACCAG	OCI-Ly7 (upstream part) J specific reverse	
IgH HVR sequencing oligos			
HBL1-V4-34_03_F	GGACTGTTGAAGCCTTCG	HBL1	
V3-53_03_F	GTGCAACCTCTGACTTCACC	HT	
Ly19_V3-48_04_F	CCAGTGTGAAGTTGAGTTGG	OCI-Ly19	
DHL4-V4-59_03_F	TACTCCTGGACTTGGATCC	SUDHL4	
U2932_V4-39_03_F	CACCTGCACTGTCTCTCG	U2932	
TMD8_V3-48_03_F	CCTGAGACTCTCCTGTGTAGC	TMD8	
IgL 5' RACE oligos			
IGK-RACE_1-R	CCTCTCTGGGATAGAAGTTATTCAGCAGGC		
IGK-RACE_2-R	CTTTGTGTTTCTCGTAGTCTGCTTTGCTCAGC		
IgL HVR forward oligos			
Ly7-KV4-1-upst_01_F	ATTAGCCAGACAAGTTTGACC	OCI-Ly7	upstream part
Ly7-KV4-1_03_F	CCTGGCTGTGTCTCTGG	OCI-Ly7	downstream part
Ly19-KV1-39-upst_01_F	ACATGAAACAATGGGAACC	OCI-Ly19	upstream part
Ly19-KV1-39_03_F	CCCTGTGAGCATCTGTAGG	OCI-Ly19	downstream part
IGKV2-28_upstr_01_F	GGGTAGATTCCAACACTTGC	SUDHL-4	
IGKV1-5_upstr_01_F	ACCTGCAGTCTTGATAGTGG	SUDHL-6	
U2932_KV3-20-upst_01_F	AAATGGTATCACTACCCTGAGG	U2932	
TMD8_KV2-30_01_upst_F	ATTAGTAAATATTTGTGGAAACATGG	TMD8	
IgL HVR reverse oligos			
Kappa_01_R	TCACTTTTGAGATCAGCTGG	U2932	
Kappa_04_R	GTTAGATCCCTGGCATCC	OCI-Ly7 (downstream part), SUDHL-6, TMD8	
Kappa_05_R	GTCCTGTGGAACAATTTCC	OCI-Ly19 (downstream part)	
Kappa_07_R	ATGAGCTCTATCTGTGAAGCC	SUDHL-4	
OCI-Ly7_J_R	TTTGATTTCCACCTTGGTC	OCI-Ly7 J specific R	upstream part
OCI-Ly19_J_R	TCTGATTTCCACCTTGGTC	OCI-Ly19 J specific R	upstream part
IgL sequencing oligo			
IGKV2-28_seq_03_F	AATGCTCTGGGTCTCTGG	SUDHL-4	
IGKV1-5_03_F	CAGTCAGAGTATTTATAACTGGTTGG	SUDHL-6	

U2932_KV3-20_03_F	TGTTAGCAGCAGCTACTTAACC	U2932	
TMD8_KV2-30_03_F	GTCTCCACTCTCCCTCTCC	TMD8	

Transfection

For experiments in which transfection of cell lines with plasmid DNA was needed, we used the Neon electroporation device (Thermo Fisher Scientific, catalog# MPK5000). The optimal electroporation conditions for each line were determined using the pre-programmed 24 well plate optimization protocol (Thermo Fisher Scientific) with 10 μ L electroporation volumes (Thermo Fisher Scientific, catalog# MPK1096). All experiments were carried out using 100 μ L volumes (Thermo Fisher Scientific, catalog# MPK10096). Cells growing in log phase were prepared for electroporation by changing cell culture medium every day for three days prior to the electroporation, and were washed once with PBS. For each electroporation, 1.2 million cells were re-suspended in 120 μ L of appropriate electroporation buffer (R or T), mixed with maxiprep plasmid DNA (PureLink® HiPure Plasmid Filter Maxiprep Kit, ThermoFisher Scientific, Catalog#: K210017), and electroporated with the conditions optimum for the cell line (see table in Cell lines and culture conditions section of Supplemental Methods). Cells were then re-suspended in 3 mL of pre-warmed antibiotic-free culture media.

Knock out experiments and complementation

The CRISPR/Cas9 system⁵ was used for all knockout (KO) experiments. We used chimeric plasmids developed in the Zhang laboratory: pX330-U6-Chimeric_BB-CBh-hSpCas9⁵ (pX330; Addgene plasmid # 42230, coding for Cas9 as well as gRNA) and pSpCas9(BB)-2A-GFP⁶ (pX458; Addgene plasmid # 48138; coding for Cas9 linked by 2A peptide with GFP and for gRNA expression). Target sequences were designed using the Zhang laboratory online CRISPR Design Tool⁷ (<http://crispr.mit.edu/>). Target sequences were ligated as annealed oligos into BbsI-opened pX330, pX335, or pX458 plasmids according to the published protocol.⁶ After verification of gRNA sequences, maxiprep DNA was used for electroporation-based cell transfection. We used 12 μ g of plasmid DNA (pX330 or pX458, with cloned gRNA sequence) per 120 μ L of cell suspension (1 million cells per 100 μ L) in electroporation buffer for each electroporation. To KO all three AKT isoforms simultaneously, 7 μ g each of pX330 AKT1/2_03 and pX330 AKT3_06 plasmids per 120 μ L of cell suspension in electroporation buffer were used together for each electroporation. When KO was attempted by Cas9/gRNA plasmids alone (i.e., without knock-in of a marker protein), cells with successful KO were detected by flow cytometry (FCM; see below) and followed over time. Targeted genes and corresponding sequences of CRISPR/Cas9 target sites are listed in table below. For KO experiments, targeting multiple sites of the gene of interest controlled for the specificity of the KO effect, and we did not detect any phenotype differences between these replicates. To further control for specificity (and set FCM parameters) in every KO experiment, a non-specific pX330 plasmid (usually targeting the HVR of a different cell line) was also electroporated. The effect of BCR KO was complemented by transiently expressing constitutively-active myristoylated murine AKT1 (MyrAKT) using the 786 pCsmAKT2Acherry mAKT and mCherry expression plasmid⁸ (Addgene plasmid #31167). This plasmid was co-electroporated with the appropriate pX330 BCR targeting plasmid (10 μ g of each per 1.2 million cells in 120 μ L of R or T buffer per electroporation), and BCR-negative, mCherry-positive cells (indicating MyrAKT expression) were followed. As a control, a GFP expression plasmid (pcDNA 6.2 emGFP, Thermo Fisher Scientific) was co-electroporated, and BCR-negative, GFP-positive cells were followed. Similarly, the MyrAKT expression plasmid was used for rescue of the effect of pan-AKT KO.

Sequences of genomic target sites used for knock out (KO) experiments.

Name	Target Sequence (5' to 3')	Plasmid	Location	Use
HBL-1_HV_01	GTTCACAGGGGTCCTGTCCCAGG	pX330	HBL-1 H-HVR V region	BCR KO in HBL-1
HBL-1_HV_03	CCTCAGGTGAGTCCTCACGTCTC	pX330	HBL-1 H-HVR J region	BCR KO in HBL-1
Ly7_HV_02	GGCAGAGTCACGATTACCGCGG	pX330	OCI-Ly7 H-HVR V region	BCR KO in OCI-Ly7
Ly7_HV_03	CTGTGTGACCGGCCCGCGGGG	pX330	OCI-Ly7 H-HVR junction	BCR KO in OCI-Ly7
Ly7_HV_04	GTTTGGAGTGCATGGGGCCAGGG	pX330	OCI-Ly7 H-HVR junction	BCR KO in OCI-Ly7
Ly19_HV_02	TGTCCAGTGTGAAGTTGAGTTGG	pX330	OCI-Ly19 H-HVR V region	BCR KO in OCI-Ly19
Ly19_HV_03	CCACCAACTCAACTTCACACTGG	pX330	OCI-Ly19 H-HVR V region	BCR KO in OCI-Ly19
Ly19_HV_04	GAAGTTGAGTTGGTGGAGTCTGG	pX330	OCI-Ly19 H-HVR V region	BCR KO in OCI-Ly19
Ly19_HV_05	CACCTGAGGAGACGGTGACCAGG	pX330	OCI-Ly19 H-HVR J region	BCR KO in OCI-Ly19
Ly19_HV_08	CAGAGGACTACCATGAAGTTGG	pX330	OCI-Ly19 H-HVR V region	BCR KO in OCI-Ly19
SUDHL4_HV_01	GTGGTTCTTCCTTCTCGTGGTGG	pX330	SUDHL-4 H-HVR V region	BCR KO in SUDHL-4
SUDHL4_HV_03	TCAAAGTTGTGCCCGTAATCAGG	pX330	SUDHL-4 H-HVR junction	BCR KO in SUDHL-4

SUDHL6_HV_02	GAAGTGCAGATGGTGGAAATCTGG	pX330	SUDHL-6 H-HVR V region	BCR KO in SUDHL-6
SUDHL6_HV_03	GAACCTTGGTACACCCGGGGGGG	pX330	SUDHL-6 H-HVR V region	BCR KO in SUDHL-6
SUDHL6_HV_04	CCGTCTCCTCGGGTGAGTCCGC	pX330	SUDHL-6 H-HVR J region	BCR KO in SUDHL-6
TMD8_HV_01	CAGAGGCCTCACCATGGATTTGG	pX330	TMD8 H-HVR V region	BCR KO in TMD8
TMD8_HV_02	ACAGCCCCAAATCCATGGTGAGG	pX330	TMD8 H-HVR V region	BCR KO in TMD8
TMD8_HV_03	TGAAGACTCACCTGAGGAGACGG	pX330	TMD8 H-HVR J region	BCR KO in TMD8
U2932_HV_02	GCAAGAAAATGAAGCACCTGTGG	pX330	U2932 H-HVR V region	BCR KO in U2932
U2932_HV_04	AGGTACTTCTTTGACTACTGGGG	pX330	U2932 H-HVR J region	BCR KO in U2932
IGHG-C1	GAACCGGTGACGGTGTCTGTGG	pX330	exon 1 of IGHG1, IGHG2, IGHG4, IGHG4	BCR KO in IgG lines
IGHG-C2	GGACTGTAGGACAGCCGGGAAGG	pX330		
IGHG-C3	ACTCTACTCCCTCAGCAGCGTGG	pX330	exon 3 of IGHG1, IGHG2, IGHG4; exon 6 of IGHG3	
IGHG-C4	CGGTGAGGACGCTGACCACACGG	pX330		
IGHG-C5	GGCAAGGAGTACAAGTGCAAGG	pX330		
IGHG-C6	TTTGAGATGGTTTTCTCGATGG	pX330		
IGHM-C1	CACGCTGCTCGTATCCGACGGGG	pX330	exon 1 of IGHM	BCR KO in IgM lines
IGHM-C2	GGCCGTTGGCTGCCTCGCACAGG	pX330		
IGHM-C3	GCCTCCAAGGACGTCATGCAGG	pX330		
IGHM-C4	AGATGAGCTTGGACTTGCGGGGG	pX330	exon 2 of IGHM	
IGHM-C5	CAGGTGTCTGGCTGCGCGAGGG	pX330		
IGHM-C6	ACCTGCCGCGTGGATCACAGGGG	pX330		
AKT1/2_03	GGATCTTCATGGCGTAGTAGCGG	pX330	exon 5 of AKT1 and exon 6 of AKT2	AKT 1/2 KO
AKT3_06	TCCCCTCAACAACTTTTTCAGTGG	pX330	exon 3 of AKT3	AKT 3 KO
CXCR4-DG1	GCTTCTACCCCAATGACTTGTGG	pX330	exon 1 of CXCR4	CXCR4 KO
CXCR4-OH3	CACTTCAGATAACTACACCGAGG	pX330	exon 1 of CXCR4	CXCR4 KO
CD19_01	TGGAATGTTTCGACCTAGGTGG	pX330	exon 3 of CD19	CD19 KO
CD19_02	GCCTCCGTGTCTCCACCGAGGG	pX330		
CD19_03	GACCGCCCTGAGATCTGGGAGGG	pX330		
SYK_01	TTTCGGCAACATCACCCGGGAGG	pX458	exon 1 of SYK	SYK KO
SYK_02	ACCATCGAGCGGGAGCTGAATGG	pX458		
SYK_03	GAAGATTACCTGGTCCAGGGGGG	pX458		
CD79B_05	AACGCCACCATCCAGTGGCTGGG	pX330	exon 1 of CD79B	CD79B KO
CD79B_06	GCAGCAACGCCACCATCCAGTGG	pX330		
GFP	GGGCGAGGAGCTGTTACCGGGG	pX330	GFP	GFP KO

Knock-in experiments

The CRISPR/Cas9 system was used also for knock-in (KI) by homologous recombination (HR). This was the case for KI alone, as well as to provide a marker for KO of genes which were not easily measured by FCM. Generally, one or more Cas9/gRNA plasmids creating DNA double strand breaks (DSB) at desired locations were co-electroporated with an HR template plasmid, which contained (in 5' to 3' order): a left homology arm (LHA), covering 200-400 bp of genomic sequence upstream of the first or only DSB; the sequence to be inserted; and the right homology arm (RHA), covering 200-400 bp downstream of the second or only DSB. All homology arms and inserts contained silent mutations to prevent targeting of the repair plasmid or modified genomic locus by the Cas9/gRNA pairs. If not stated elsewhere, homology arms and KI sequences for insertion were ordered as gBlocks Gene Fragments (Integrated DNA Technologies), captured in a pSC-B-amp/kan plasmid using the StrataClone Ultra Blunt PCR Cloning Kit (Agilent Technologies, catalog#: 240218), verified by sequencing, and then used for cloning. The general approach to construct the HR template plasmids was to design the upstream and downstream homology arms as one gBlock, in which they were separated by a cassette containing two type IIS restriction enzyme sites in opposite orientation. The cassette was consequently used for “seamless” insertion of the sequence for KI. Details and specific sequences of all HR templates are given in the Sequences section below.

In general, KI was used to: 1) replace the endogenous H-HVR and L-HVR sequences at the genomic level, together with KI of a fluorescent protein (FP) as a marker of genomic modification; 2) achieve “KI/KO” (i.e., mark KO cells for further analysis), by KI of a marker protein (FP or mCD8a), in frame in a translated exon, followed by a STOP codon and polyA signal sequence; 3) KI variants of CD79A, together with a FP as a marker of modification; and 4) KI to repair a single nucleotide deletion in the H-HVR of cell line HT, to cause re-expression of its BCR. In all cases, modified cells were detected and followed by FCM (see below). To confirm specificity of KI, each KI experiment included a parallel electroporation of non-specific pX300 or paired pX335 plasmids, usually targeting HVRs of a different cell line, in combination with the specific HR template plasmid. From few to no marker-positive cells were detected in the specificity controls. In all cases, modified cells were detected and followed by FCM (see below). Additional details of these types of KI are as follows:

1) H-HVR and L-HVR replacement. For each cell line, in regions flanking the genomic sequence coding for the IgH or IgL HVR, we identified a suitable upstream Cas9/gRNA target site (near the translation start site of the IMGT/V-QUEST-predicted V segment) and a downstream Cas9/gRNA target site (in the 3' end of the predicted J region or the following intron). The general structure of the repair template plasmid, from 5' to 3', was: LHA; FP; 58-AA F2A; HVR; and RHA. In more detail, the homology arms were 200-400 bp each, as described above; the FP cDNA was positioned, relative to a Kozak sequence (original or added), to be the start of in-frame translation; the FP was emGFP for H-HVR replacement and mTurquoise2 for L-HVR replacement; the F2A sequence was 58 amino acids long, found to work best to separate the FP from the following HVR⁹; and the inserted HVR sequences included the leader sequence of the new HVR as well as the V intron. After HR-mediated KI, the modified genomic sequence extended from the V region translation initiation site to the 3' end of the J segment. The endogenous IgH or IgL promoter thus drives the expression of the FP (as a marker of modification) as well as the separate IgH or IgL, containing replaced HVRs. The emGFP sequence was cloned from the pcDNA 6.2 emGFP plasmid (Thermo Fisher Scientific), and the mTurquoise2 sequence was cloned from the pLifeAct-mTurquoise2 plasmid¹⁰ (Addgene Plasmid #36201). If cells were already expressing GFP as marker of CD79A modification (see below), mRFP (Addgene Plasmid #13032) was used as the marker of H-HVR replacement.

HVRs recognizing tetanus toxoid (TTox) were based on paired HVR sequences from TTox-reactive single B cells;¹¹ two pairs of IgH and IgL HVRs (TTox 3 and TTox 6) were chosen because of the similarity of their predicted V segments to those of some of the lymphoma cell lines studied. To re-create the full TTox HVR sequences, we added sequences coding for the leader sequence, and the intron, based on the V segment predicted by IMGT/V-QUEST from the published partial TTox HVR sequences. For experiments in which HVRs of the U2932 cell line were “reverted” to their naïve form, free of somatic hypermutation, we designed HVRs based on the unmutated reference sequences of the IMGT/V-QUEST-predicted V, D, and J segments. Additional nucleotides predicted to have been inserted at the V-D and D-J junctions of U2932 HVRs were not modified. HVRs recognizing ovalbumin (OVA) were designed based on published HVR sequences from OBI RAG1^{-/-} mice with OVA-reactive B-cells.¹² To re-create the full OVA HVR, we added 5' parts of the full HVRs (including leader sequence and V intron) based on the mouse reference sequence of the V segment predicted by IMGT/V-QUEST. CRISPR/Cas9 target sequences used in HVR replacement are listed in table below. HA fragments with inserted FPs and F2A sequence, as well as individual H-HVR and L-HVR fragments that were ligated into them, are listed in the Sequences section below. For the majority of HVR replacement experiments, we replaced the IgH and IgL HVRs simultaneously, by electroporating six plasmids (upstream and downstream CRISPR/Cas9 plasmids and an HR template plasmid for each Ig chain) at once, using 4 µg of each per electroporation of 1.2 million cells re-suspended in 120 µL of R or T buffer. We followed the double HVR-replaced (GFP- and mTurquoise2-positive) cells by FCM and bead assays (see below). In all experiments, we used control HVR replacements in which the original (endogenous) HVR was inserted together with the fluorescent marker.

2) Knock-in/knockout (KI/KO) approach. We used this “gene trapping” approach to express GFP instead of PTEN in multiple lines, and to express mCD8a instead of the BCR in the OCI-Ly19 cell line. For PTEN, we used paired nickases¹³ to target the region just downstream of the PTEN translation initiation site, using D10A Cas9 mutant (expressed from pX335-U6-Chimeric_BB-CBh-hSpCas9n(D10A) plasmid; Addgene plasmid #42335).⁵ The HR template plasmid had the following structure: LHA-GFP-STOP-PolyA-RHA. After HR-mediated DNA repair, the GFP sequence was inserted in frame immediately after the PTEN translation initiation site, ending with a stop codon and bGH polyA signal sequence. For this, three plasmids were co-electroporated: two pX335 plasmids (6 µg each) and the HR template plasmid (7 µg) per 1.2 million cells re-suspended in 120 µL of R or T buffer. A similar approach inserted mCD8a-STOP-PolyA in the IgH locus in the OCI-Ly19 cell line, serving as a reporter for BCR KO. The sequence coding for mCD8a, excluding its signal peptide, was inserted in frame just after the end of the OCI-Ly19 H-HVR leader sequence. 12 µg of one of the pX330 plasmids, together with 8 µg of the HR template plasmid, was electroporated per 1.2 million cells re-suspended in 120 µL of R or T buffer. The mCD8a sequence for cloning was ordered as a gBlock gene fragment and inserted between OCI-Ly19 H-HVR specific homology arms. CRISPR/Cas9 target sequences used for the KI/KO approach are listed in table below.

3) Modifications of CD79A. These were made in the region of the gene coding for the ITAM domain, involving the end of exon 4 and the beginning of exon 5, which are the last two exons of CD79A. Two pX330 plasmids were used to create DSB in both exons (see table below). The HR template plasmid contained homology arms upstream of the CRISPR/Cas9 target site in exon 4 and downstream of the CRISPR/Cas9 target site in exon 5, so that translation of the endogenous CD79A exon 4 continues to exon 5 in the knocked-in sequence version, followed by a STOP and bGH polyA signal sequence. Modified versions of CD79A were: wild-type (WT) full-length CD79A-GFP fusion; WT full-length CD79A-3xFLAG fusion; truncated CD79A (ending with L187

and thus deleting the ITAM) fused to 3xFLAG; full-length CD79A-GFP fusion with mutation of both ITAM Tyr residues (Y188F and Y199F); full-length CD79A-GFP fusion with Y188F mutation only; and full-length CD79A-GFP fusion with Y199F mutation only. For the CD79A modification, we co-electroporated the two pX330 plasmids (6 µg each) and the HR template plasmid (7 µg) per 1.2 million cells re-suspended in 120 µL of R or T buffer. Details of the sequence of the CD79A HR template plasmids are provided in the Sequences section below.

4) BCR re-expression. Analysis of the genomic sequence coding for the H-HVR of the HT cell line, first identified from cDNA (indicating active transcription), showed a single nucleotide deletion in the VDJ junction region, causing a frame shift with consequent downstream premature termination of translation (Figures S8A-S8C). A pX330 plasmid was used to create a DSB close to the deletion, and an HR template plasmid carrying a corrected HVR sequence allowed KI of a frame-restoring nucleotide. We co-electroporated the two pX330 plasmids (6 µg each) and 7 µg of the HR template plasmid per 1.2 million HT cells re-suspended in 120 µL of T buffer. The sequences of the HT H-HVR and HR plasmid are provided in the Sequences section below. Used target sites are listed in table below.

Sequences of genomic target sites used for knock-in (KI) experiments.

Name	Target Sequence (5' to 3')	Plasmid	Location	Use
HVR replacement				
HBL1_HV_07	GAAGTGCTTTCTGAGAGTCATGG	pX330	V 5' UTR	HBL-1 H-HVR replacement
HBL1_HV_04	AAACCAGGAGAGACGTTGTGAGG	pX330	beginning of post J intron	HBL-1 H-HVR replacement
HBL1_LV_01	TGGAGAAGAGCTGCTCAGTTAGG	pX330	V 5' UTR	HBL-1 L-HVR replacement
HBL1_LV_04	TCGTGAGATTTTAGTGCCATTGG	pX330	beginning of post J intron	HBL-1 L-HVR replacement
Ly7_HV_06	CCCAGGGGCTTCTTTAGAGGAGG	pX330	V 5' UTR	OCI-Ly7 H-HVR replacement
Ly7_HV_07	CTCATAATCTATCATAATGTAGG	pX330	beginning of post J intron	OCI-Ly7 H-HVR replacement
Ly7_LV_02	CTGAGCTACAACAGGCAGGCAGG	pX330	V 5' UTR	OCI-Ly7 L-HVR replacement
Ly7_LV_04	ACAGAAGACACAGACAAGTGG	pX330	beginning of post J intron	OCI-Ly7 L-HVR replacement
Ly19_HV_08	CAGAGGACTCACCATGAAGTTGG	pX330	beginning of V	OCI-Ly19 H-HVR replacement
Ly19_HV_06	AAAGTAAATGAGACGTTGTGAGG	pX330	beginning of post J intron	OCI-Ly19 H-HVR replacement
Ly19_LV_01	AGAGATTTTCCCTGAAGTTCCGG	pX330	V intron	OCI-Ly19 L-HVR replacement
Ly19_LV_03	ATATATCACTTCATAGACACAGG	pX330	beginning of post J intron	OCI-Ly19 L-HVR replacement
SUDHL4_HV_01	GTGGTTCCTTCTCGTGGTGG	pX330	beginning of V	SUDHL-4 H-HVR replacement
SUDHL4_HV_04	CCACAACACTTCTCACTCTGAGG	pX330	beginning of post J intron	SUDHL-4 H-HVR replacement
SUDHL4_LV_02	AGATGATGCTCCTCTAACACAGG	pX330	V intron	SUDHL-4 L-HVR replacement
SUDHL4_LV_04	TTTCGGCGGAGGGACCAAGGTGG	pX330	J region	SUDHL-4 L-HVR replacement
SUDHL6_HV_05	TCAGAGTTAAGGTTGGACTGAGG	pX330	beginning of post J intron	SUDHL-6 H-HVR replacement
SUDHL6_HV_06	TGGAAATGCCTTGAATCCAGGG	pX330	V 5' UTR	SUDHL-6 H-HVR replacement
SUDHL6_LV_01	AGGCTGGTCACACTTTGTGCAGG	pX330	V 5' UTR	SUDHL-6 L-HVR replacement
SUDHL6_LV_03	ACCGAATACACAGACAATTGAGG	pX330	beginning of post J intron	SUDHL-6 L-HVR replacement
U2932_HV_02	GCAAGAAAATGAAGCACCTGTGG	pX330	beginning of V	U2932 H-HVR replacement
U2932_HV_03	AAAGCAGGAGAGAGGTCGTGAGG	pX330	beginning of post J intron	U2932 H-HVR replacement
U2932_LV_01	TGGAGAAGAGCTGCTCAGTTAGG	pX330	V 5' UTR	U2932 L-HVR replacement
U2932_LV_04	TAGATCACTTCATAGACACAGGG	pX330	beginning of post J intron	U2932 L-HVR replacement
KI/KO experiments				

PTEN_TS_01:	TTGACCTGTATCCATTTCTGCGG	pX335	translation initiation region	PTEN KO/GFP KI
PTEN_TS_02:	TTGATGATGGCTGTCATGTCTGG	pX335	translation initiation region	PTEN KO/GFP KI
Ly19_HV_02	TGTCCAGTGTGAAGTTGAGTTGG	pX330	beginning of OCI-Ly19 H-HVR V region 2 nd exon	BCR KO/mCD8a KI
Ly19_HV_03	CCACCAACTCAACTTCACACTGG	pX330	beginning of OCI-Ly19 H-HVR V region 2 nd exon	BCR KO/mCD8a KI
Ly19_HV_04	GAAGTTGAGTTGGTGGAGTCTGG	pX330	beginning of OCI-Ly19 H-HVR V region 2 nd exon	BCR KO/mCD8a KI
CD79A modifications				
CD79A_01	ACCCTTCACTCACTTCATAAAGG	pX330	End of CD79A exon 4	CD79A modification by KI
CD79A_02	GGACGACTGCTCCATGTATGAGG	pX330	Beginning of CD79A exon 5	CD79A modification by KI
HT cell line BCR re-expression				
HT_HV_02	CTACTTTGACTCCTGGAGTCAGG	pX330	VDJ junction	BCR re-expression
HT_HV_03	CACCTGAGGAGACGGTGACCAGG	pX330	J region	BCR re-expression

Inducible B-cell receptor expression and isotype comparison

To control expression of the BCR at varied surface levels, the general approach was to KO the endogenous IgH chain and express a cDNA encoding a complete IgH chain (with HVR and constant region) through a doxycycline (Dox)-inducible transposon-based system.¹⁴ The SUDHL-4 line was chosen for these experiments, because of its extreme dependence on tonic BCR signaling, but that same dependence required a system by which cells with KO of the endogenous IgH could be detected while expressing an exogenous IgH of the same isotype. This was accomplished by using SUDHL-4 cells that had been modified, by KI at the IgH locus, to express GFP in the 5' portion of the endogenous IgH transcript, in front of the H-HVR; those cells had served as controls for H-HVR replacement experiments. These cells were then transduced with pSBtet-Bla plasmid (Addgene Plasmid #60510) for inducible expression of a cDNA containing the SUDHL-4 H-HVR joined to an IgH constant region, either IgG4 (the isotype used by SUDHL-4) or IgM constant. After selection of transduced SUDHL-4 cells with Blasticidin (ThermoFisher Scientific, #A1113903) at 10µg/mL, KO of the endogenous IgH chain was done using a GFP-targeting CRISPR/Cas9 pX330 plasmid (see above); the target site, in 5' to 3' orientation, was GGGCGAGGAGCTGTTACCG. First, we verified that GFP negative cells were also BCR KO (48 hours after electroporation) and then viably sorted GFP-negative cells by FCM (see below). Immediately after the sorting, cells were re-suspended in media containing doxycycline hyclate (Dox; Sigma, #D9891-5G; final concentration, 200 ng/mL) to express the SUDHL-4 HVR IgM/IgG from the integrated inducible transposon cassette, so as to rescue and expand the modified cells. A similar but different method was used to create OCI-Ly19 cells with inducible surface BCR expression. WT OCI-Ly19 cells were transduced with pSBtet-Bla plasmid for inducible expression of a cDNA containing the OCI-Ly19 H-HVR joined to IgM or IgG4 constant regions. Blasticidin-selected cells were then electroporated for KI/KO (see above) of the endogenous IgH chain, marked by mCD8a expression, and mCD8a-positive cells were viably sorted for further experiments. Final modified versions of SUDHL-4 and OCI-Ly19 were cultured in medium containing Dox at full concentration (200 ng/mL) for maximal BCR expression (to compare IgM vs. IgG isotypes), or with Dox over a dilution series of concentrations (to determine the effect of varied BCR levels). BCR levels were analyzed using FCM (see below) and cell growth was assessed using bead assay (see below). To determine the relationship between GFP fluorescence (from GFP fused to CD79A; see above) and BCR surface expression (estimated using Ab staining), OCI-Ly19 cells expressing WT CD79A fused to GFP were modified similarly to enable controllable BCR expression.

Flow cytometry, image cytometry, and cell sorting

For detection of cell-surface antigens, approximately 1 million cells for each sample were washed once with FACS buffer (PBS with 1% FBS) and then re-suspended in 100 µL of FACS buffer containing the working dilution of antibody (see table below) and incubated 30 min on ice in the dark. Cells were then washed once with FACS buffer and re-suspended in 200 µL of FACS buffer containing a 1:1000 dilution of SYTOX® Blue (Thermo Fisher Scientific; catalog#: S34857) or SYTOX® Red (Thermo Fisher Scientific; catalog#: S34859) dead cell stains and analyzed using an LSR Fortessa flow cytometer (BD Biosciences). Intracellular antigens were detected as follows: approximately 1 million cells per sample were washed once with PBS and re-suspended in PBS with 1:1000 dilution of Ghost Dye Violet 450 (Tonbo Biosciences; catalog#: 13-0863-T500) to stain for dead cells. Cells were then washed once with FACS buffer and stained for surface antigens (30 min incubation in 100 µL of FACS buffer with the working dilution of Ab followed by one wash with FACS buffer). Fixation, permeabilization, and intracellular staining was consequently done using the Cytofix/Cytoperm™ Fixation/Permeabilization Solution Kit (BD Biosciences; catalog#: 554714). In brief, cells were incubated 20 minutes on ice in fixation/permeabilization buffer, then washed once with permeabilization/wash buffer and cell pellets re-suspended in 50 µL of permeabilization/wash buffer containing the working dilution of desired antibody (see table below) followed by 30 min incubation on ice in dark. Cells were then washed once with the permeabilization/wash

buffer, re-suspended in 200 μ L of FACS buffer, and analyzed on an LSR Fortessa flow cytometer (BD Biosciences). FCM data were analyzed by FlowJo software (FlowJo). Cell surface density of GFP or CD79B surface staining was calculated on a per-cell basis as fluorescence intensity divided by the squared forward scatter (FSC) value and multiplied by 10^6 . When needed for other purposes, such as gene expression profiling or Western blotting, the KO or KI fraction of viable cells was sorted by FCM to purity at the MD Anderson Flow Cytometry core facility using FACS Aria™ II or FACS Aria™ Fusion sorters (both from BD Biosciences). Cells for imaging cytometry measuring cell size were prepared by the same procedures as for cell cycle analysis (see below) including surface BCR staining and FxCycle™ PI/RNase Staining Solution (ThermoFisher Scientific, catalog#: F10797). Cells for imaging colocalization were prepared similarly as for flow cytometry (see above). Data were acquired using an ImageStream®X Mark II Imaging Flow Cytometer (ED Millipore) with data analyzed using IDEAS® Software (ED Millipore), including the similarity bright detail score (SBDS) calculation feature. The SBDS, calculated for each cell image separately, is based on goodness of correlation between two fluorescent intensities across individual pixels.¹⁵

Antibodies used for flow cytometry and microscopy.

Antibody	Conjugation	Working Dilution	Company	Catalog #
Cell surface antigens				
F(ab') ₂ -Goat anti-Human IgM Molecular Probes™ Secondary Antibody	FITC	1:100	Thermo Fisher Scientific	H15101
Goat anti-Human IgM Molecular Probes™ Secondary Antibody	FITC	1:100	Thermo Fisher Scientific	H15001
Goat anti-Human IgM Molecular Probes™ Secondary Antibody	RPE	1:100	Thermo Fisher Scientific	H15104
Goat anti-Human IgM Heavy Chain Secondary Antibody	Alexa Fluor® 647	1:100	Thermo Fisher Scientific	A-21249
Goat anti-Human IgG Molecular Probes™ Secondary Antibody	FITC	1:100	Thermo Fisher Scientific	H10001C
Goat anti-Human IgG Molecular Probes™ Secondary Antibody	Alexa Fluor® 488	1:100	Thermo Fisher Scientific	H10120
Goat anti-Human IgG Molecular Probes™ Secondary Antibody	RPE	1:100	Thermo Fisher Scientific	H10104
Mouse anti-Human Kappa Light Chain Molecular Probes™ Secondary Antibody	APC	1:100	Thermo Fisher Scientific	MH10515
Mouse anti-Human Kappa Light Chain Molecular Probes™ Secondary Antibody	RPE	1:100	Thermo Fisher Scientific	MH10514
Mouse anti-Human Kappa Light Chain Molecular Probes™ Secondary Antibody	Alexa Fluor® 488	1:100	Thermo Fisher Scientific	MH10520
Mouse anti-Human Lambda Light Chain Molecular Probes™ Secondary Antibody	RPE	1:100	Thermo Fisher Scientific	MH10614
Lambda Light Chain Antibody (1-155-2),	APC	1:100	Thermo Fisher Scientific	A15730
Mouse Anti-Human CD19	APC	1:10	BD Biosciences	555415
Anti-Human CD184 (CXCR4)	APC	1:50	eBioscience	17-9999-42
Mouse Anti-Human CD79b	PE	1:10	BD Biosciences	557931
Rat Anti-Mouse CD8a	PE	1:50	BD Biosciences	553033
Goat F(ab') ₂ IgG FITC - Isotype Control	FITC	1:50	Abcam	ab37394
Intracellular antigens				
Anti-Human Syk	APC	1:20	eBioscience	17-6696-42
Phospho-Syk (Tyr525/526) (C87C1) Rabbit mAb	PE	1:20	Cell Signaling Technology	6485
DYKDDDDK Tag Antibody	Alexa Fluor® 647	1:50	Cell Signaling Technology	3916
Akt (pan) (C67E7) Rabbit mAb	PE	1:50	Cell Signaling Technology	8790
Rabbit (DA1E) mAb IgG XP® Isotype Control	PE	1:200	Cell Signaling Technology	5742
Mouse Anti-Human CD79a	APC	1:10	BD Biosciences	551134
Ab used for BCR KO detection in FRET experiments				
AffiniPure Fab Fragment Goat Anti-Human IgM	Alexa Fluor® 647	1:100	Jackson ImmunoResearch	109-607-043
AffiniPure Fab Fragment Goat Anti-Human IgM	Rhodamine Red™-X (RRX)	1:100	Jackson ImmunoResearch	109-297-043
AffiniPure Fab Fragment Goat Anti-Human IgG (H+L)	Alexa Fluor® 647	1:100	Jackson ImmunoResearch	109-607-003

AffiniPure Fab Fragment Goat Anti-Human IgG (H+L)	Rhodamine Red™-X (RRX)	1:100	Jackson ImmunoResearch	109-297-003
---	------------------------	-------	------------------------	-------------

Bead assay

The absolute growth rates of WT and modified cell lines were assessed by the change over time in the calculated absolute number of cells in culture.¹⁶ At any point in time, this number was determined as follows: an aliquot of well-suspended cells in culture, representing a known fraction of the culture volume, was removed and stained for FCM as described above, so as to be able to identify a population (or populations) of interest (e.g., KO cells). In the last re-suspension of pelleted cells before FCM, the buffer included 10 μ L of a stock solution containing 6.0-8.0 μ m polystyrene particles (beads; Spherotech Inc.; Catalog#: PP-60-10; a 1:20 dilution of the original solution). The beads are a distinguishable separate population of events by FCM, with low forward scatter and high side scatter (Figures 5D and 5E). From the ratio of the FCM-determined counts of beads and the cell population of interest, and the volume of the culture aliquot used, the absolute number of the cells of interest in the culture can be calculated. If the culture is maintained over time by passaging via known dilutions, the growth curve of exponential increase in absolute cell number (logarithmic) over time (linear) can be constructed. For each line, the relative proliferation after BCR KO was quantified as the slope of the growth curve after BCR KO divided by the slope of the growth curve for control cells.

Cell viability assays of drug sensitivity

Cell suspensions, adjusted to approximately 5×10^4 cells/mL, were plated in triplicate with drug dilutions in 96 well-plates at 200 μ L/well. After 72 hour incubations, cultures were sampled for detection of ATP by the CellTiter-Glo assay (Promega) according to the manufacturer's instructions. Dose-response curves and IC₅₀ values were generated using GraphPad Prism software. Small-molecule inhibitors P505-15 (SYK) and CAL-101 (PI3K p110 δ isoform) were obtained from Selleck Chemicals.

DNA content for cell cycle analysis

Approximately 1 million cells from mixed cultures of WT and BCR KO cells were first stained for BCR expression according to the protocol above, with all steps performed at 4°C. Cells were then fixed with 1% paraformaldehyde (to preserve surface BCR staining) and washed with FACS buffer (PBS+1% FBS). Cell pellets were then re-suspended in 0.3 mL of neat PBS (no protein) and 2 mL of cold 54% ethanol was slowly added while vortexing. Cells were then incubated at 4°C overnight before washing once with FACS buffer. Cell pellets were re-suspended in 0.5 mL of FxCycle™ PI/RNase Staining Solution (ThermoFisher Scientific, catalog#: F10797) and incubated for 30 min at RT. Cells were then analyzed without washing on an LSR Fortessa flow cytometer (BD Biosciences) with linear scale detection of propidium iodide signal on slow acquisition speed.

Apoptosis detection

Apoptotic cells were detected in mixed cultures of WT and BCR KO live cells using the green fluorogenic apoptotic substrate PhiPhiLux® G1D2 (OncoImmunin) measuring the activity of caspase-3 and caspase-3 like activity. Cells were processed according to the manufacturer's protocol; in brief, pelleted cells were re-suspended in the provided 10 μ M substrate solution (in RPMI 1640 medium with 25 mM HEPES, both Gibco) with added FBS to a final concentration of 10%. Cells were incubated at 37°C for 40 min and washed with the provided FCM dilution buffer and consequently stained for BCR expression with APC-conjugated anti-human kappa Ab (see table in Flow cytometry, image cytometry, and cell sorting section of Supplemental Methods) and SYTOX Blue dead cell dye (Thermo Fisher Scientific; catalog#: S34857) as described above, with all steps at 4°C. The apoptotic cells were detected on a BD LSR Fortessa flow cytometer using 488 nm laser excitation with 530/30 filter setting (FITC channel).

Calcium flux

Sorted pure cultures of HVR double-replaced cells (expressing GFP and mTurquoise2) or CD79A modified cells (expressing GFP) were mixed with WT cells and loaded with Indo-1 as follows: cells were re-suspended in cell loading media (CLM; RPMI with 2% FBS and 25mM HEPES) containing 2 μ M Indo-1 (AM, cell permeant; ThermoFisher Scientific, catalog#: I1223) and 0.05% of Pluronic® F-127 (ThermoFisher Scientific, catalog#: P-6866) and incubated for 45 minutes at 37° C in the dark. Cells were then washed twice with DMEM medium containing 2% FBS and re-suspended in CLM for analysis. Cells were stimulated with F(ab')₂ anti-human IgM goat Ab (Jackson ImmunoResearch, catalog#: 109-006-129), F(ab')₂ anti-human IgG goat Ab (Jackson ImmunoResearch, catalog#: 109-006-098) (12 μ g per 1 mL of cell suspension), or a complex of tetanus toxoid (TTTox) mixed with anti-TTTox Ab; the latter was made by mixing 2 μ L of TTTox (Colorado Serum Company, catalog#: 11401) for 10 minutes at RT with 2 μ L (8 μ g) of anti-TTTox goat polyclonal Ab (Abcam; catalog#: ab156655) for stimulation of 1 mL of cell suspension. To stimulate the OVA-recognizing BCR, we used an OVA 17-mer peptide (biotin-FDKLPGFGDSIEAQGGK,

custom-synthesized at GenScript) previously published to bind to the OB1 HVR sequences.¹⁷ To induce BCR activation, OVA 17-mer-biotin was mixed with avidin (Pierce™ Avidin; ThermoFisher Scientific; catalog#: 21128) in a 4:1 molar ratio, respectively, and 20 µL of 10 µM solution (calculated as molarity of added avidin) was used for stimulation of 1 mL of cell suspension. Calcium response was measured as the ratio of emission intensity of Indo-1 with bound Ca²⁺ (using 379/28 filter without LP filter) and unbound Ca²⁺ (using 509/20 and 470 LP filters) when excited with a 355 nm laser on an LSR Fortessa flow cytometer (BD Bioscience).

Chemotaxis assay

Electroporation of GCB-DLBCL cell lines OCI-Ly7, OCI-Ly19, and SUDHL-4 with Cas9/gRNA vectors produced a stable proportion of viable CXCR4 KO cells, determined by FCM with anti-CXCR4 antibody conjugated with APC (eBioscience, clone 12G5) and a dead cell dye, SYTOX Blue (ThermoFisher). Chemotaxis was assayed as previously published.¹⁸ Cells in mixed cultures of CXCR4-positive and CXCR4-KO cells were counted and then conditioned in RPMI1640 medium without fetal bovine serum for one hour. 500,000 cells in 0.1 mL complete medium were then placed in the upper insert of a 24-well Transwell plate (Corning, catalog# 3421) with 5 µm pore size, with 0.6 mL of complete medium in the lower chamber, with 10 nM CXCL12 (R&D Systems, catalog# 350-NS). After 6 hours, cells in the lower chamber were collected and examined by FCM for proportions by CXCR4 expression.

Western blotting

As described above, cells with BCR KO were isolated by flow cytometric sorting. Specifically, 4-7 days after electroporation with chimeric Cas9/gRNA plasmids, cells were stained with fluorescent antibody to human IgM or IgG, appropriate to the line being sorted, and cells lacking surface BCR expression were collected and returned to culture for an additional 1-7 days. Variation in times depended on the sensitivity of the line to BCR KO, and the rapidity of surface BCR decline after KO. 2-4 different gRNA sequences targeting the IgH chain, whether in the HVR or constant region, were used in separate electroporations and sortings. As controls for the effect of electroporation, sorting, and subsequent culture, 1-2 replicates of GFP+ cells were collected that had been electroporated in parallel with empty px458 plasmid. Aliquots of the sorted and cultured cells were re-examined by FCM for purity just before harvest.

Harvested cells were lysed in RIPA Buffer (Sigma Aldrich) containing PhosSTOP Phosphatase Inhibitor Cocktail and cComplete Protease Inhibitor Cocktail (Roche, Indianapolis, IN) and loaded onto NuPAGE® Novex® 4%-12% gradient gels (Life Technologies). After electrophoresis protein was transferred onto PVDF membranes (EMD Millipore, Darmstadt, Germany). Membranes were blocked for 1 h at room temperature with PBS containing 0.1% Tween (PBS-T) and either 5% BSA (when detecting phosphoproteins) or 5% milk (when detecting total protein). Primary antibodies were diluted in blocking solution at the recommended concentrations. Membranes were incubated overnight at 4 °C. The following day membranes were washed three times for 10 min with PBS-T and incubated with species-specific HRP-linked secondary antibody (GE Healthcare) (diluted 1:10,000) for 1 h at room temperature. Protein was visualized via ECL detection (Pierce, Rockford, IL) according to the supplier's instructions.

The following antibodies were used for immunoblot analysis: anti-SYK, anti-pZAP-70 (T319)/pSYK(Y352), anti-AKT, anti-pAKT (S473), anti-PTEN, and anti-GAPDH (Cell Signaling Technologies, Danvers, MA); anti-IgM, anti-IgG (Abcam, Cambridge, MA).

Electrochemiluminescent assay

To detect changes in AKT phosphorylation at Ser473 and Thr308, we used electrochemiluminescent assay kits from Meso Scale Discovery: Phospho (Ser473)/Total Akt Whole Cell Lysate Kit and Phospho-Akt (Thr308) Whole Cell Lysate Kit. BCR KO and control cells were generally prepared similarly as for Western blotting (see above). To overcome the limitation of high toxicity of BCR KO in the SUDHL-4 line, cells prepared for inducible IgH expression (see above) in this cell line were used, comparing BCR-positive cells (fully Dox-stimulated) and BCR-negative cells (4 days after Dox withdrawal). All cells were lysed with lysis buffer consisting of 1% Triton X-100, 50mM HEPES (pH 7.4), 150 mM NaCl, 1.5 mM MgCl₂, 1 mM EGTA, and 10% glycerol with freshly added MSD Phosphatase Inhibitor I, Phosphatase Inhibitor II, and Protease Inhibitor Solution. Protein concentration was measured using Pierce™ BCA Protein Assay Kit (ThermoFisher Scientific) and 10 µg of total protein was loaded per MSD assay well. Measurement of phosphorylated Ser473 and Thr308 was done in duplicates and in parallel using the same lysates according to the manufacturer's instructions. Plates were imaged by the QuickPlex SQ 120 instrument (Meso Scale Discovery) and signal normalized by subtraction of negative control values.

Super resolution microscopy

To visualize the distribution of the BCR complex in the cell membrane, live cells expressing the CD79A-GFP fusion protein (see above), growing in suspension, were washed once with FACS buffer (PBS with 1% FBS), stained for 1 minute at RT in 1:1000 CellMask™ Deep Red Plasma Membrane Stain (ThermoFisher Scientific, catalog#: C10046) solution in FACS buffer, and washed once again with FACS buffer. 150,000 cells were re-suspended in 200 μ L of PBS per well of an 8-well coverslip bottom chamber slide (Nunc™ Lab-Tek™ II Chambered Coverglass, Thermo Scientific, catalog#: 155409) coated with poly-L-lysine (SigmaAldrich, catalog#: P4832-50ML). Chamber slides containing cell suspensions were centrifuged at 600 g for 10 minutes to promote cell attachment. The PBS was then gently exchanged for complete culture medium (see above) containing 1:100 ProLong™ Live Antifade Reagent (ThermoFisher Scientific, catalog#: P36975), and cells were returned to an incubator for 30 minutes at 37°C with 5% CO₂ until imaging. Super-resolution images were obtained using a structured illumination (SI) based DeltaVision OMX Blaze V4 Microscope (GE Healthcare Life Sciences) with UPLSAPO 100x (Olympus) objective, N = 1.514 immersion oil, and a 488 nm laser with 528/48 filter for GFP detection and a 642 nm laser with 683/40 filter for CellMask™ Deep Red plasma membrane stain detection. Z stack images were taken at the plane of contact of the cells with the coverglass \pm 1.5 μ m using sequential SI mode with dual EMCCD cameras operated at 5 MHz and 170 gain, 512 x 512 image resolution, and 0.125 μ m section spacing. Acquired raw images were processed in softWoRx™ software (GE Healthcare Life Sciences) using OMX SI reconstruction algorithm. For the final image, 2-3 sections at the point of contact of the cells with the chamber bottom were merged in maximum intensity projection. Brightness levels were adjusted for each image individually using Adobe Photoshop. Videos with 3D projections were generated with softWoRx™ software. All images of the z-stacks were enhanced by the Local Contrast Enhancement tool and 3D reconstructions created by Volume Viewer tool, calculating 350 maximum intensity projections for 360° rotation. After brightness adjustment, maximum intensity projections were saved as AVI formatted videos with speed set at 18 frames per second.

Förster resonance energy transfer (FRET)

To measure AKT activity directly, we used the FRET-based AKT activity reporter AktAR2 (Addgene plasmid #64932).¹⁹ In brief, from N terminus to C terminus (Figure S2A), the reporter protein consists of: Cerulean3 (donor fluorescent protein); a phospho-amino acid (AA) binding domain from FHA1; a phosphorylation target sequence surrounding Thr-24 of FOXO1; and circularly permuted Venus (cpVenus[E172], acceptor fluorescent protein). AKT-mediated phosphorylation of the reporter causes binding of the FHA1 domain to the phosphorylated threonine, resulting in bending of the reporter that brings the fluorescent proteins in close proximity, increasing the FRET efficiency (*E*). As was done previously,²⁰ we added to the N terminus of AktAR2 the ten N-terminal AA from Lyn kinase, targeting Lyn-AktAR2 to lipid rafts through myristoylation and palmitoylation. As adjuncts to FRET determination, we created the following constructs expressing: Cerulean3 alone; cpVenus[E172] alone; C3-cpV (Cerulean3-cpVenus[E172]) as a fusion protein without a linker, serving as a maximum FRET control; C3-spacer-cpV, in which the FoxO1 phosphorylation site was replaced with a 230-AA TRAF2-derived spacer, as done before for a low-FRET control;²¹ and a “Dead” Lyn-AktAR2, in which the FoxO1 Thr-24 was changed to a similar but unphosphorylatable residue (Val), serving as a baseline FRET control. For measurement of AKT activity in response to small molecule inhibitors, we used an improved version of the AKT activity reporter (Lyn-AktAR2-EV) in which a long flexible linker called “EV”²² was inserted to lower the baseline FRET. The improved reporter was also used to measure AKT activity in cells modified to express the BCR at variable levels. Sequences of all constructs used for FRET-based detection of AKT activity are listed in the Sequences section below.

Cells were stably transfected to express the FRET constructs using the Sleeping Beauty transposon system.¹⁴ Specifically, Lyn-AktAR2 and the above-mentioned constructs were inserted into the donor transposon plasmid pSBbi-Pur (Addgene plasmid #60523¹⁴), and 9 μ g of each transposon plasmid was electroporated together with 5 μ g of the transposase plasmid pCMV(CAT)T7-SB100 (Addgene plasmid #34879²³) per 1.2 million cells, resuspended in appropriate buffer (see above). Cells were consequently selected for integration by puromycin at a final concentration of 2 μ g/mL.

To measure the change in FRET efficiency (*E*) with BCR KO, indicating its effect on AKT activity, we knocked out the BCR in cells stably expressing the Lyn-AktAR2 reporter by CRISPR/Cas9 methods as described above. *E* was determined in BCR-negative cells (as identified by staining using fluorescently labeled antibody, see below) in mixed cultures after BCR targeting, and compared to the *E* of BCR-expressing cells. We found that staining for BCR expression, even with Fab’ fragment antibodies, increased the *E* level (data not shown); therefore, the *E* of BCR-expressing cells was determined in parallel unstained cultures after electroporation with gRNA/Cas9 plasmids targeting the HVR of a different cell line.

E was measured in live cells by two methods, fluorescent microscopy and FCM, at 5 days after electroporation to achieve BCR KO. For fluorescent microscopy, mixed cultures of BCR-positive and BCR-KO Lyn-AktAR2-expressing cells were stained with non-crosslinking anti-IgG Fab’ or anti-IgM Fab’ fragment antibody (see table in Flow cytometry, image cytometry, and cell sorting section of Supplemental Methods) by the same methodology as for FCM staining (see above), to allow identification of BCR-negative cells. Cells after staining, as well as all cells expressing adjunct constructs (which went through the same staining procedure but without antibody), were then attached to 8-well coverslip-bottom chamber slides as described above, and incubated for one hour at 37°C with 5% CO₂ until imaging. Fluorescent microscopy for FRET was done according to the “3-filter cube”

methodology developed by Zal and Gascoigne²⁴ using a DeltaVision OMX Blaze V4 Structured Illumination Microscope (GE Healthcare Life Sciences) with a 60x TIRF oil objective (Olympus) in the widefield mixed-FRET mode with dual electron multiplied charge-coupled device (EMCCD) cameras operated without EMCCD gain. We used excitation with a 445 nm laser with 478/35 filter to measure donor fluorescence with donor excitation (I_{DD} , donor channel), excitation with a 445 nm laser with 541/22 filter to measure acceptor emission with donor excitation (I_{DA} , FRET channel), and excitation with 514 nm laser with 541/22 filter to measure acceptor emission with acceptor excitation (I_{AA} , acceptor channel). Exposure times were 200-400 ms, always the same for all channels for one cell image. Single images through the middle of cells were used to calculate mean fluorescent intensities for each cell and channel using softWoRx™ software (GE Healthcare Life Sciences). For each cell, a region of background was defined in the image and subtracted from the measured intensities. The cpVenus[E172] and Cerulean3 single-color constructs were used to calculate the a and d channel cross-talk coefficients, respectively. The C3-cpV construct of maximal FRET was used to calculate the G factor by the acceptor photobleaching method.²⁴ Each coefficient was calculated as the average of at least 10 measurements. Average values of the individual coefficients were: $d = 0.282$ ($SD = 0.9253 \times 10^{-3}$), $a = 0.1283$ ($SD = 4.697 \times 10^{-3}$), and $G = 1.0205$ ($SD = 0.181$).

For E determination by FCM, mixed cultures of BCR-positive and BCR-KO cells were re-suspended in complete culture medium (see above) containing a final dilution of anti-IgG or anti-IgM Fab' fragment antibody (see table in Flow cytometry, image cytometry, and cell sorting section of Supplemental Methods) and incubated for 20 minutes at 37°C with 5% CO₂ or until FCM analysis. All cells expressing adjunct constructs went through the same procedure without antibody. Our approach to E determination by FCM was adapted from methods developed by Chen et al.,²⁵ in which calculation of the G factor is based on a pair of FRET reporters with identical fluorophores but differing highly in FRET efficiency due to differences in proximity of the fluorophores. Our C3-cpV and C3-spacer-cpV constructs provided maximum and minimal FRET controls, respectively. Filter settings on the LSR Fortessa flow cytometer (BD Biosciences) used for FRET were as follows: excitation with a 405 nm laser with 450/50 filter for I_{DD} measurement, excitation with a 405 nm laser with 525/50 filter for I_{DA} measurement, and excitation with a 488 laser with 530/30 filter for I_{AA} measurement. For each cell line, non-fluorescent unmodified cells were used to measure autofluorescence, providing average values for each channel to be subtracted from corresponding intensity values obtained for reporter-expressing cells. Cells expressing cpVenus[E172] alone were used to measure the a and b coefficients, and cells expressing Cerulean3 alone were used to measure the c and d coefficients. To calculate coefficients, only cells with fluorescent protein expression levels in the higher half of expression intensity were used, and linear regression was used to calculate the coefficient values. Similarly, cells with higher expression of the C3-cpV and C3-spacer-cpV constructs were used to calculate the G value. Average values of sensitized acceptor emissions (F_c) and corrected I_{DD} and I_{AA} intensities were used for final calculation of the G factor.²⁵ All constants were separately measured for each experiment. Coefficient values from a representative experiment were: $a = 7.718 \times 10^{-3}$ (standard error = 0.179×10^{-3}), $b = 0$, $c = 11.102 \times 10^{-3}$ (standard error = 0.171×10^{-3}), $d = 0.982$ (standard error = 1.597×10^{-3}), and $G = 1.719$. From the experimental data, an E value was calculated for each cell, and values for all cells of a particular line, reporter, and condition were plotted as a moving median of E versus corrected I_{DD} (I_{dd}) (Figure S2E). For comparing BCR-positive and BCR-KO cells of the same cell line, a single average overall E value for each condition was calculated from cells in the same range of donor emission intensities, with all parts of the range having enough cells to generate a consistent moving average. For each cell line, data points in the very low range of donor emission intensities (usually I_{dd} below 2000) were excluded, because of non-robust E values at low fluorescence intensities.

Gene expression profiling (GEP)

BCR KO cells were isolated as described above for Western blotting. For cell lines with little effect on growth of BCR KO, such that stable BCR negative cultures were created, the parental lines were used as controls. Total RNA was isolated from harvested cells with the RNAqueous Total RNA Isolation Kit (Thermo Scientific, catalog#: AM1912). Subsequent RNA quality assessment, generation of biotinylated aRNA for hybridization on Illumina HT-12 BeadArrays (Illumina, Inc., San Diego, CA), and data processing was as previously described.²⁶ Data from microarray studies are submitted to Gene Expression Omnibus as GSE80615. Values for probes expressed above background in at least 10% of samples were used for heat mapping and correlation analysis. After log₂ transformation and mean centering, heat maps showed good agreement between replicates as to the effect of BCR KO on gene expression, even though the replicates for BCR KO used different gRNA sequences. Therefore, for each line, log₂ values for each probe were averaged to give a single value for each state (BCR KO or Control), and then subtracted to give a log₂ value for the fold-change in gene expression caused by BCR KO. Using data from 10 GCB-DLBCL lines, an r value was calculated for each gene probe of the Pearson correlation between the change in log₂ gene expression caused by BCR KO and the relative proliferation after BCR KO; this correlation for the HRK gene is illustrated in Figure 3A. For each gene probe, a metric of correlation between change in gene expression and change in proliferation after BCR KO was then based on this r value as follows:

$$\text{correlation metric} = \text{sign}(r) \times \frac{\text{variance}(\text{gene expression change})}{\text{abs}(\log_2(\text{abs}(r)))}$$

Absolute values of the correlation metric, which is positive or negative according to the r value, increase with increasing variance in the change in gene expression, and with increasing correlation (r values approaching 1 or -1) between gene expression change

and proliferation change, potentially selecting for genes with both large change and high correlation. Probe-averaged gene values for this correlation metric were then used to rank genes to perform Gene Set Enrichment Analysis (GSEA),²⁷ using a custom collection of gene sets from the scientific literature, as well as gene sets in the C2, C3, C5, and C6 categories in the Molecular Signatures Database (MSigDB) web service release version 3.84.

SUPPLEMENTAL TABLE**Table S1. Relative proliferation of GCB-DLBCL cell lines after BCR KO**

Slopes of absolute growth curves of BCR-KO and BCR-replete cells of each line yield a ratio (BCR-KO/BCR-replete) quantifying the relative proliferation of BCR-KO cells. The order of cell lines, from top to bottom, is those most affected by BCR KO to those least affected.

Cell line	Relative proliferation	IgH isotype	IgL isotype
SUDHL-4	-0.0322	G4	K
SUDHL-6	0.430746	M	K
OCI-Ly7	0.455293	M	K
Pfeiffer	0.648559	G	K
OCI-Ly19	0.727581	M	K
OCI-Ly18	0.735202	M	not expressed
SUDHL-7	0.904983	G	K
OCI-Ly8	0.912752	M	L
DB	0.939476	G	L
SUDHL-10	0.941596	G	L

SUPPLEMENTAL FIGURES

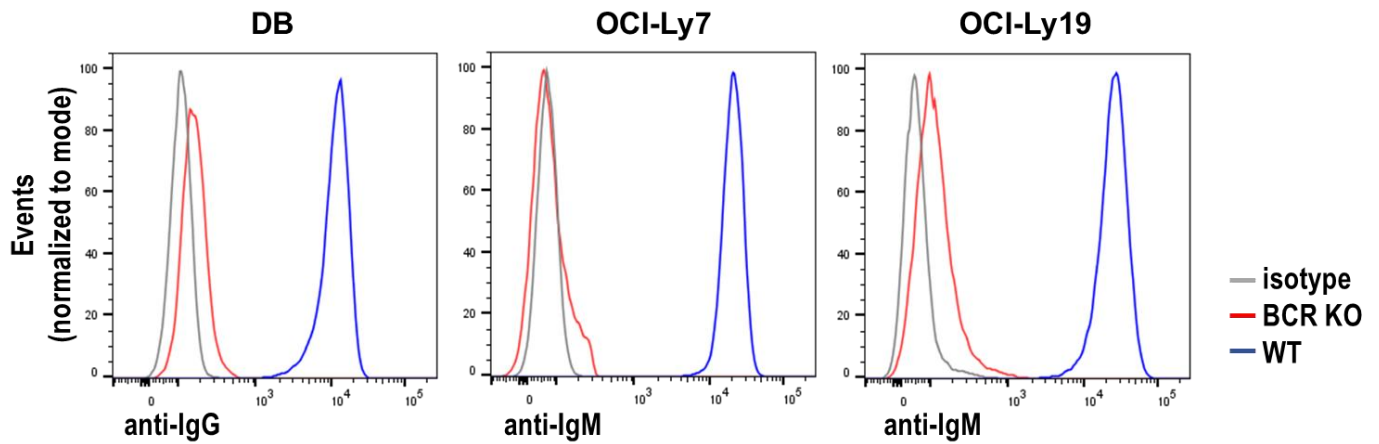


Figure S1. Targeting of IgH reduces surface BCR to undetectable levels

Viable cultured cells from three representative GCB-DLBCL cell lines were assessed by flow cytometry for surface binding of goat fluorescent antibody, either specific for the IgH isotype expressed by the particular cell line (WT or BCR KO) or a non-specific antibody of the same goat isotype (isotype). For each cell line, cultures were either unmodified cells (WT and isotype) or had undergone BCR KO at least 10 days earlier, followed by flow cytometric sorting to eliminate unmodified cells and further culture.

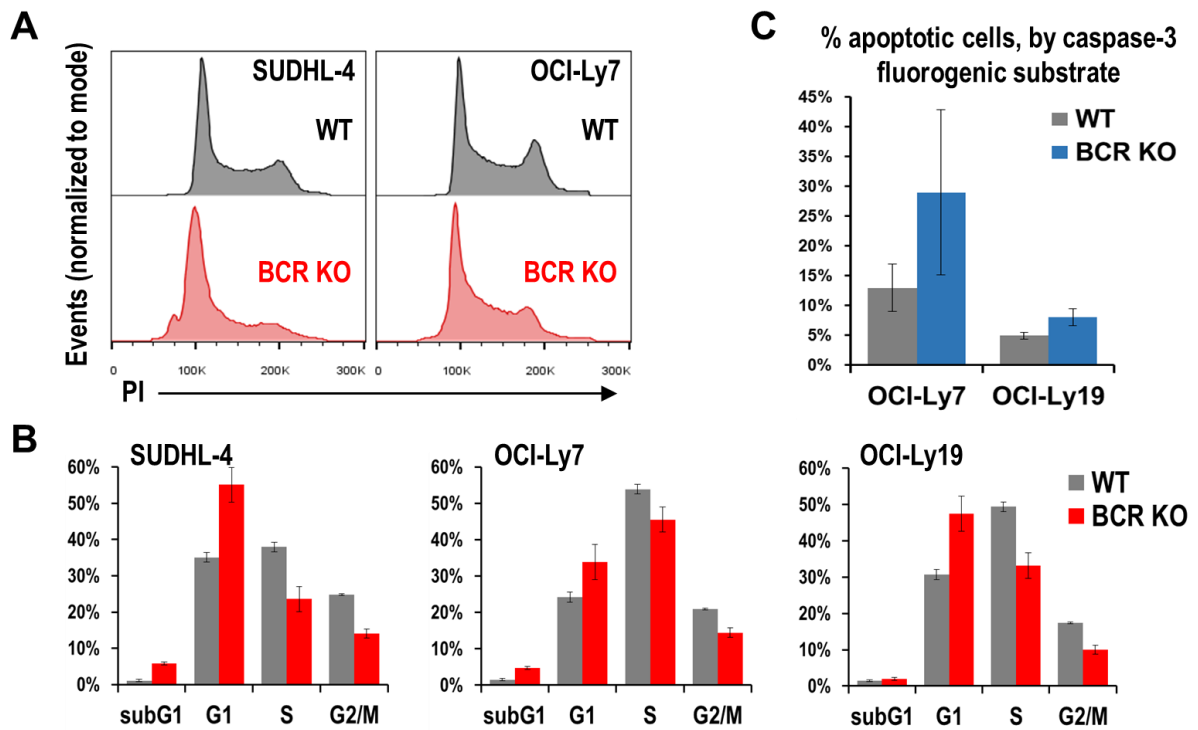


Figure S2. BCR KO reduces proliferation and can induce apoptosis in GCB-DLBCL lines

(A) Effect of BCR KO (via targeting of IgH) in two GCB-DLBCL lines on histograms of DNA content, based on propidium iodide staining and flow cytometry.

(B) Effect of BCR KO on proportions of cells of 3 GCB-DLBCL lines in active cell-cycle phases or apoptosis (sub-G1), based on propidium iodide staining for DNA content. The mean \pm s.d. from 3 (OCI-Ly7), 4 (OCI-Ly19), and 6 (SUDHL-4) biological replicates is displayed.

(C) Effect of BCR KO on proportions of apoptotic cells of two GCB-DLBCL lines, based on flow cytometry with a caspase-3 fluorogenic substrate. The mean \pm s.d. from 3 biological replicates is displayed.

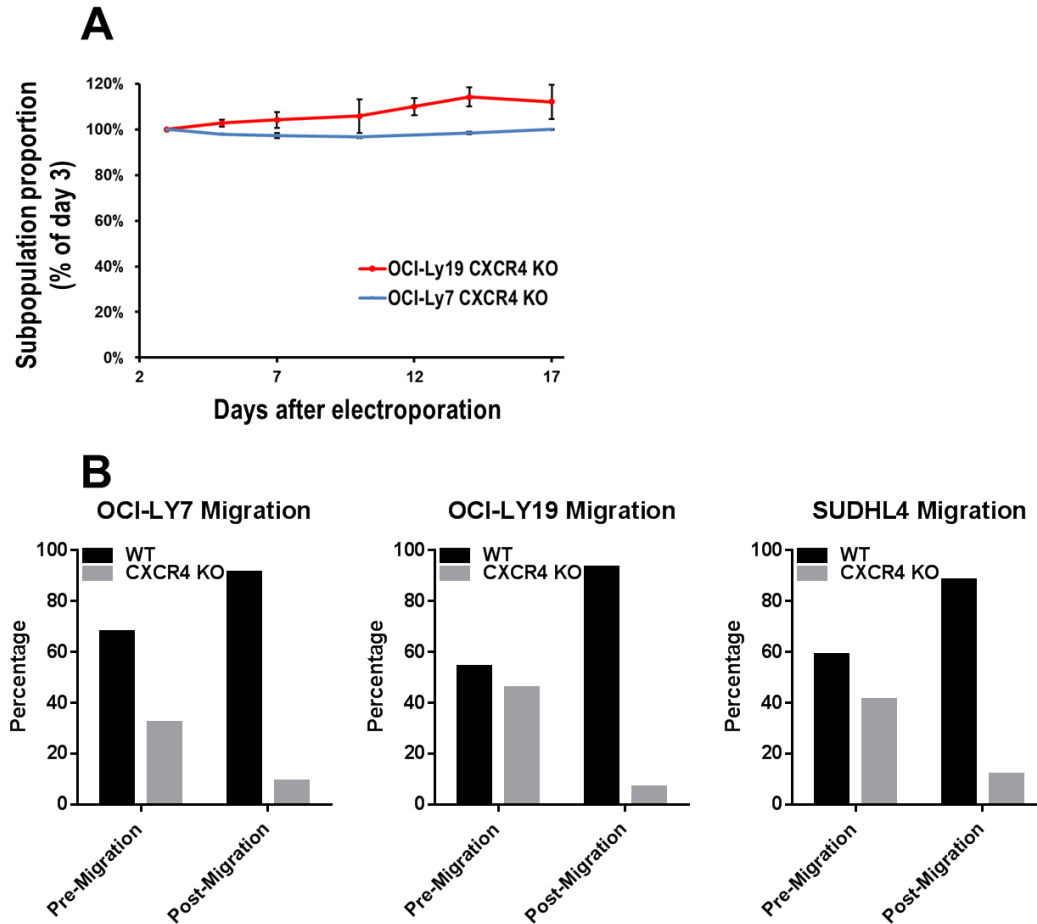


Figure S3. CXCR4 KO in GCB-DLBCL lines affects chemotaxis but not proliferation.

(A) The proportion of CXCR4 KO cells in mixed cultures (KO and unmodified cells) for 2 GCB-DLBCL lines, normalized to its initial value (determined 3 days after electroporation), is stable over time.

(B) The 3 GCB-DLBCL lines shown underwent KO of CXCR4, creating mixed cultures of WT and CXCR4 KO cells, whose relative proportions (determined by flow cytometry for CXCR4 surface expression) are shown as “Pre-Migration”. Aliquots of these cultures were then placed in the upper insert of a 24-well Transwell plate, for challenge by chemotaxis to a CXCL12 gradient through a 5 μ m pore-size filter. After 6 hours, cells in the lower chamber (“Post-Migration”) were examined by flow cytometry for surface CXCR4 expression. The increase in relative proportion of WT cells post-migration provides functional confirmation of the loss of CXCR4 in CXCR4 KO cells.

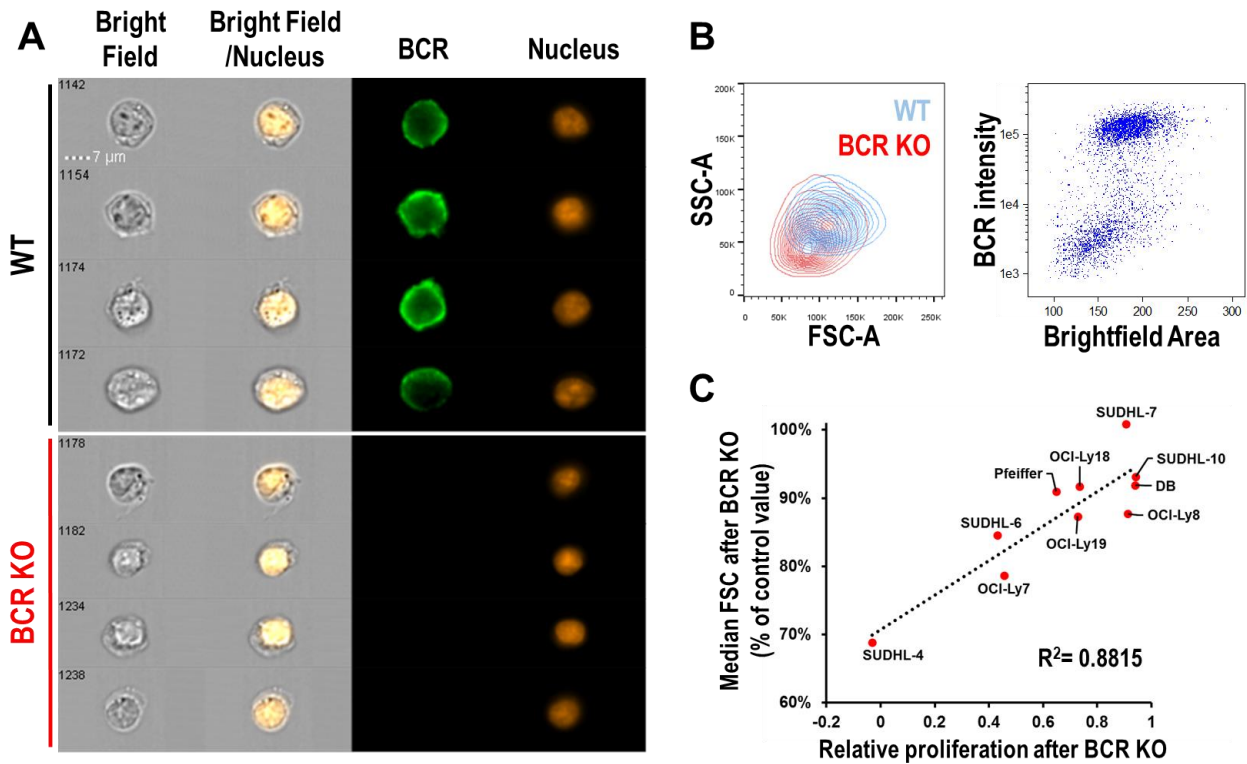


Figure S4. BCR KO reduces cell size in GCB-DLBCL lines

(A) Individual representative images of cells of the GCB-DLBCL line SUDHL-4, detected with an ImageStream image cytometer, showing reduced size of BCR-KO cells. Cells were stained with FITC labeled antibody to IgM (BCR) and then fixed, permeabilized, and stained with propidium iodide.

(B) Aggregate measures of SUDHL-4 cell size by flow cytometry (left panel; FSC = forward scatter; SSC = side scatter) or image cytometry (right panel) according to BCR status.

(C) Correlation between BCR KO-induced reductions in proliferation and cell size, reflected by forward scatter (FSC), of GCB-DLBCL lines. The average of FSC median values from 2-3 biological replicates, each performed with a different IgH-targeting gRNA, is shown for each line.

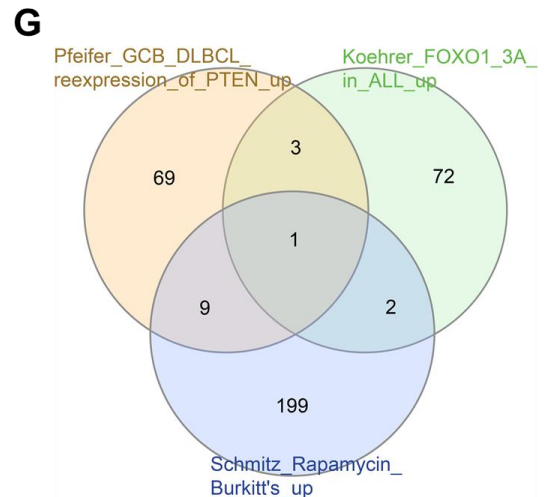
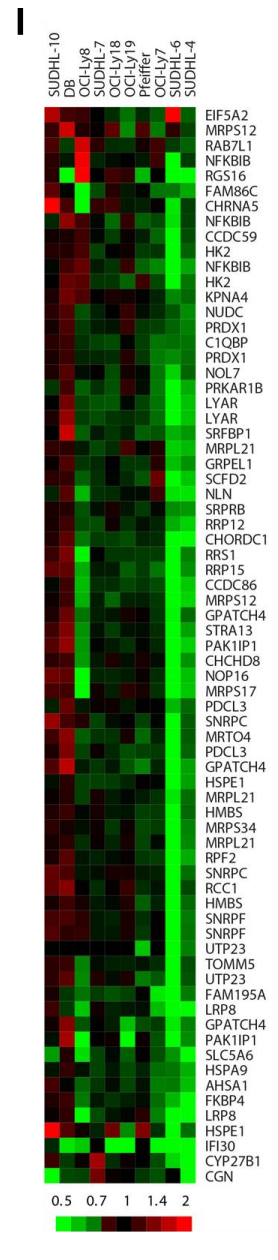
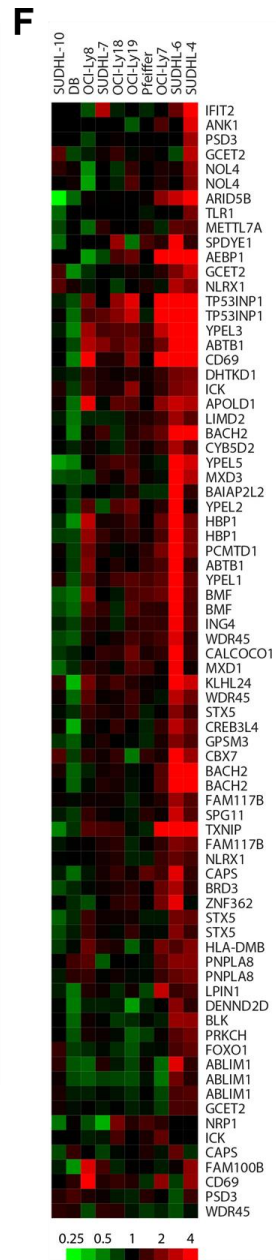
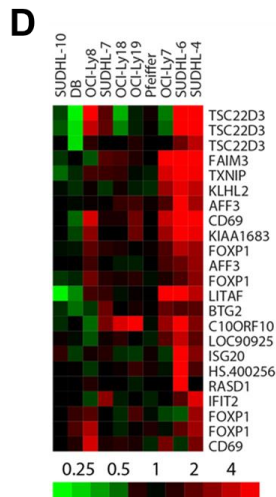
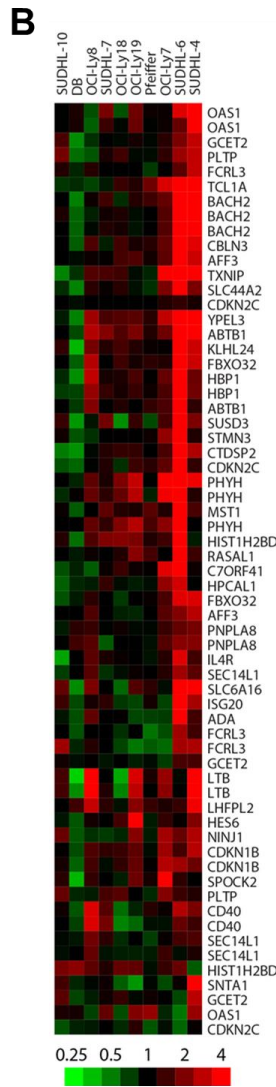
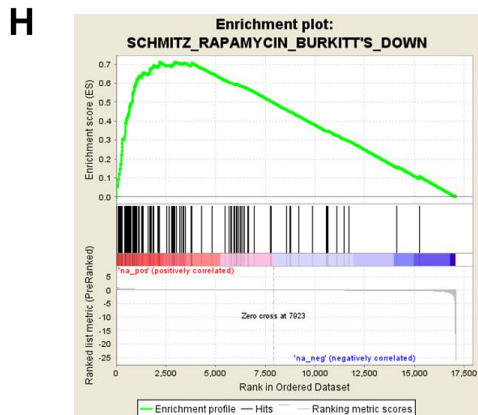
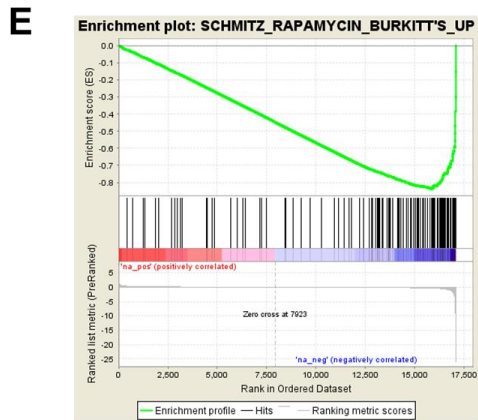
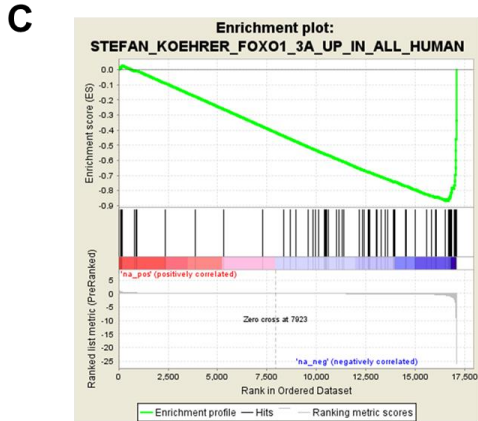
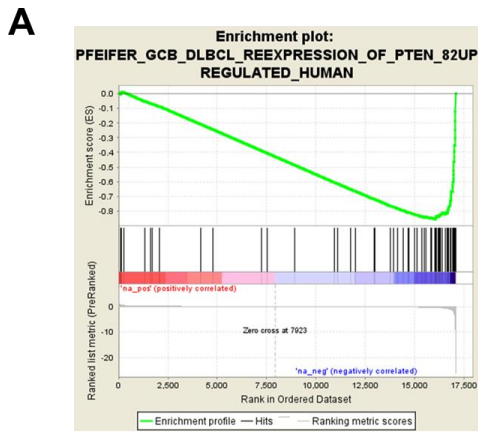


Figure S5. Gene set enrichment analysis (GSEA) indicates that effects of BCR KO correlate with reduced AKT activity

(A) Applied to genes ranked by correlation between BCR KO-induced changes in expression and relative proliferation in 10 GCB-DLBCL lines, GSEA enriched a set of 82 genes upregulated by the forced expression of PTEN in HT, a GCB-DLBCL line lacking PTEN protein expression. Shown is the enrichment plot (FDR = 0.008).

(B) Subtracted heat map of gene expression changes caused by BCR KO in GCB-DLBCL lines, arranged by BCR KO-induced growth reduction (left, least; right, most), for the 40 core genes of the gene set in (A). Results are based on 3-4 BCR KO replicates, each using a different IgH-targeting gRNA. The color bar shows fold-change.

(C) GSEA enrichment plot (FDR = 0.002) for 78 genes upregulated in RCH-ACV (a cell line expressing a pre-BCR) by a non-phosphorylatable mutant form of FOXO1, which avoids inhibition by AKT.

(D) Subtracted heat map for the 17 core genes of the gene set in (C).

(E) GSEA enrichment plot (FDR = 0.004) for 211 genes upregulated in Burkitt's lymphoma cell lines treated with rapamycin.

(F) Subtracted heat map for the 54 core genes of the gene set in (E).

(G) Venn diagram²⁸ showing overlap of the 3 gene sets used for (A)-(F).

(H) GSEA enrichment plot (FDR = 0.000) for 133 genes downregulated in Burkitt's lymphoma cell lines treated with rapamycin.

(I) Subtracted heat map for the 53 core genes of the gene set in (H).

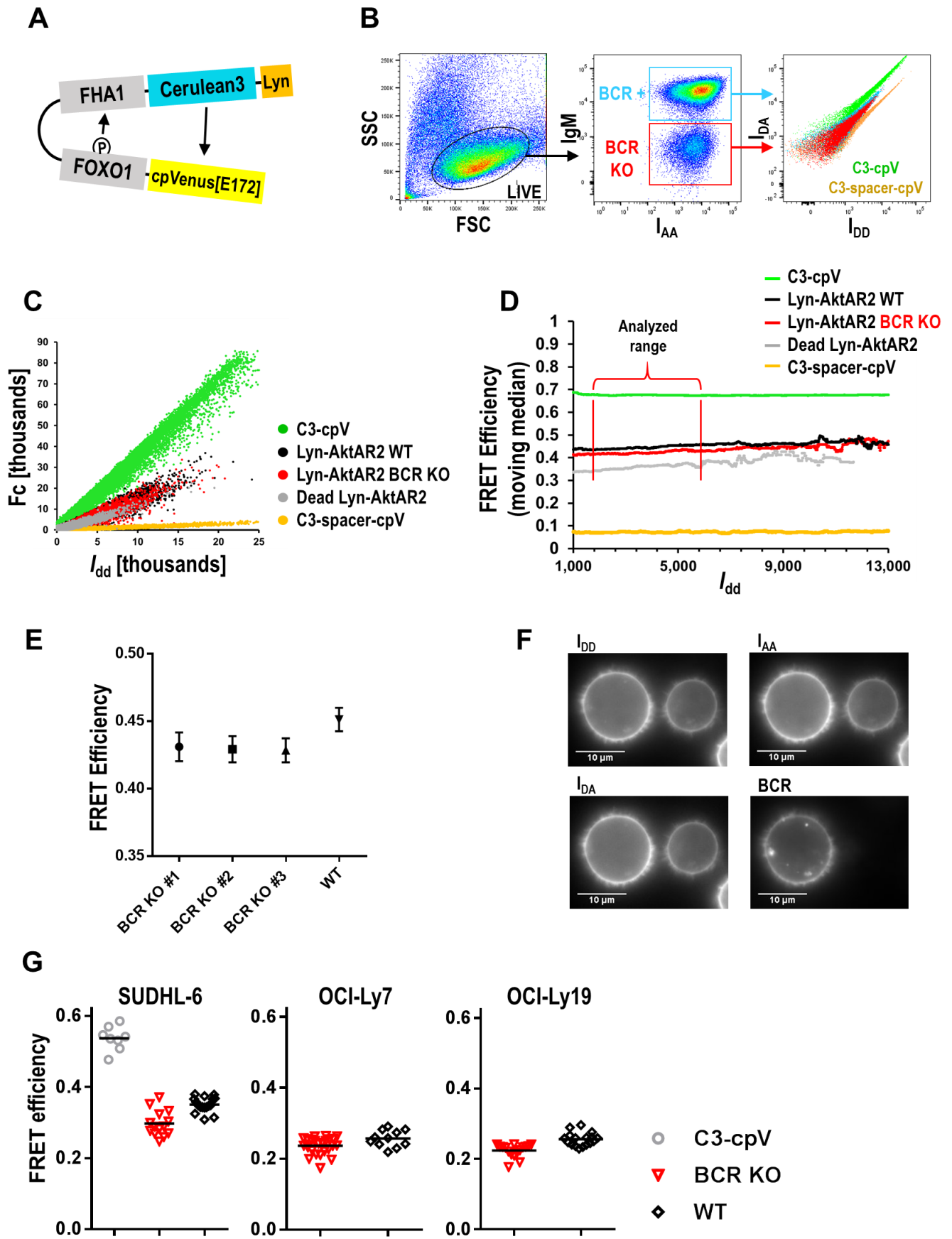


Figure S6. Effect of BCR KO on AKT activity in GCB-DLBCL lines

- (A) Lyn-AktAR2 reporter schematic. The N-terminal domain from LYN mediates plasma membrane localization. Phosphorylation of the AKT target site from FOXO1 induces binding by the FHA1 domain, bringing Cerulean3 (donor) and cpVenus[E172] (acceptor) fluorescent proteins closer.
- (B) Uncompensated flow cytometry data and gating strategy for OCI-Ly7 cells stably expressing Lyn-AktAR2, 5 days post-electroporation for BCR KO. FRET (I_{DA} versus I_{DD}) of Lyn-AktAR2, between high (C3-CpV) and low (C3-spacer-cpV) control constructs, is slightly lower in BCR-KO than WT cells.
- (C) Sensitized acceptor emission (F_c) versus corrected donor emission (I_{dd}) in OCI-Ly7 cells expressing FRET control constructs, Lyn-AktAR2-expressing WT or BCR-KO SUDHL-6 cells 5 days post-electroporation, and SUDHL-6 cells expressing non-phosphorylatable (Dead) form of Lyn-AktAR2.
- (D) Moving median of per-cell E value versus I_{dd} for same cells as in (C). The average of moving median values of E (E_{ave}) was determined in the marked region.
- (E) E_{ave} (+/- standard deviation) of BCR-replete (WT) and BCR-KO (3 biological replicates) Lyn-AktAR2-expressing SUDHL-6 cells 5 days post-electroporation.
- (F) OCI-Ly7 cells (BCR-replete, left; BCR-KO, right) 5 days post-electroporation show Lyn-AktAR2 donor emission after donor excitation (I_{DD}), acceptor emission after acceptor excitation (I_{AA}), acceptor emission after donor excitation (I_{DA}), and surface BCR (BCR) detected with red fluorescence-emitting anti-IgM.
- (G) FRET efficiency (E) from microscopy of Lyn-AktAR2-expressing single cells of 3 GCB-DLBCL cell lines (horizontal line = mean), either BCR-replete (WT) or with BCR KO. C3-cpV is a high-FRET control construct with Cerulean3 fused directly to cpVenus[E172].

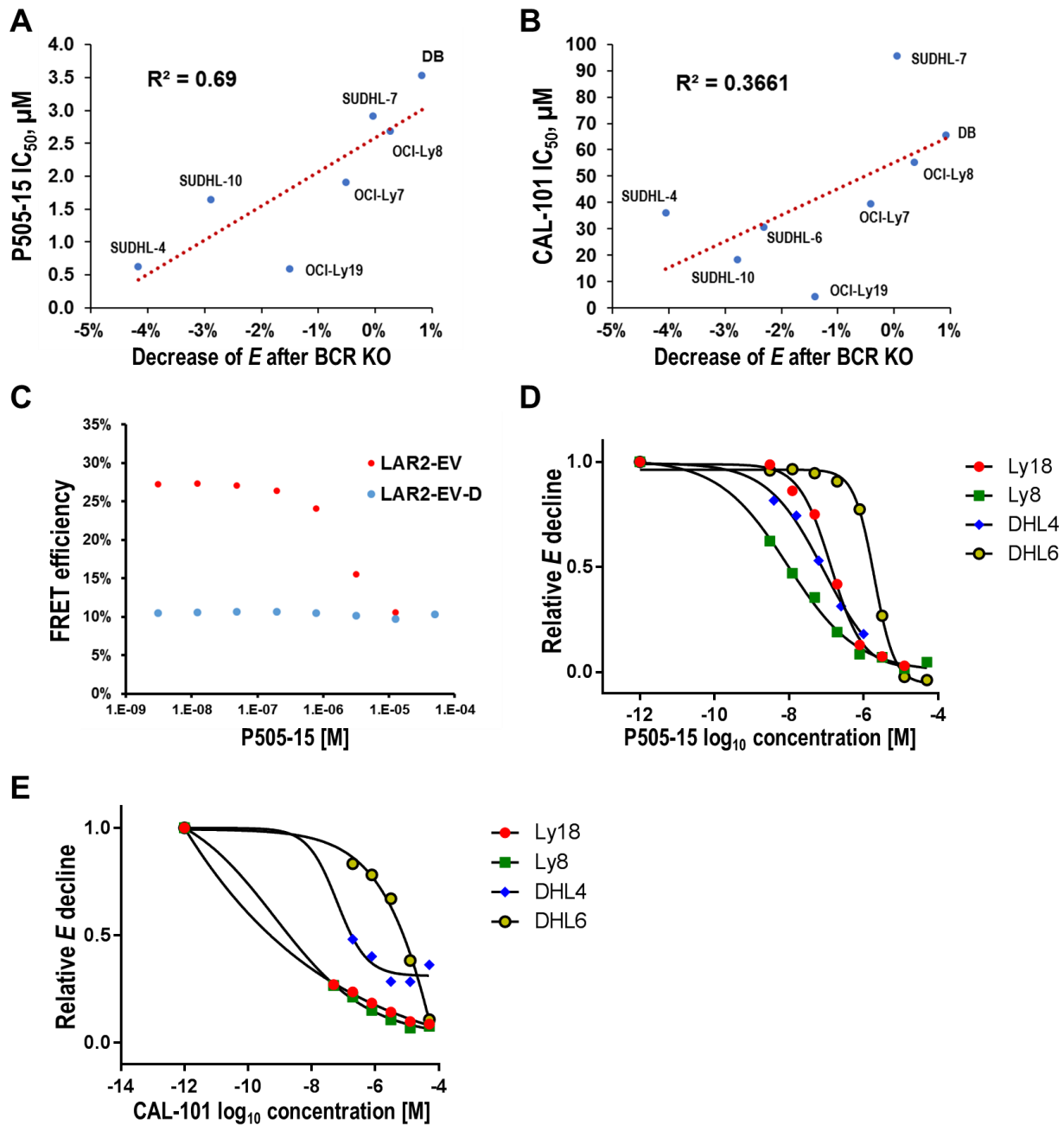


Figure S7. Measures of effect on AKT activity in GCB-DLBCL lines on inhibitors of tonic BCR signal transmission

(A) Correlation between sensitivity of GCB-DLBCL lines to a small-molecule SYK inhibitor P505-15,²⁹ determined by CellTiter-Glo viability assays, and the BCR KO-induced reduction in AKT activity, as measured by percentage decrease of E with the Lyn-AktAR2 reporter.

(B) Correlation between sensitivity of GCB-DLBCL lines to CAL-101, a small-molecule inhibitor of the PI3K p110 δ isoform,³⁰ and the BCR KO-induced reduction in AKT activity, as measured by percentage decrease of E .

(C) Dose-response curves of FRET efficiency, for linker-enhanced versions of the “live” (phosphorylatable) and “dead” (non-phosphorylatable) forms of the Lyn-AktAR2 reporter, in SUDHL-6 cells treated for 1 hour with SYK inhibitor P505-15. AKT activity measured by the live reporter is inhibited by increasing concentrations of P505-15, without a change in FRET efficiency of the dead reporter.

(D) Dose-response curves for inhibition of AKT activity by 1 hour treatment of 4 GCB-DLBCL lines with SYK inhibitor P505-15. Values are normalized to 100% of the baseline difference for each line in FRET efficiency between the linker-enhanced live and dead Lyn-AktAR2 reporters.

(E) Dose-response curves for inhibition of AKT activity by 1 hour treatment of 4 GCB-DLBCL lines with PI3K p110 δ isoform inhibitor idelalisib. Values are normalized as in (D).

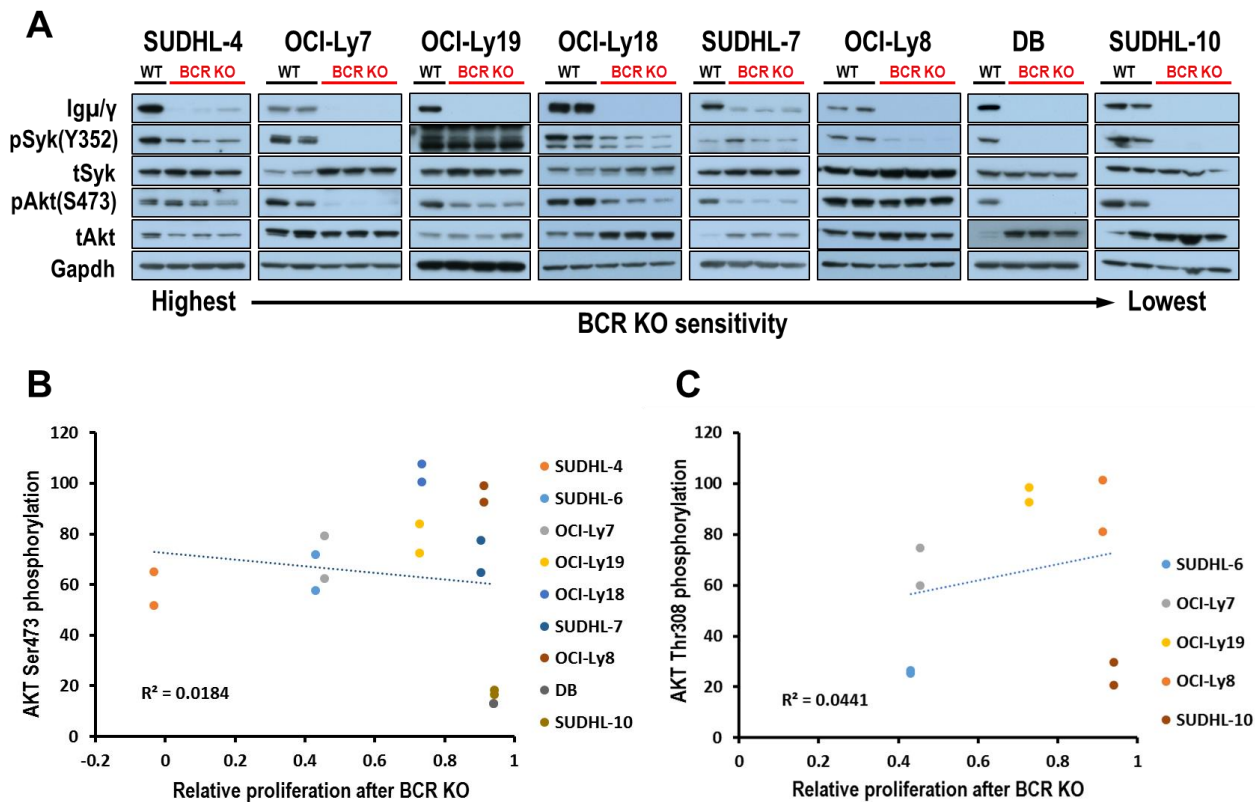


Figure S8. BCR KO reduces AKT phosphorylation, but to a degree not well correlated with BCR KO-induced reduction in proliferation

(A) Western blot for abundance and phosphorylation of BCR-relevant proteins in GCB-DLBCL lines after BCR KO. BCR KO replicates used different IgH-targeting gRNAs. Lines are arranged by effect of BCR KO on proliferation (left, most; right, least).

(B) Electrochemiluminescence assay for AKT Ser473 phosphorylation (pSer473) was performed on protein lysates, balanced for total protein content, from unmodified (WT) and BCR KO cells of 9 GCB-DLBCL lines. Results are displayed for BCR KO cells assayed in duplicate, normalized to the pSer473 value of WT cells from the same line and correlated with the effect of BCR KO on relative proliferation in that line.

(C) Results of electrochemiluminescence assay for AKT Thr308 phosphorylation, performed and displayed similarly to (B). Lines in (B) not included in (C) did not have detectable signal for pThr308.

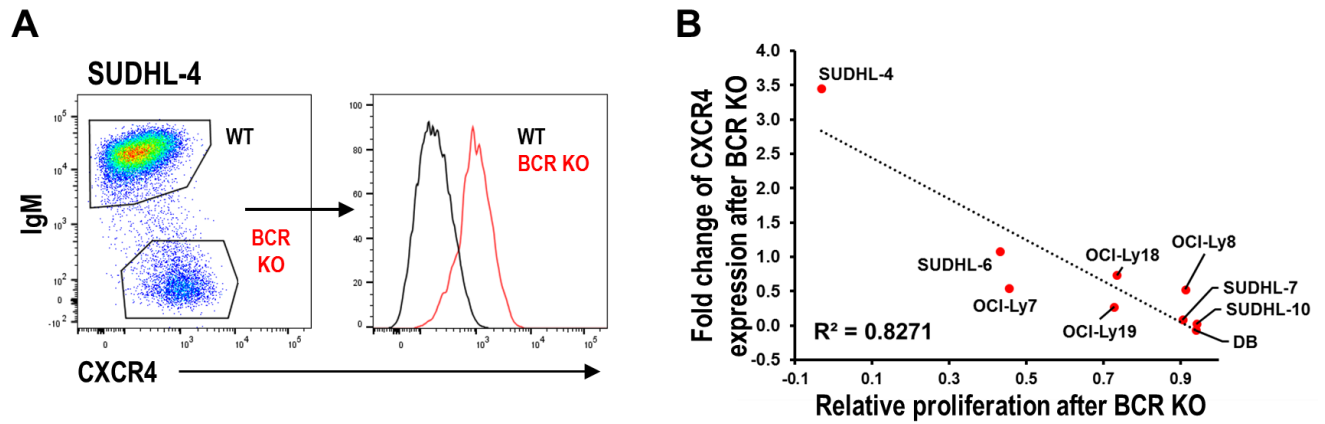


Figure S9. Upregulation of surface CXCR4 by BCR KO correlates with BCR KO-induced reduction in proliferation

(A) CXCR4 surface levels in SUDHL-4 cell line 5 days after electroporation for BCR KO.

(B) Correlation in GCB-DLBCL lines between BCR KO-induced relative proliferation and upregulation of CXCR4 surface expression 5 days after electroporation for BCR KO. Results are the average of 2 (CXCR4) and 3 (proliferation) biological replicates with different IgH-targeting gRNAs.

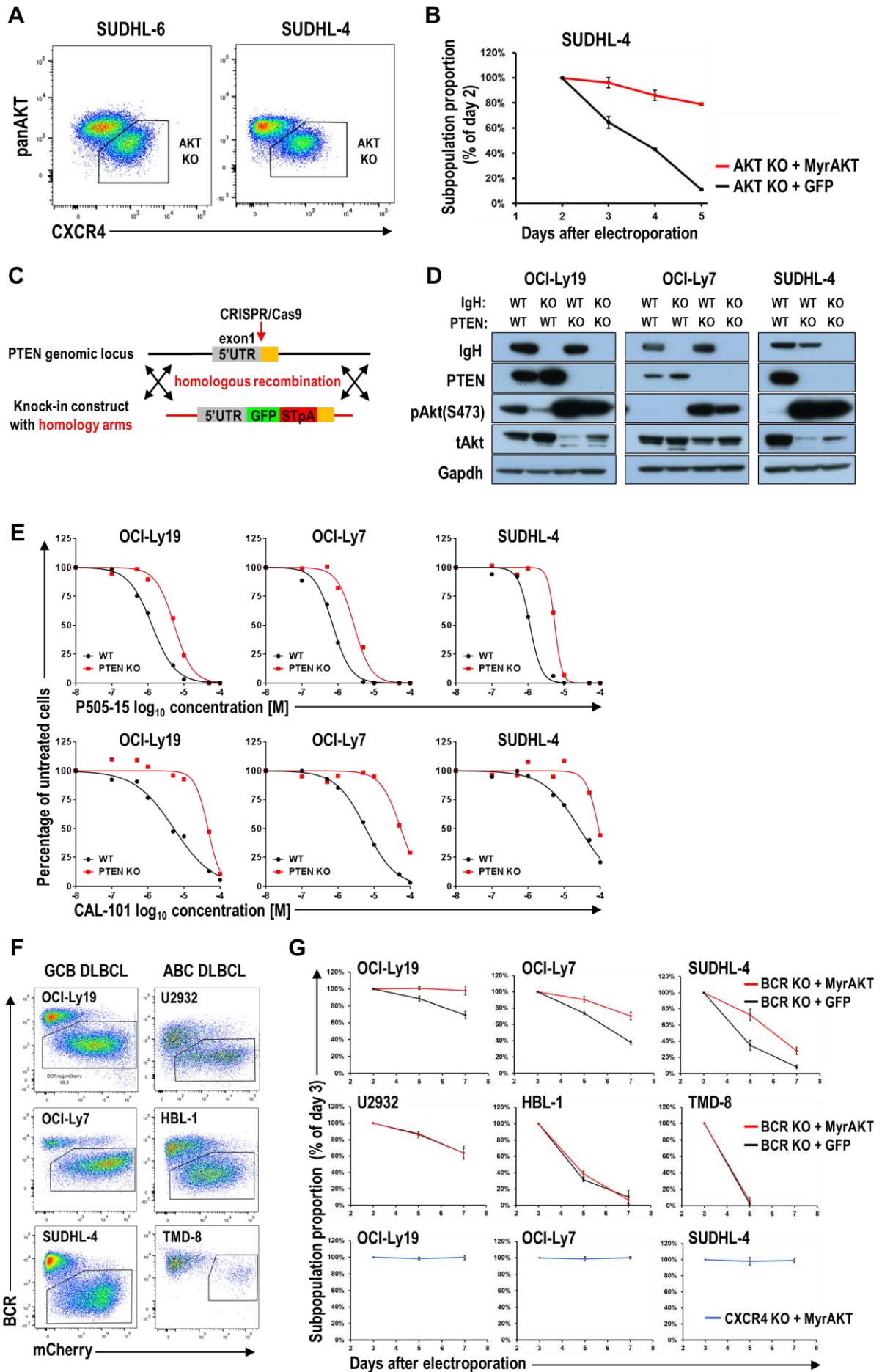


Figure S10. Manipulations showing role of BCR signaling and AKT in GCB-DLBCL lines

- (A) Flow cytometry of GCB-DLBCL lines 3 days post-electroporation with plasmids targeting all 3 AKT genes shows CXCR4 upregulation in AKT-KO cells.
- (B) Constitutively-active murine AKT1 (MyrAKT, co-expressed with mCherry) rescues SUDHL-4 cells from effect of AKT KO (shown in Figure 3C), but cells expressing GFP alone undergo rapid decline. Mean \pm s.d. from 3 biological replicates is displayed.
- (C) Schematic of “gene trapping” KO of PTEN by knock-in of a reporter cDNA (GFP) ending with a stop codon followed by a polyA signal sequence (STpA).
- (D) Western blots showing effects of KO of IgH and/or PTEN in 3 GCB-DLBCL lines. BCR KO was too rapidly toxic in SUDHL-4 for isolation of BCR-KO cells.
- (E) Effect of PTEN KO on sensitivity of GCB-DLBCL lines to small-molecule inhibitors of SYK (P505-15) and the PI3K p110 δ isoform (CAL-101).
- (F) Flow cytometric measurement of mCherry (indicating co-expression of MyrAKT) and surface BCR, 3 days post-electroporation of mCherry-2A-MyrAKT and CRISPR/Cas9 IgH-targeting plasmids. mCherry expression is largely confined to BCR-KO cells and high in all DLBCL lines.
- (G) Proportion over time of BCR-KO cells also expressing a marker (mCherry, indicating co-expression of MyrAKT, or GFP alone) from a co-transfected plasmid, normalized to its initial value 3 days post-electroporation, in GCB-DLBCL (top panels) and ABC-DLBCL lines (middle panels). Bottom panels show proportion over time of CXCR4-KO cells also expressing MyrAKT in 3 GCB-DLBCL lines. Growth advantage (rescue) by MyrAKT is restricted to BCR-KO GCB-DLBCL lines. Mean \pm s.d. from 3 biological replicates (each with a different gRNA) is displayed.

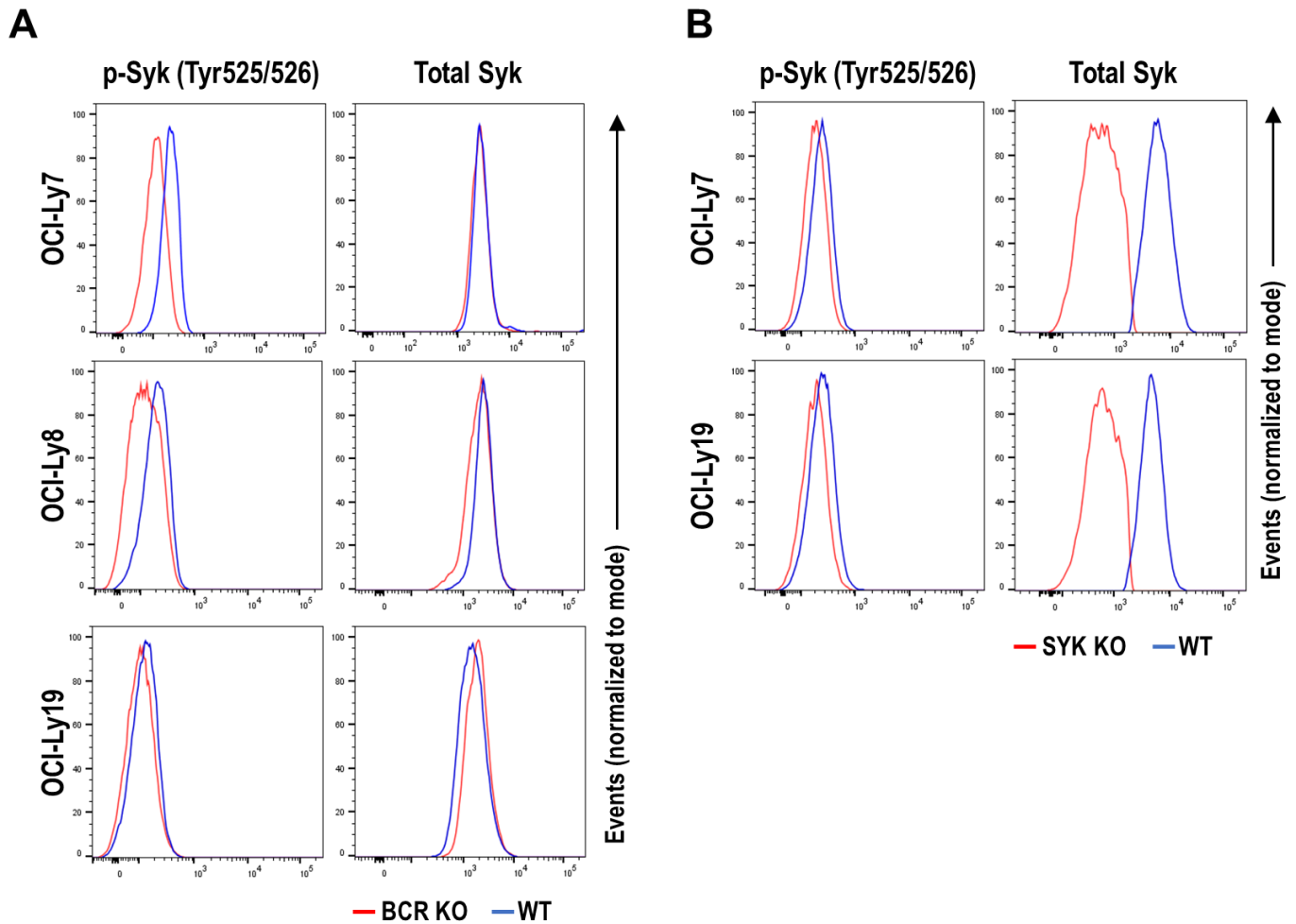


Figure S11. Effect of BCR KO on SYK autophosphorylation sites Y525/Y526

(A) Viable cultured cells from three representative GCB-DLBCL cell lines were assessed by flow cytometry in mixed cultures of unmodified (BCR-positive) and BCR-KO cells, after fixation and permeabilization, for BCR expression, total SYK content, or the level of phosphorylation of SYK (p-Syk) at residues Y525/Y526, a site of autophosphorylation.³¹ For OCI-Ly7, aliquots from separate cultures of stably-growing unmodified and BCR-KO cells were mixed; for OCI-Ly8 and OCI-Ly19, cells were analyzed 5 days after electroporation to create BCR-KO cells (by IgH targeting), producing mixed cultures of unmodified (BCR-positive) and BCR KO cells. For each line, results for one of two similar replicates are displayed. Results show that p-Syk is reduced by BCR KO in all lines.

(B) In two of the GCB-DLBCL lines shown in (A), cells with fusion of cpVenus (cpV) to the 5' end of SYK were created by KI, then sorted by flow cytometry to purity for further culture. These cells then underwent targeting of cpV, for the purpose of creating SYK-KO cells, and the resulting mixed culture of unmodified (cpV-positive) and SYK-KO (cpV-negative) cells was assessed by flow cytometry, after fixation and permeabilization, for cpV expression, total SYK content and p-Syk as in (A). Results show that the reduction in p-Syk staining caused by SYK KO is roughly the same as is caused by BCR KO, shown in (A).

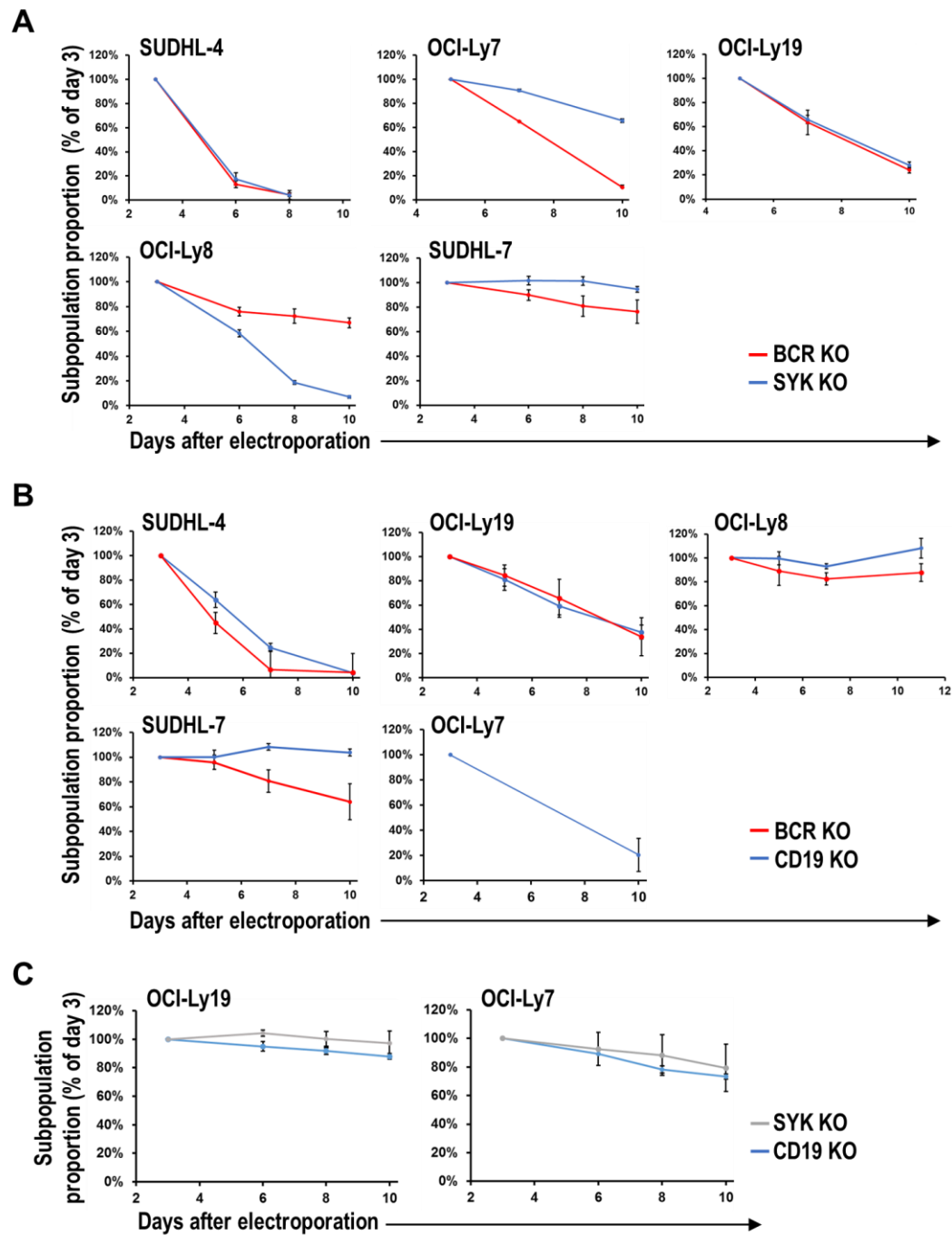


Figure S12. SYK and CD19 KO replicate growth-retarding effect of BCR KO in GCB-DLBCL lines

(A) Flow cytometry-determined proportions over time of cells with KO of SYK or BCR (by targeting IgH), normalized to their initial values 3 days post-electroporation. Cells with SYK KO were determined by staining after fixation and permeabilization. Mean \pm s.d. from 3 biological replicates, each with a different gRNA, is displayed.

(B) Flow cytometry-determined proportions over time of cells with KO of CD19 or BCR (by targeting IgH), normalized to their initial values 3 days post-electroporation. Decrease in proportion of CD19-KO cells in the OCI-Ly7 cell line is similar to the effect of BCR KO in previous experiments (decrease to 10-20% on day 10 post-electroporation). Mean \pm s.d. from 3 biological replicates (each with a different gRNA) is displayed.

(C) Flow cytometry-determined proportions over time of cells with KO of SYK or CD19, in 2 GCB-DLBCL lines which previously underwent sequential PTEN KO/GFP KI and BCR KO and were sorted to purity each time. Proportions are normalized to their initial values 3 days post-electroporation. Mean \pm s.d. from 3 biological replicates (each with a different gRNA) is displayed.

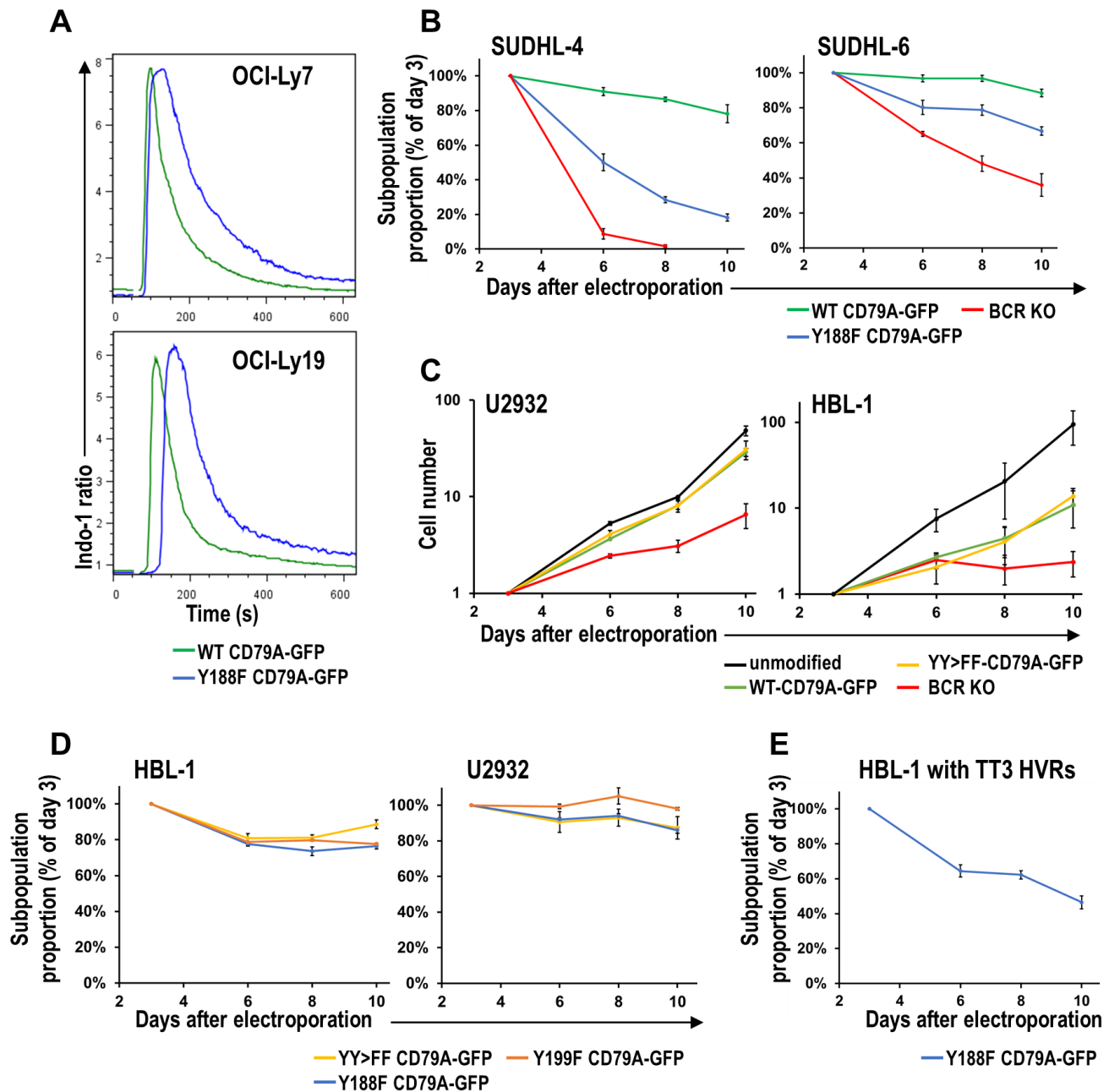


Figure S13. Effect of CD79A ITAM tyrosine mutations on DLBCL lines

(A) Calcium flux in response to BCR crosslinking with anti-IgM in CD79A-GFP knock-in cells is slightly prolonged by Y188F mutation in OCI-Ly7 and OCI-Ly19 GCB-DLBCL lines.

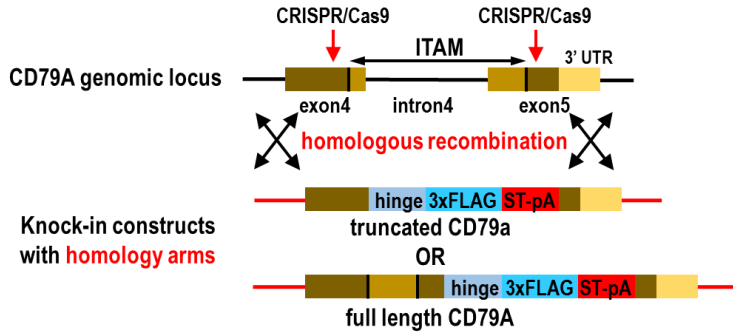
(B) Proportions of SUDHL-4 and SUDHL-6 cells modified by BCR KO or CD79A-GFP KI, relative to unmodified cells in the same cultures, at time points after electroporation. The results show a marked growth-inhibitory effect of the Y188F CD79A mutation. Relative decline with WT CD79A-GFP is attributed to subnormal BCR levels (which are the same as with Y188F CD79A-GFP; data not shown) in these highly BCR-dependent lines. Mean \pm s.d. from 3 biological replicates is displayed.

(C) Absolute growth curves for U2932 and HBL-1 ABC-DLBCL lines after BCR KO or CD79A-GFP knock-in (WT or ITAM YY>FF). In both lines, there is essentially no difference in growth between the two types of CD79A-GFP KI cells. Mean \pm s.d. from 3 biological replicates is displayed.

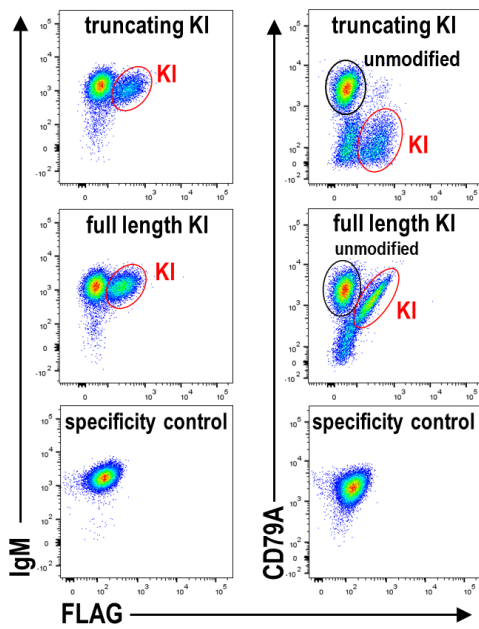
(D) Proportions of HBL-1 and U2932 cells modified by mutant CD79A-GFP KI, relative to unmodified cells in the same culture, and further normalized to the relative proportion of WT CD79A-GFP KI cells in a parallel culture. There is no significant effect of any mutation to Tyr residues in the CD79A ITAM. Mean \pm s.d. from 3 biological replicates is displayed.

(E) HBL-1 cells, previously modified by KI of an HVR (TT3) specific for tetanus toxoid, were further modified by KI of CD79A-GFP. Shown is the proportion of Y188F mutant cells, relative to unmodified cells in the same culture, and further normalized to the relative proportion of WT CD79A-GFP KI cells in a parallel culture. Mean \pm s.d. from 3 biological replicates is displayed.

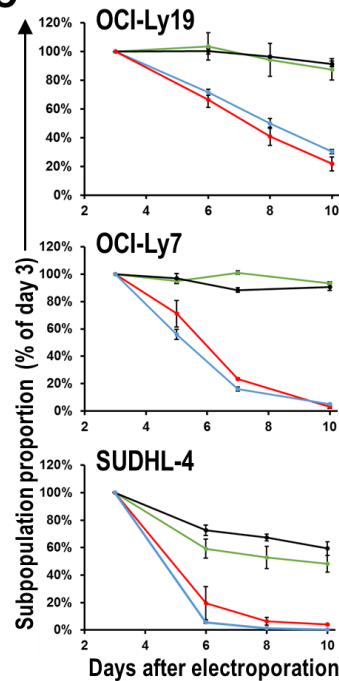
A



B



C



D

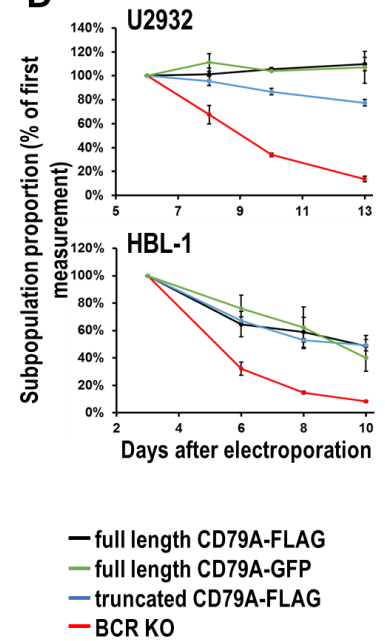


Figure S14. Effect of CD79A truncation on growth of DLBCL lines

(A) Schematic of knock-in approach to fuse 3xFLAG to the 3' end of full-length or truncated CD79A.

(B) BCR surface levels vs. intracellular staining for FLAG or CD79A (using an antibody recognizing the cytoplasmic terminal portion of CD79A) of OCI-Ly7 cells 5 days post-electroporation to KI CD79A-FLAG constructs. Absence of CD79A staining in FLAG-positive cells confirms truncation. No FLAG-positive cells were detected when non-specific gRNA was used in combination with the full length CD79A-FLAG KI construct (bottom panels).

(C) Flow cytometry-determined proportions over time of cells with KI of full-length or truncating CD79A-FLAG constructs or BCR KO (by targeting IgH), normalized to their initial values 3 days post-electroporation in 3 GCB-DLBCL cell lines, showing similar growth-retarding effects of CD79A truncation and BCR KO. Mean \pm s.d. from 3 biological replicates is displayed.

(D) Similar graphs as C for 2 ABC-DLBCL lines, showing no effect of CD79A truncation as compared to full length CD79A KI. Mean \pm s.d. from 3 biological replicates is displayed.

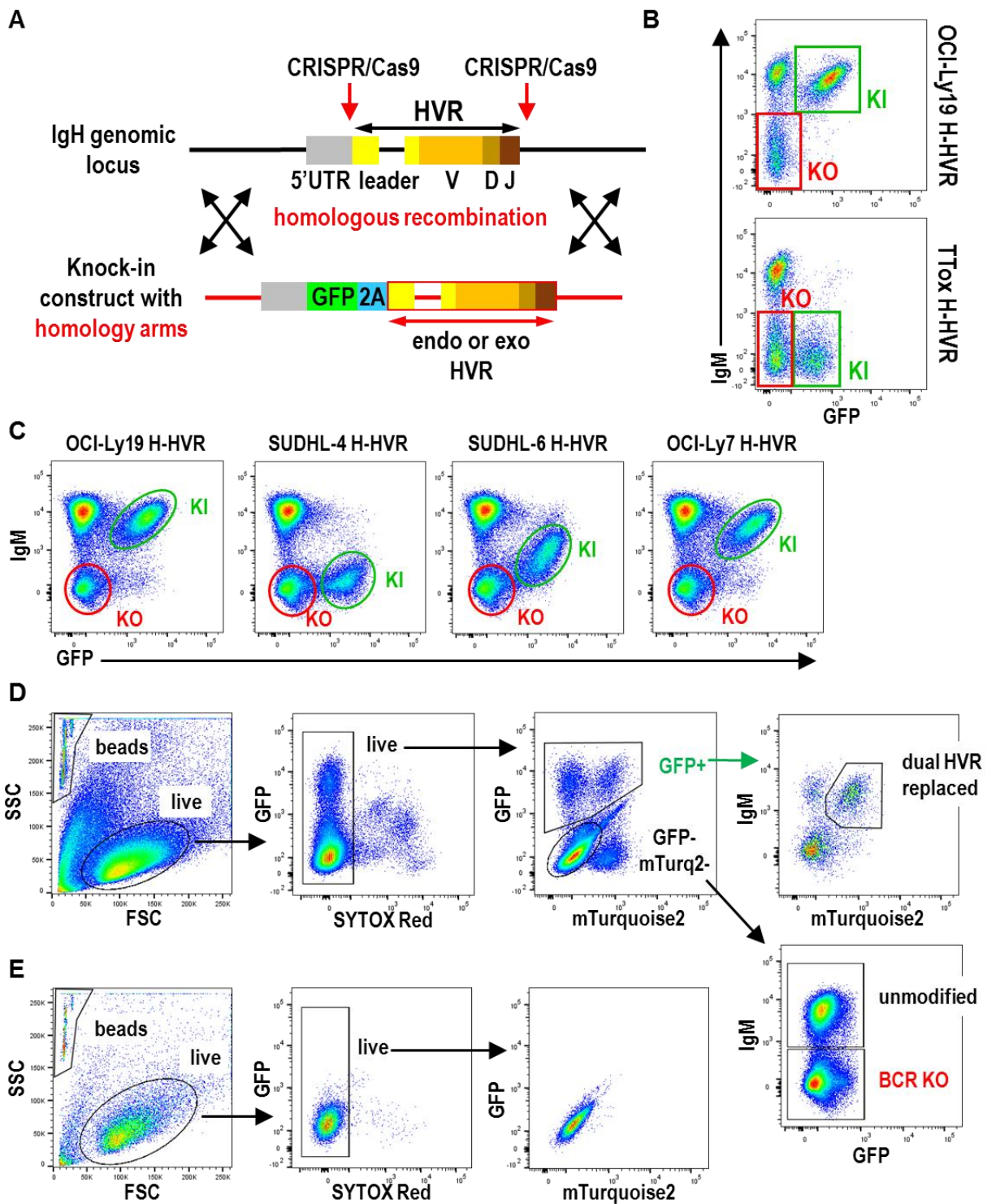


Figure S15. Design, gating strategy, and compatibility of HVR replacement

(A) Schematic for replacement of IgH HVR (H-HVR). GFP cDNA, knocked in at the start of IgH translation, is followed in frame by a 2A peptide sequence, which creates a break during translation. The post-break translated polypeptide resembles a normal IgH chain; beginning with an IgH leader sequence (signal peptide, spanning an intron) followed by an HVR, either endogenous (endo; i.e., the H-HVR of the cell line being targeted) or exogenous (exo, from another B cell), and is inserted into the plasma membrane and incorporated into a BCR complex, depending on compatibility with the IgL chain. The design for replacement of the IgL HVR is similar, but a CFP variant (mTurquoise2) is used rather than GFP, and there is no D segment.

(B) Levels of surface BCR and GFP (the marker of H-HVR replacement) of OCI-Ly19 cells 5 days post-electroporation. Knock-in of endogenous H-HVR (top) produces normal surface BCR levels in GFP-expressing cells, but exogenous TTox-reactive H-

HVR (bottom) produces low BCR levels in GFP-expressing cells. At lower left of both panels are cells that underwent simple BCR KO.

(C) Surface BCR and GFP levels of OCI-Ly19 cells 6 days post-electroporation with H-HVRs from other GCB-DLBCL lines. Endogenous H-HVR (left panel) again yields normal surface BCR levels in GFP-expressing cells. Exogenous H-HVR sequences (remaining panels) yield variably-subnormal surface BCR levels in GFP-expressing cells.

(D) Gating strategy to distinguish dual HVR-replaced, BCR-KO, and unmodified cells. Levels of GFP (marker for IgH HVR replacement), mTurquoise2 (marker for IgL HVR replacement), BCR (stained for IgM), and SYTOX Red (dead cell dye) are shown for SUDHL-6 cells 5 days post-electroporation.

(E) As a specificity control, SUDHL-6 cells were electroporated with the same IgH and IgL HVR replacement constructs as in (D), along with four Cas9/gRNA plasmids designed to target the IgH and IgL HVR regions of another cell line (SUDHL-4).

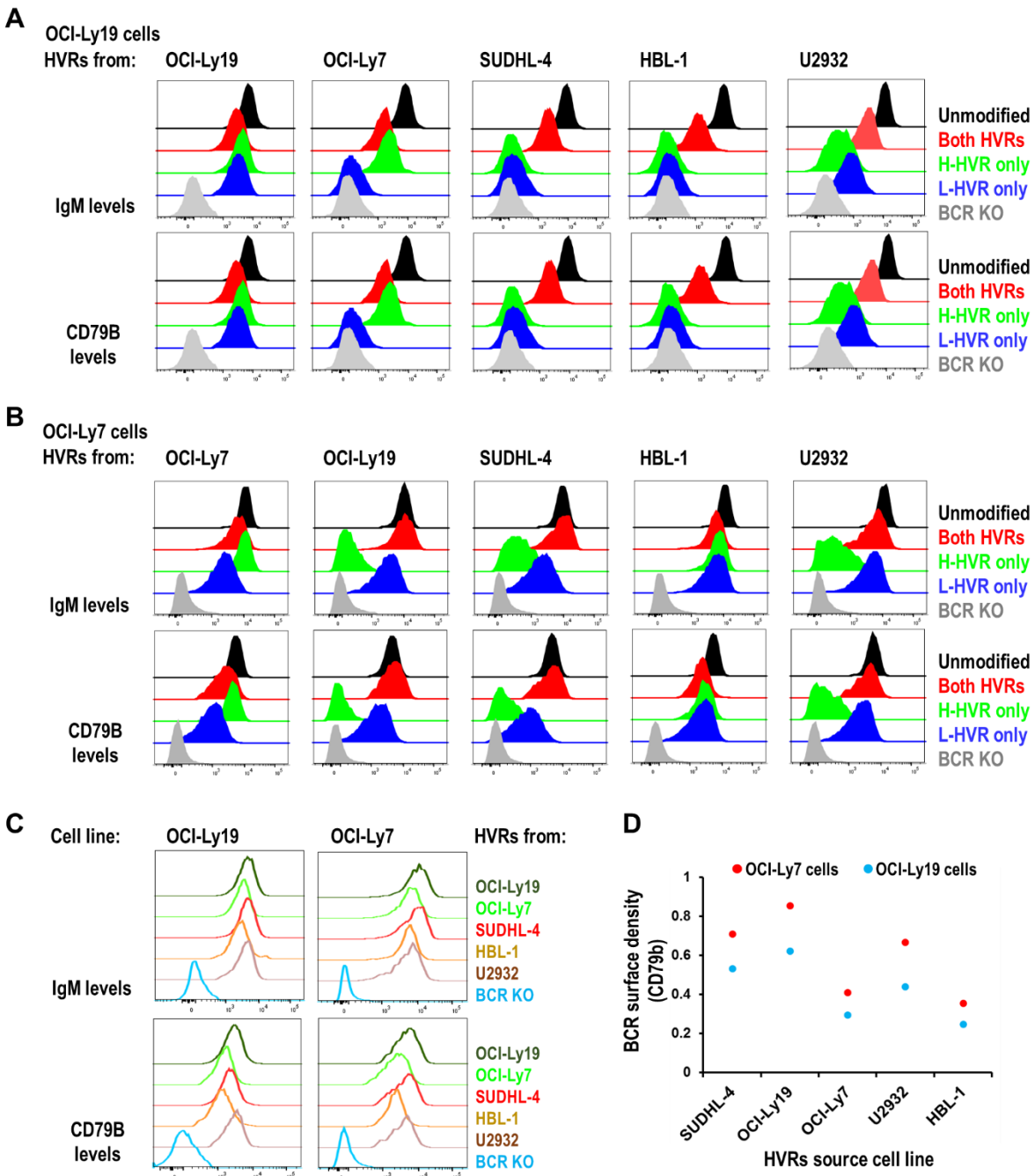


Figure S16. Surface BCR levels after single and dual HVR replacements in 2 GCB-DLBCL lines with HVR sequences from other DLBCL lines

(A) Histograms of surface IgM (top panels) and CD79B (bottom panels) levels in OCI-Ly19 cells 6 days after knock-in of HVR sequences (IgH, IgL, or both) or BCR KO (by targeting IgH). In each set of histograms, all donor HVR sequences come from the DLBCL line indicated, of GCB-DLBCL (OCI-Ly7, OCI-Ly19, and SUDHL-4) or ABC-DLBCL type (U2932 and HBL-1). Cells generating each histogram were identified as viable (by scatter properties and a dead-cell dye) and expressing the marker protein(s) specific for IgH (GFP) and/or IgL (mTurquoise2). Donor HVR sequences from OCI-Ly19 are free from incompatibility issues, as expected; the slightly lower BCR levels (as compared to unmodified OCI-Ly19 cells) are attributed to adding a marker protein and 2A peptide sequence to the Ig transcripts.

(B) Similar to (A), but with OCI-Ly7 as the recipient line and analysis 4 days after knock-in of HVR sequences.

(C) Histograms of surface BCR levels (by anti IgM and CD79B) in OCI-Ly19 and OCI-Ly7 cells after knock-in of dual HVR sequences (IgH and IgL) from the DLBCL lines indicated; these data are a subset of data shown in (A) and (B).

(D) From the experimental data in c, average BCR surface density was calculated for each recipient GCB-DLBCL line (OCI-Ly7 or OCI-Ly19) modified by dual replacement with paired HVRs from a DLBCL cell line.

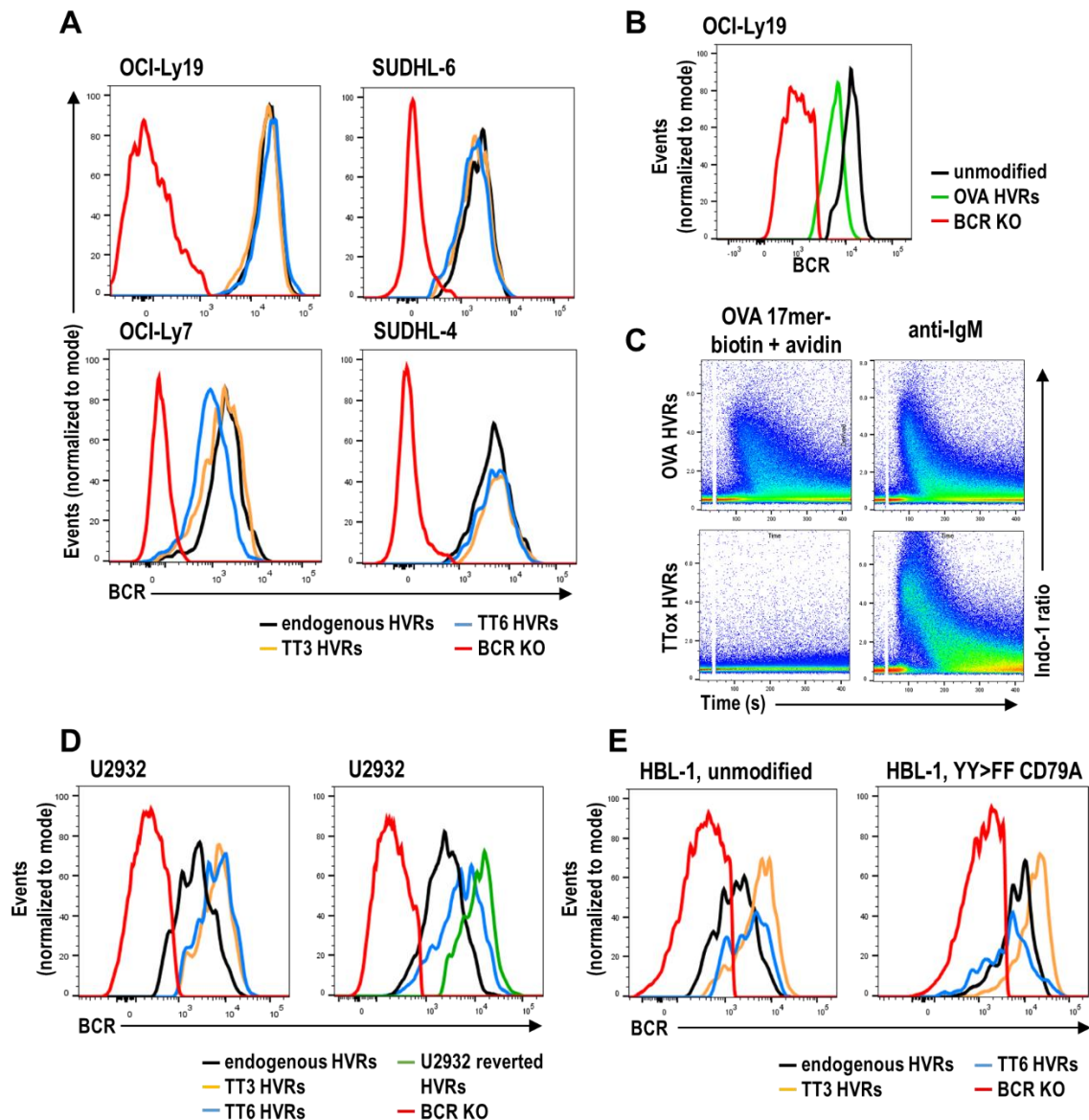


Figure S17. Surface BCR levels and functional response after dual HVR replacements in DLBCL lines

(A) Dual replacement with TTox-reactive HVRs in 4 GCB-DLBCL lines, whose effect on absolute growth curves are shown in Figure 6B. BCRs were expressed at levels similar to those of endogenous HVRs. Results were obtained post-electroporation for OCI-Ly19 (day 7), SUDHL-6 (day 5), OCI-Ly7 (day 6), and SUDHL-4 (day 6).

(B) BCR levels of OCI-Ly19 cells 3 days post-electroporation for dual HVR replacement with OVA-specific HVRs, in comparison to unmodified and BCR-KO cells from the same experiment.

(C) Calcium flux in response to BCR stimulation in OCI-Ly19 cells with OVA- or TTox-reactive HVRs. BCR crosslinking with anti-IgM triggers calcium flux for both HVR types, but only cells with OVA-specific HVRs respond to OVA-17mer-biotin complexed with avidin.

(D) Dual replacement with TTox-reactive HVRs and reverted endogenous U2932 HVRs in the U2932 cell line produced BCRs that were expressed at higher levels than endogenous HVRs. Effects of these HVRs on absolute growth are shown in Figure 6C. Results shown are from 5 days post-electroporation.

(E) Similar to (D), but with unmodified and YY>FF CD79A-GFP HBL-1 cells analyzed 3 days post-electroporation for dual HVR replacement. For the YY>FF CD79A-GFP HBL-1 cells, RFP was used as the marker for H-HVR replacement. The effects of these HVRs on absolute growth curves are shown in Figure 6D.

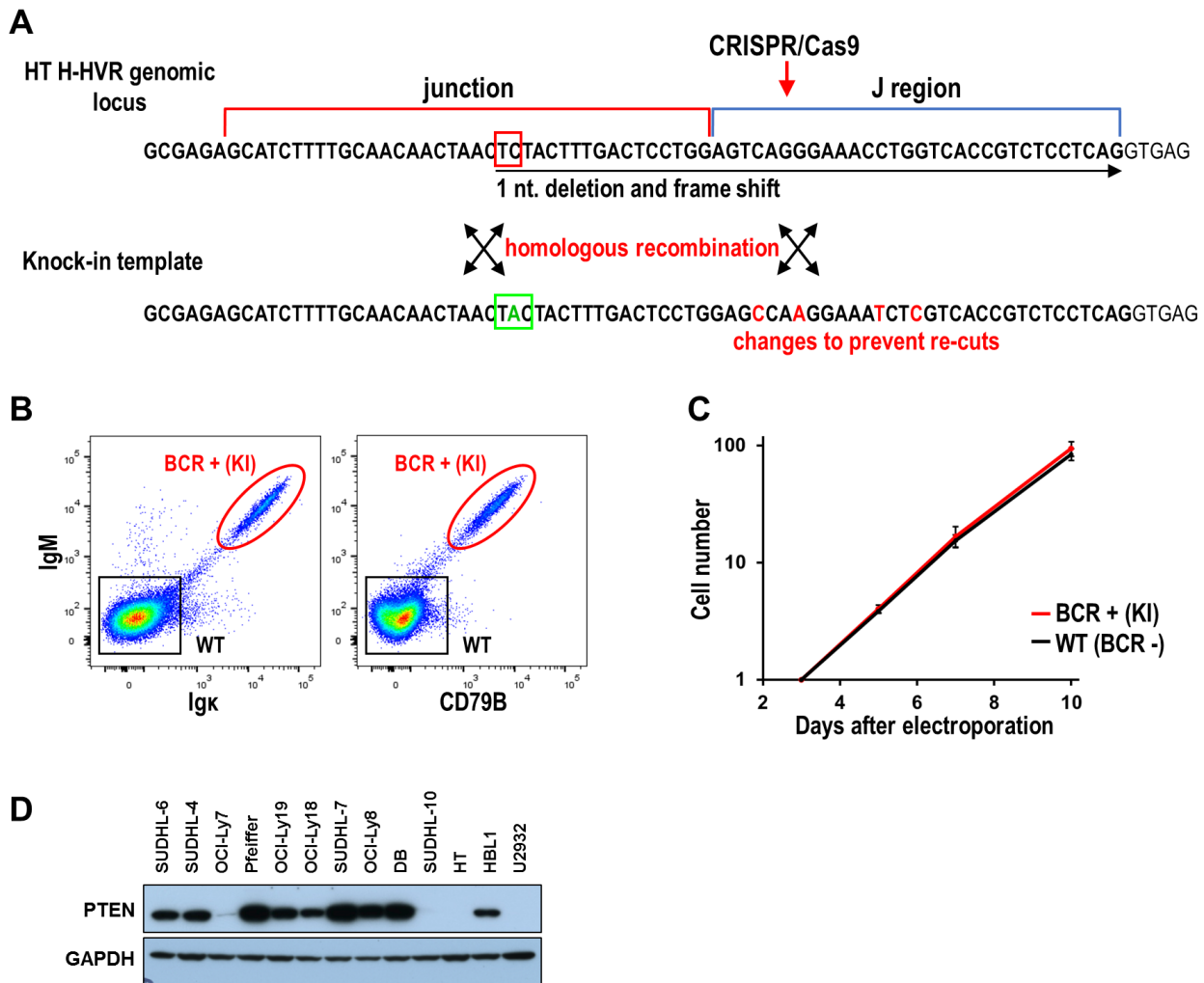


Figure S18. BCR re-expression in cell line HT, one of two naturally PTEN-deficient GCB-DLBCL lines studied

(A) Schematic of knock-in approach to repair the single nucleotide deletion in the HT H-HVR sequence. The presumed deficient codon in the genomic sequence is indicated by a red box, and the donor repair codon by a green box.

(B) Levels of IgM, Igk, and CD79B in HT cells 7 days post-electroporation to knock in the missing nucleotide; a population of cells has re-expressed BCR components on their cell surface.

(C) Similar rates of absolute growth curves for WT (BCR-negative) and re-expressed BCR-positive (KI) HT cells. Mean \pm s.d. from 3 biological replicates is displayed.

(D) Western blot for PTEN protein expression by DLBCL used in this study, showing loss in SUDHL-10, HT, and U2932.

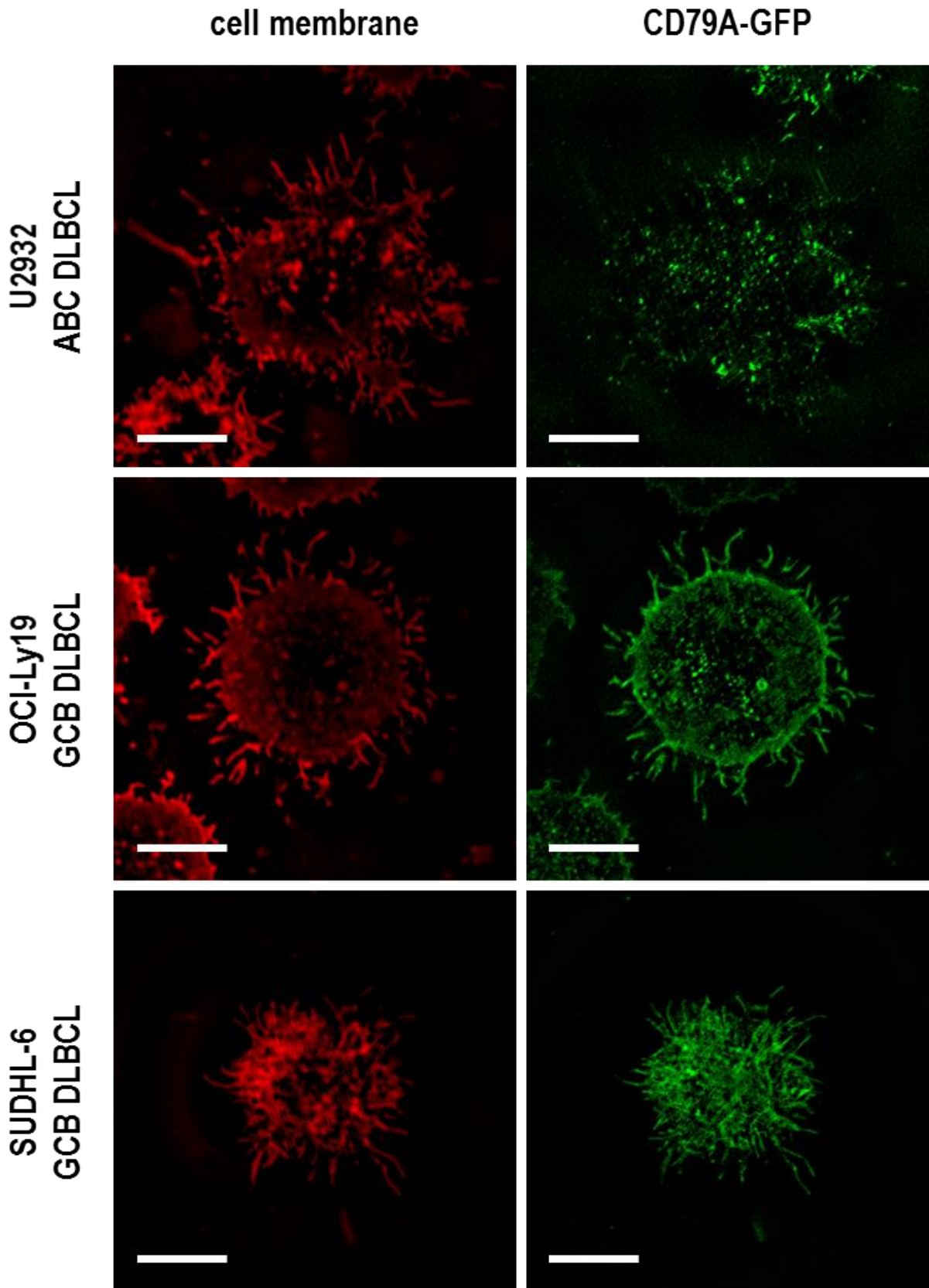


Figure S19. BCR surface distribution in DLBCL cell lines differs according to subtype

Super-resolution microscopy shows clustering of BCR units in the ABC-DLBCL line U2932, but diffuse distribution in the GCB-DLBCL lines OCI-Ly19 and SUDHL-6. BCR units were labeled by knock-in fusion of GFP to CD79A. Red CellMask dye marks the surface membrane. Live cells were imaged at the point of contact with glass coverslip chamber slides (bars = 5 μ m).

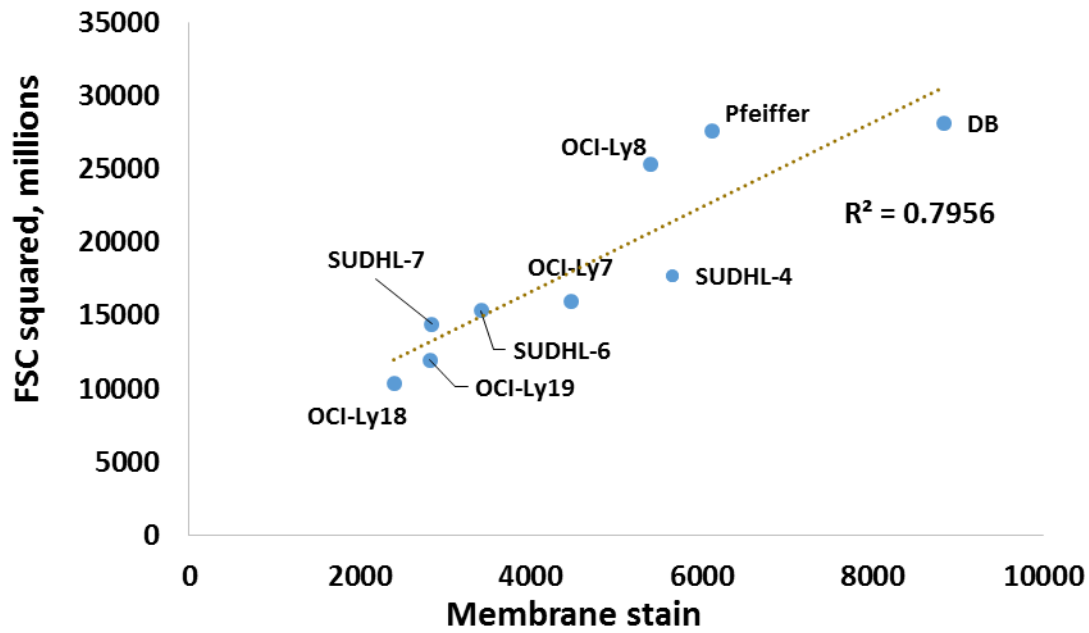


Figure S20. Correlation between squared FSC value and cell membrane content

Squared FSC value and cell membrane content (determined by fluorescence after staining with CellMask™ Deep Red plasma membrane stain) of unmodified GCB-DLBCL lines. The correlation supports the use of the squared FSC value as a measure of cell surface area.

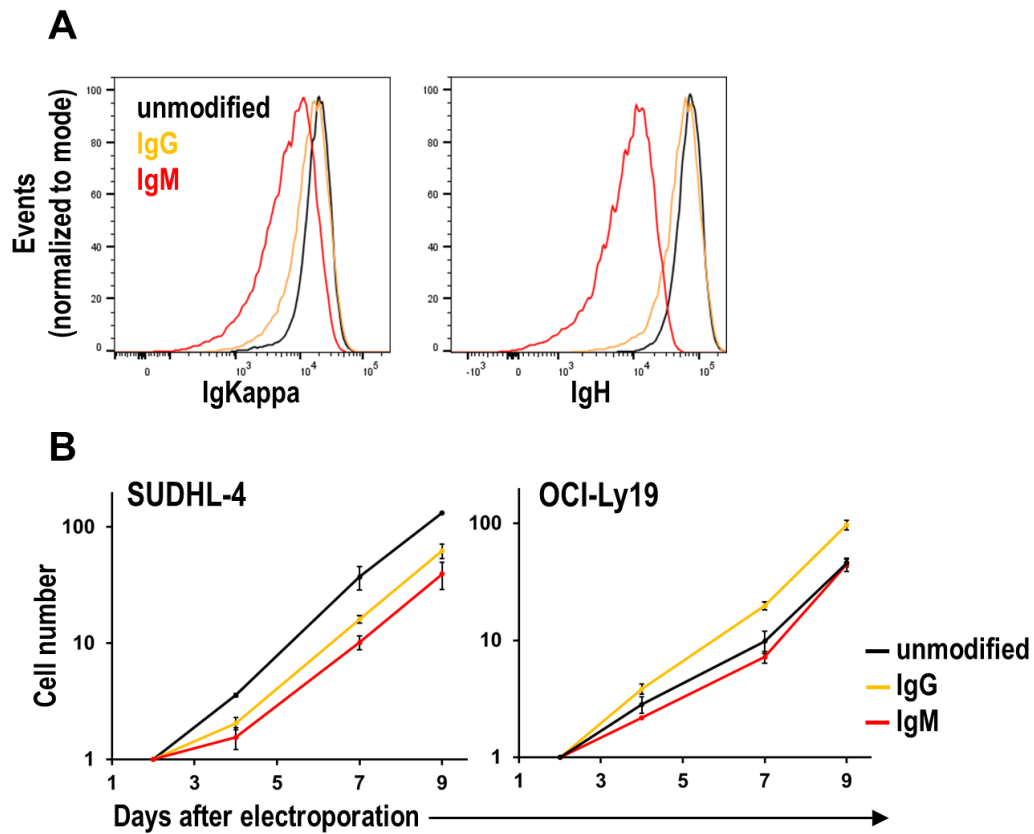


Figure S21. Effect of IgH isotype on surface BCR level and growth rates of GCB-DLBCL lines

(A) Surface BCR levels of SUDHL-4 cells, stained for either IgL kappa or the expressed IgH isotype: unmodified (WT, naturally IgG4), or with maximal expression of inducible IgG4 or IgM at a high concentration of doxycycline (200 ng/mL). IgL kappa staining between the two isotypes is more similar than results obtained with different IgH isotype-specific antibodies.

(B) Absolute growth rates of SUDHL-4 and OCI-Ly19 cells: unmodified (WT), or with maximal expression of inducible IgG4 or IgM. Cell number is normalized to its value 2 days after induction. Mean \pm s.d. from 3 biological replicates is displayed.

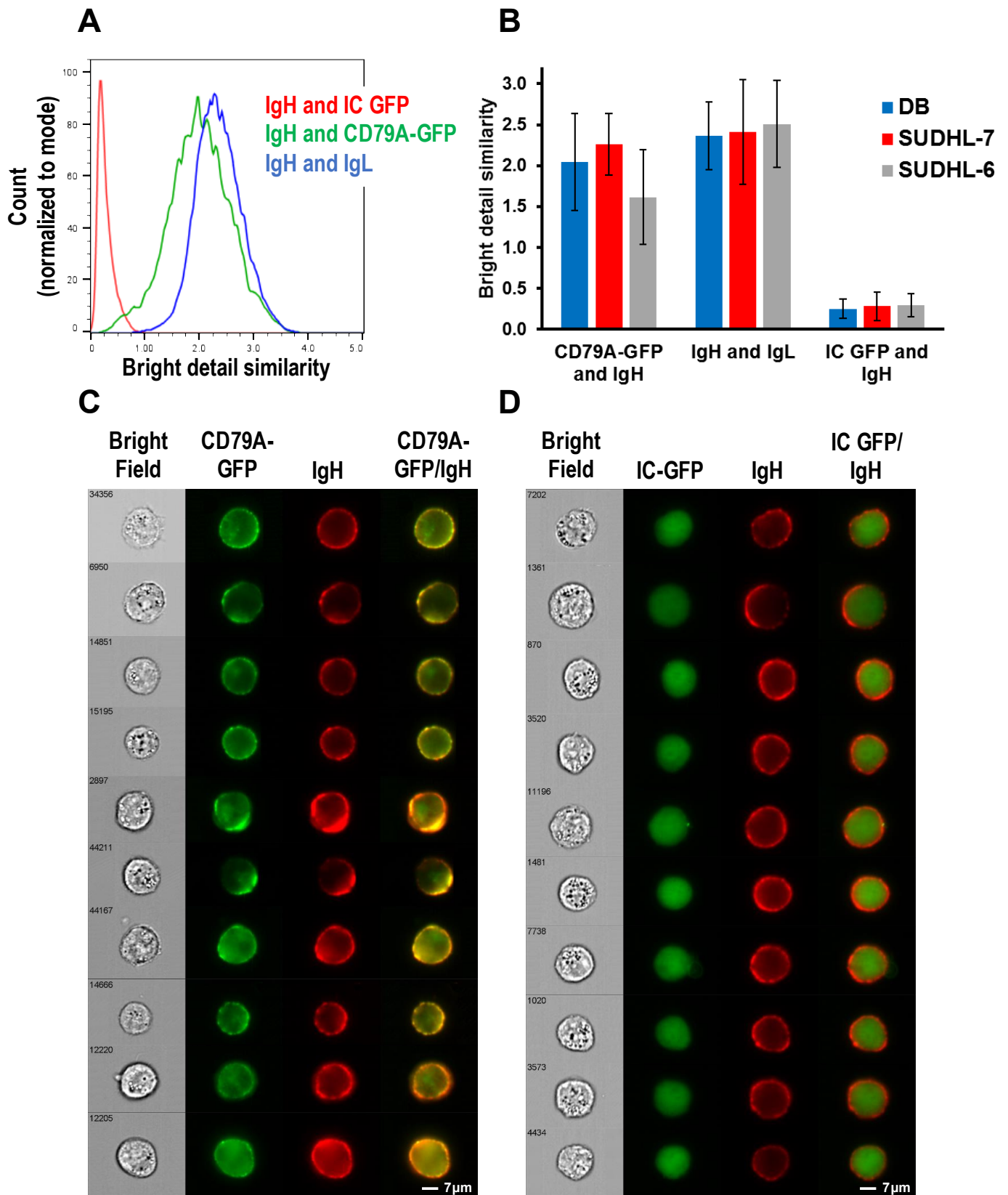


Figure S22. Image cytometry shows predominant colocalization of CD79A-GFP with surface IgH

(A) The similarity bright detail score (SBDS)¹⁵ was determined with the ImageStream imaging flow cytometer. Histograms of the SBDS for 3 types of cells of the GCB-DLBCL line are shown overlaid: cells modified (only) by CD79A-GFP knock-in and stained with APC-labeled anti-IgH (green line); unmodified cells stained with FITC-labeled anti-IgH and APC-labeled anti-IgL, as an SBDS-high control (blue line); and cells expressing unfused (cytoplasmic) GFP and stained with APC-labeled anti-IgH, as

an SBDS-low control (red line). The histogram for CD79A-GFP cells is similar to the SBDS-high control histogram from IgH/IgL dual-stained cells, and very different from the SBDS-low control histogram from cells with cytoplasmic GFP, supporting predominant colocalization of CD79A-GFP with surface IgH.

(B) The median and MAD (median absolute deviation) were calculated from the SBDS histograms for 3 GCB-DLBCL lines, each analyzed by 3 types of cells as in A. Again, results support predominant colocalization of CD79A-GFP with surface IgH.

(C) Individual representative images of CD79A-GFP knock-in cells of the GCB-DLBCL line DB, stained with APC-labeled anti-IgH. The predominantly yellow color of the overlaid GFP and IgH images (rightmost column) supports colocalization of CD79A-GFP with surface IgH.

(D) Individual representative images of cells of the GCB-DLBCL line DB expressing unfused (cytoplasmic) GFP, stained with APC-labeled anti-IgH. The overlaid GFP and IgH images (rightmost column) show an absence of colocalization.

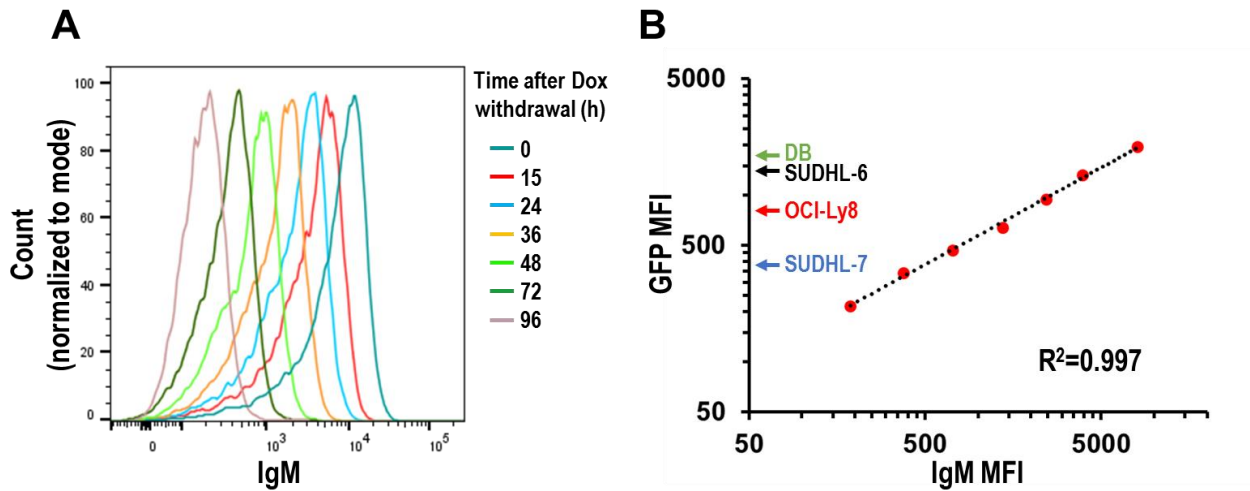


Figure S23. Correlation of BCR surface level and CD79A-GFP fluorescence in cells with inducible IgH expression

(A) Surface BCR level, detected by flow cytometry with anti-IgM, in OCI-Ly19 cells with inducible IgM expression (and stable KI of WT CD79A-GFP) at different time points after withdrawal of doxycycline.

(B) Correlation between BCR surface level and CD79A-GFP fluorescence after doxycycline withdrawal in OCI-Ly19 cells with inducible IgM and stable KI of WT CD79A-GFP. Arrows on the Y-axis indicate “natural” levels of GFP fluorescence in otherwise-unmodified CD79A-GFP versions of 4 GCB-DLBCL lines with intermediate to low levels of BCR surface density as measured by CD79A-GFP

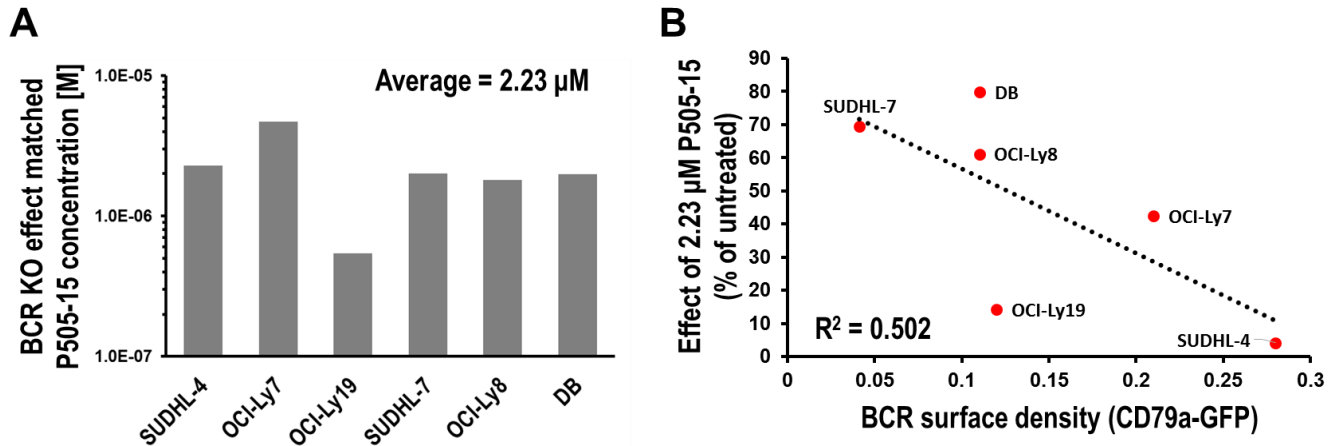


Figure S24. Correlations of BCR surface density with sensitivity of GCB-DLBCL lines to BCR KO or SYK inhibitor P505-15

(A) Comparison of the concentration of SYK inhibitor P505-15 in various GCB-DLBCL lines at which the relative reduction in the number of viable cells after 4 days' incubation is the same as the reduction produced by BCR KO. The latter was calculated from absolute growth curves of unmodified and BCR-KO cells, from which "relative proliferation" was also calculated; then, this value for %reduction value after 4 days of BCR KO was used to interpolate the P505-15 concentration from the dose-response curves of 4-day P505-15 treatment. The general similarity of this "BCR-inhibitory" concentration of P505-15 in different GCB-DLBCL lines is consistent with the effect of this SYK inhibitor at lower doses being specifically determined by its interruption of tonic BCR signaling and AKT activity.

(B) BCR surface density in GCB-DLBCL lines, based on CD79A-GFP fluorescence, correlated with calculated relative reduction in cell number after 4 days of treatment with the average BCR-inhibitory concentration of P505-15 (2.23 μ M), calculated from (A).

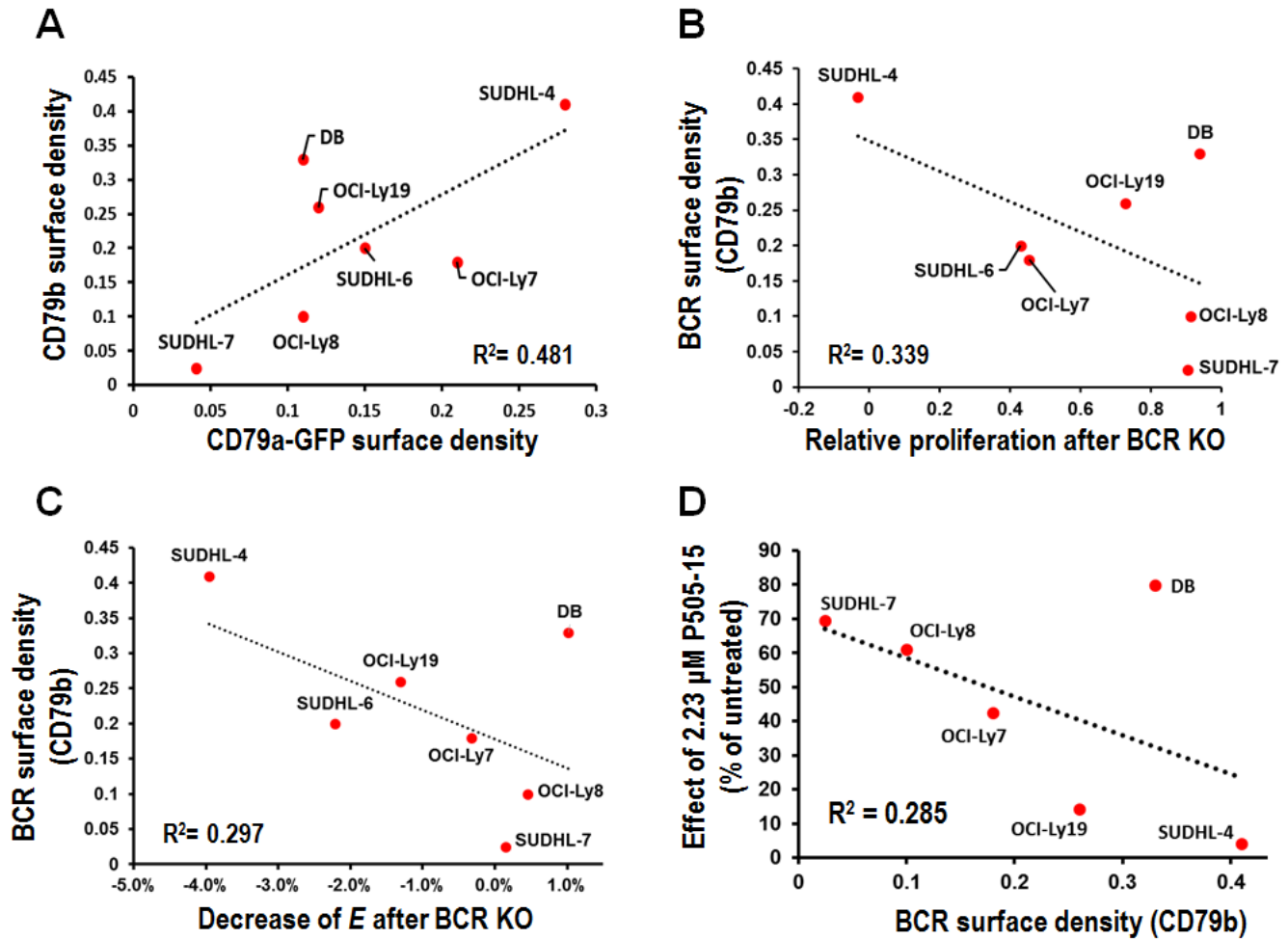


Figure S25. BCR surface density based on surface CD79B staining shows non-uniform correlation with other measures

(A) Correlation between BCR surface densities based on surface CD79B staining and CD79A-GFP fluorescence, across a spectrum of GCB-DLBCL lines. IgG-expressing line DB is an outlier.

(B) Correlation between surface CD79B-based BCR surface density and effect of BCR KO on proliferation in GCB-DLBCL lines.

(C) Correlation between BCR surface density based on CD79B staining and BCR KO-induced reduction in AKT activity, as measured by percentage decrease of E, FRET efficiency, determined by flow cytometry in 3 biological replicates (each with a different gRNA).

(D) Correlation between surface CD79B-based BCR surface density and sensitivity to a “BCR-inhibitory” concentration of P505-15 (see Figure S24).

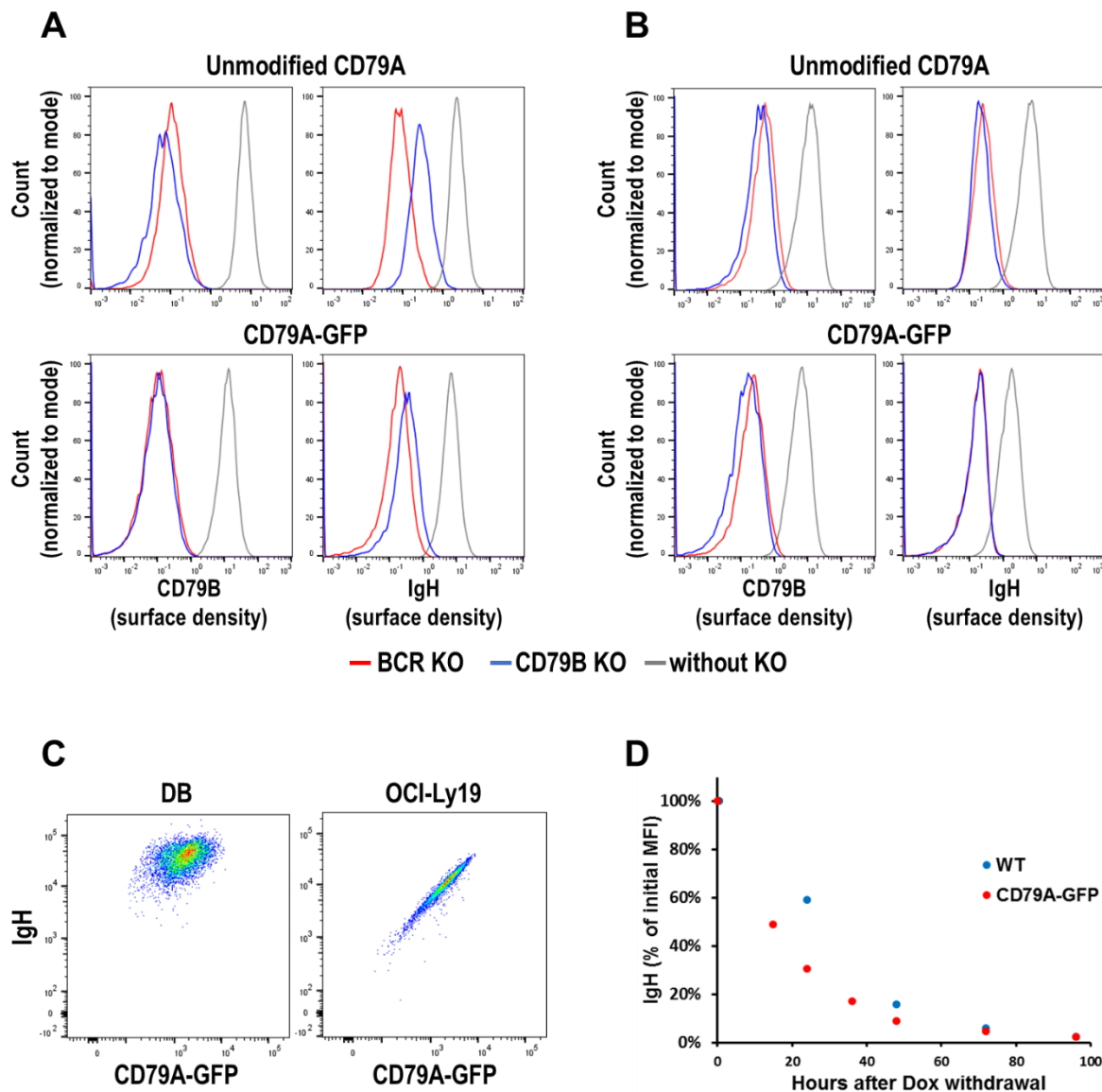


Figure S26. Effect of CD79A-GFP on surface expression of BCR components by GCB-DLBCL lines

(A) The surface expression of BCR components CD79B (left panels) and IgH (right panels), normalized to per-cell squared FSC values to yield surface density, were examined without (gray) or with KO of CD79B (blue) or IgH (red) in cell line DB that was either otherwise-unmodified (top panels) or had undergone knock-in to fuse GFP to unmutated CD79A (bottom panels). CD79A-GFP fusion eliminates residual surface CD79B that is still present after IgH KO in otherwise-unmodified cells (left panels), and reduces residual surface IgH that is still present after CD79B KO (right panels).

(B) Results of an experiment identical to the one shown in (A), except that it was performed in the cell line SUDHL-6. There is no difference between unmodified and GFP-fused CD79A in the amount of residual surface CD79B still present after IgH KO, and there is no residual surface IgH present after CD79B KO.

(C) Two-parameter dot plot of IgH surface staining vs. CD79A-GFP fluorescence in cells that had undergone knock-in to fuse GFP to unmutated CD79A. Whereas the OCI-Ly19 cell line (right) shows very tight correlation between per-cell levels of surface IgH and CD79A-GFP, representative of most GCB-DLBCL lines, cell line DB (left) displays a “cloud” of less-correlated values. Since IgH and CD79A-GFP are translated from independent gene loci in both cell lines, this suggests highly-coordinated post-translational regulation of amounts of these proteins in OCI-Ly19, but some degree of independence in DB.

(D) Time course of disappearance of surface IgH after doxycycline (Dox) withdrawal from OCI-Ly19 cells with Dox-inducible IgH, either without CD79A modification (blue, as used in Figure 6) or that had undergone knock-in to fuse GFP to unmutated CD79A (red, as used in Supplementary Figure S23). Disappearance is more rapid in cells with CD79A-GFP fusion.

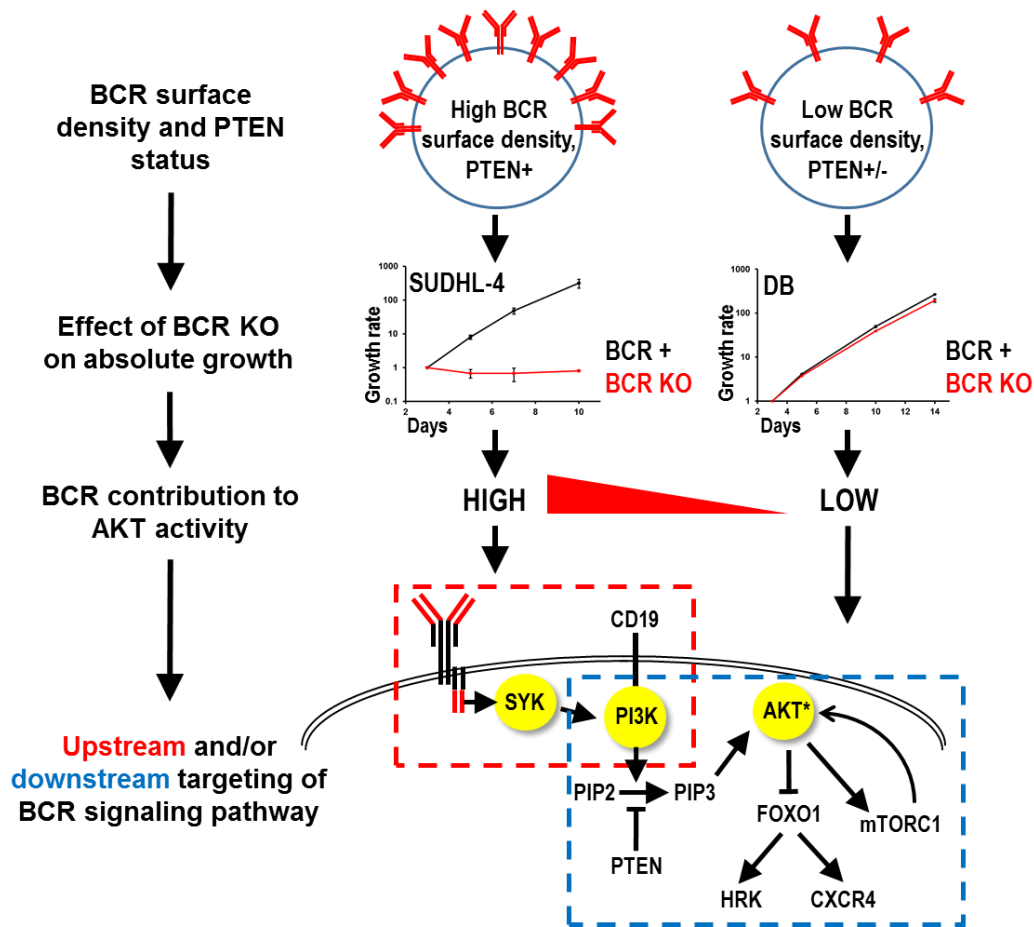


Figure S27. Potential biomarker-guided strategy for targeted therapy of GCB-DLBCL

The schematic illustrates implications of findings from studies of GCB-DLBCL lines. If primary GCB-DLBCL tumors similarly utilize tonic BCR signaling to activate AKT, patients with higher surface BCR density may be more likely to respond to inhibitors of tonic BCR signaling at upstream points. PTEN deficiency may be a biomarker indicating low likelihood of responding to upstream inhibitors of tonic BCR signaling. Downstream inhibition of AKT may synergize with upstream inhibitors and be more widely effective in GCB-DLBCL.

SEQUENCES

Sequences of BCR hypervariable regions of individual cell lines as sequenced from gDNA

Exons are highlighted in bold, all other characteristics of hypervariable regions are marked as follows:

Translation initiation

Splice donor/acceptor sites

First amino-acid of mature peptide

Junction

J region

HBL-1 H-HVR

IGHV4-34, D3-10, J4

ACCAGTCTCCTTCAGCACATTTCTACCTGGAAGAAGAGGACTCTGGGTTTGGTGAGGGGAGGCCACAGGAAGAGAAGCTG
 AGTTCTCAGAGGGCACAGCCAGCATAACCTCCCAGGGTGAGCCAAAAGACTGGGGCCTCCCTCATCCCTTTTTACCT
 ATCCATACAAAGGCACCACCCACATGCAAATCCTCACTTAGGCACCCACAGGAAATGACTACACATTTCTTAAATTCA
 GGGTCCAGCTCACATGGGAAGTGC~~TTTCTGAGAGT~~CATGGACCTCCTGCACAAGAACATGAAACACCTGTGGTTCCTTC
 TCCTCCTGGTGGCAGCTCCCGGATGTGAGTGTCTCAGGAATGCGGATATGAAGATATGAGATGCTGCCTCTGATCCCAG
 GACTCACTGTGGGTTTCTCTGTTCCACAGGGTCCCTGTCCAGGTGCAGCTACAGCAGTGGGGCGCAGGACTGTTGAAGC
 CTTCCGAGACCTGTCCCTCACTTGCCTGTCTATGGTGGGTCTTCAGTGATTACTACTGGACCTGGATCCGTCAGTC
 CCCAGGAAAGGGGCTGGAGTGGATTGGGGAAATCAATCGTAGTGGAAGTACCGACTACAACCCGTCCCTCAAGAGTCGA
 GTCACCATATCACTAGACACGTCCAAGAACCAATTCTCCCTGCATCTGACCTCTGTGACCCGCCGGACACGGCTCTAT
 ATTACTGTGCGGGGGACAAGACTACGGTACTATGTTAGGGGGGGTAGTGACTACTGGGGCCAGGGAACCTGGTCCAC
 CGTCTCCTCAGGTGAGTCCACACAGTCTCTCCTGGTTAACTCTGAAGGGTTTTATTGTATTATTGGGGGAAGTTC
 GGGTGTGGGTCTCCTGCCAGGAGAACCCCGGAGCAGTCTGGGTGACTCAAGAGGATGCCCTGAGGCAACCCGACCCAC
 ACAGACGAGGGCAAGGGCTCCAGATGTTCTCTCCTGAGCCCAACAATACTAATCTCTGTGGCCAGGGCCACCC
 TAGGCCTCTGGGGTCCAATGCCGACAATCCCCGGGCCCTCCCC

HBL-1 L-HVR

IGKV3-20, J3

AGGAAAGATCACTAACAAGTAAATACAAGTATATCCGGAGAATAAAGTTGTAATAGACTCTTCCTTTCAACCTGATCCA
 TCATGCATTTAGGGAGCTGACTGGGCACAAGTTGGAGCAGAAAGAGAAAAATGAAACCACAGCCTTCTATTTTGTCTTCT
 AACAGACTTGTACCAAACATTCTGTGGCTCAATCTAGGTGATGGTGAGACAAGAGGACACAGGGGTTAAATTTCTGTGGC
 CGCAGGGGAGAAGTTCTACCCTCAGACTGAGCCAACGGCCTTTTCTGGCCTGATCACCTGGGCATGGGCTGCTGAGAGC
 AGAAAGGGGAGGCAGATTGTCTCTGCAGCTGCAAGCCCAGCACCCGCCAGCTGCTTTGCATGTCCCTCCAGCCGCC
 CTGCAGTCCAGAGCCCATATCAATGCCTGGGTGAGAGCTCTGGAGAAGAGCTGCTCAGTTAGGACCCAGAGGGAACCAT
 GGAAACCCAGCGCAGCTTCTCTTCTCCTGCTACTCTGGCTCCAGGTGAGGGGAACATGGGATGGTTTTGCATGTCA
 GTGAAAACCCCTCTCAAGTCTGTACCTGGCAACTCTGCTCAGTCAATAACAATAAAGCTCTGTATAAAGCAATAA
 TTCTGGCTCTTCTGGGAAGACAATGGGTTTGATTTAGATTACATGGGTGACTTTTCTGTTTTATTTCCAATCTCAGATA
 CCACCGGAGAAATGTGTTGACGCAGTCTCCAGGCACCCTGTCTTTGTCTCCAGGGGAAAGAGCCACCCTCTCCTGCAG
 GGCCAGTCAGAGTATTAGCAGCAACTACTTAGCCTGGTTCAGCTGAAAGGTGGCCAGGCTCCAGGCTCCTCATCTTT
 GGTGCATCCAACAGGGCCACTGGCATCCAGACAGGTTGAGTGGCAGTGGGTCTGGGACAGACTTCACTCTCACCATCA
 GCAGACTGGAGCCTGAAGATTTTGCAGTGTATTACTGTGAGCAGTATGGTAGCTCACCGATCACTTTCCGGCCCTGGGAC
 CAAAGTGGATATCAAACGTAAAGTACATCTGTCTCAATTATTCGTGAGATTTTAGTGCCATTGGATCATTTGTGCAAATT
 TTGTGATATTTTGGTTGAATAAACCTGGTGACCCAGAAGTAAATAGCAGGACACCAGAAAATGAACTTAAAAATCTGAG
 CAAATAGACGAATCATTGGGTTTGGAGAGGAGAATAGGATTCATGGGGGAAATGGGGAAGAAAATAGCTAGATTTTCTCT
 GAACAAGCAGCCTATCTCGTATGATTGGCTTCAAGAGAAGTTTTTGTGAGGGGAAAGGGTGAGATCCCTCACTGTGAC
 TCACTTTCGGCGGAGGGACCAAGGTGGAGATCAAACATAAGTGCACTTTCTAATGCTTTTTCTTATAAGGTTTTAAAT
 TTGGAGCATTTTTGTGTTTGGAGATATTAGCTCAGGTCAATTCCAAAGAGTACCAGATTCCTTCAAAGAGTCAAGATTTT
 AAGGGATAGAAAATTAGTTCATCTTAAGGAACAGCCAAGCGCTAGCCAGTTAAGTGGGATCTCAATTGCAAGATTTT
 GTCTGCATCGGTGAGTTAGTGAGATTAACAGCGAAAAGAGATTTTTGTTAAGGGGAAAGTAATTAAGTTAACACTGTG
 GATCACCTTCGGCCAAGGGACACGACTGGAAATTAACGTAAGTAATTTTTCACTACTGTCTTCTGAAATTTGGGTCTG
 ATGGCCAGTATTGAGTTTTAGAGGCTTAAATAGGAGTTTGGTGAAGATTGGTAAATGAGGGCATTAAAGATTTGCCATG
 GGTGCAAAAAGTTAAACTCAGCTTCAAAAATGGATTTGGAGAAAAAAGATTAAAGT

HT H-HVR

IGHV3-53, D5-24, J4

CTGCCTCCTCCAGTGGTTAGAGCACAGGCCAGGTAATAGGACTCATTTTTTTTAGATGTGTAATTTTTAGACACACTGCA
 CAACTGCTGTGTTCTCTGTGCAAATTATCTCCTGTAAAATGTAACATTGAAACCTGCCTTAAATATATTGTGTAATAT
 GTAAAAATAAAATCAGATTGTGAGAGCTAAATGCTAATCAAGGCGCAATCACGTAATATAACAATTATATTTTCTGAAT
 GATGGAATTAATACCAATCTCCCCAGGACACTTCATCTGCACGGAGCCCGCCTCTCCTCAGATGTCCACCCAGAG
 CTTGCTATATAGTCGGGGACATGCAAATAGGGCCCTCCCTCTGCTGATGAAAACCAGCCCAGCTGACCCTGCAGCTCTG
 GGAGAGGAGCCAGCAGTGGGATTCCGAGGTGTTTCATTGATGATCAGCACTGAACACAGAGGACTCACCATGGAGT
 TTTGGCTGAGCTGGGTTTTCTTGTGCTTTTTCAAAGGTAAATTCATGGAGAAGTACGAGAAATCGAGTGTGAGTGGAC
 ACGAGTGAGAGAAACAGTGGATATGTGTGGCTCTTTCTAACCAATGTCTCTGTGTTTGCAGGTGTCCAGTCTGGGTGC
 AGTTGGTGGAGACTGGAGGAGGCTTGTTCAGCCGGGGGAGTCCCTGAGACTCTCCTGTGCAACCTCTGACTTCACCGT
 CAGTAACAACACTACATGGCCTGGGTCCGCCAGGCTCCAGGGAAGGACTGAATTGGGTCTCACTTATCTCTGCCGTGGT
 GTCACATTCTACGCAGACTCCGTGAAGGGCCGATTCTCCATTTCCCGAGACAACCTCCAAGAACACACTATATCTTCAA
 TGACCAGCCTGAGAGCCGAGGACACGGCCATGTATTACTGTGCGAGAGCATCTTTTGAACAACCTAACCTACTTTGAC
 TCCTGGAGTCAGGGAACCTGGTCACCGTCTCCTCAGGTGAGTCTCAGAACCCTCTCTCGGGGTCTGCTTCTGAAGGAT
 ATTGCTACATTTTCGGGGAATAAAGGATGCTGGGTACCTGGCCAGACAGACGCGGACCACCCTGGGGGTCTCAGGA
 GGAGGCCCTGAGGCAACAGCGGCCGCACAGACGAGGTACAAGGACTCCAGATGTCCCTTCCCTCCAGAGCCCAAAACCAC
 GGGTCTCTCTGTGCCTAGGACCACCCTAGGCCTCTGGGGTCCAATGTCCCAAGTCCCGGGCCCTCCCCGGCCTCAGT
 CTAGAGGGTCCCAGGGACGTGGCGGGGCGCCCGTTCTTGCTGGGGTCTGGCACTATTGTTACATTGTGACAGCTGA
 TTCGACCCCTGGGGCCAGGGAACCCGGTGAGTCTCACCACCCCTCTCTGAGTCCACTTAGGGAGACTCAGGTTGCCA
 GGGTCTAGGGGTGAGAGTCTTGAGGCATTTTGGACGTGAGGAAAAAAGCTGGGGAGAGGGACCCTTCGAATGGGAAG
 TCGCCTGTCTCCCAAGTCCGCCACAGATGTCGGCAACTGGGGCCCTCCTTCGGCTGGTCTGGGGTGACCTCTCTC
 CGCTTACCTGGAGCATTCTCAGGGGTGTCGTGATGAGTGCAGGTCGACTCTGTCCCGCTCCAAGGCACCCGCTCT
 CTGGGACGGGTGCCCCCGGGGTTTTTGGACTCCTGGGGGTGACTGAGTAGCCGTCTGCTTGCAGTTGGACTTCCAGG
 CCGACAG

Note: **TC** - highlighted codon with deletion causing frame shift and premature termination of translation in HT cell line.

OCI-Ly7 H-HVR

IGHV1-69, D6-19, J4

CTCTCCATGGGTCTGCTGGACACTCATGTAGGGTAACGAGTGGCCACCTTTTTCAGTGTACCAGTGAGCTCTGAGTGT
 TCCTAATGGGACCAGGATGGGTCTAGGTGCTCAATGTCAGAGACAACAATGGTCCCACAAAAAACCAGGTAATC
 TTTAGGCCAATAAAATGTGGGTTCACAGTGAGGAGTGCATCCTGGGGTTGGGTTTTGTTCTGCAGCGGGAAGAGCGCTG
 TGCACAGAAAGCTTAGAAATGGGGCAAGAGATGCTTTTCTCAGGCAGGATTTAGGGCTTGGTCTCTCAGCATCCCACA
 CTTGTACAGCTGATGTGGCATCTGTGTTTTCTTCTCATCGTAGATCAGGCTTTGAGCTGTGAAATACCCTGCCTCATG
 CATATGCAAATAACCTGAGGTCTTCTGAGATAAATATAGATATATTGGTGCCTGAGAGCATCACATAACAACCACATT
 CCTCCTCTAAAGAAGCCCCTGGGAGCACAGCTCATCACCATGGACTGGACCTGGAGTTCTCTTTGTGGTGGCAGCAG
 CTACAGCTAAGGGGCTTCCCTAGTCCTAAGGCTGAGGAAGGGATCCTGGTTTAGTTAAAGAGGATTTTATTACCCCTGT
 GTCTCTCCACAGGTGTCCAGTCCAGGTACAGTTGGTGCAGTCTGGGGCTGAGGTGAAGAAGCCTGGGTCTCGGTGA
 ATGTCTCCTGCAAGACTTCTAGAGACACCTTCAGCAGCTATGCTATCAACTGGGTGCGACAGGCCCTGGACAAGGGTT
 TGAGTGGATGGGAGGGATCATCCCTATCGTTGGTACAGCAAACCTACACACAGAAGTTCAGGGCAGAGTCACGATTACC
 GCGGACGAATCCACGAGCACAACCTACATGGAACCTGAGCAGCCTGACATATGAAGACACGGCCGTTTATTACTGTGTGA
 CCGGCCCGGGGGGCTGTTTGGAGTGCATGGGGCCAGGGAATCCTGGTCAACGCTCTCCTCAGGTGAGTCTCATAATC
 TATCATAATGTAGGATTTTGGTGCCTTTTTGGGGGAAATAAAGGTCTGGGTCTCCTGCCAAGAAAGACCCGGAGCAG
 CCGGGGGGGGCTCAGGAGGATGCCCTGGGGCAACAGCGGACACGCAGACGAGGGTCAAGGGCTCCAGAAGCCCCTTCT
 CCTGAGGCCGACAGCGGGTCTCTCTGTGGCCAGGGCCACCCTAGGCCTCTGGGGTCCAATGCCAACAACCCCGGG
 CCTCCCCGGGTTCACTCTGAGAGGGTCCCAGGGACGTGGCGGGGCGCCAGTCTTGCCTGGGGTCTTGACATTGTTGT
 CACAATGTGACAACCTGGTTCGACCCCTGGGGCCAGGGAACCTGGTCAACGCTCTCCTCAGGTGAGTCTCACCACCCCT
 TCTGTGAGTCCACTTAGGGAGACTCAGCTTGCCAGGGTCTCAGGGTCAAGTCTTGGAGGCATTTTGGAGGTGAGGAAA
 GAAAGCGGGGAGAGGGACCCTTCGAATGGGAATTCAGCCTGTCTCCCCAAGTCCGGCCACAGACGTCCGCAGCTGGG
 GGGTCTCTTCGGCTGGTCTGGGGTGACCTCTCTCCGTTACCTGGAGCATCTCAGGGGCTGTCTGTCTGTCCCGCTCC
 AAGGCACCCGCTCTCTGGGACGGGTGCCCCCGGGGTTTTTGGACTCCGGGGGGTACTTAGCAGCCGTCTGCTTGCAA
 TTGGACTTCCCAGGCCGACAGTGGTCTGGCTCTGAGGGGTGAGGCCAGAATGTGGGGTCCGTGGGAGGCCAGCAGAGG
 CTTCATGAGAAGGACAGGACAGGGCCACGGACAGTCACTTCCATGTGACGCCCGGAGACAGAAGGTCTCTGGGTGGC
 TGGGTTTTTGTGGGGTGGAGGATGGACATTCTGCCATTGTGATTAATACTACTATTACGGTATGGACGTCTGGGGCCAA

GGGACCACGGTCACCGTCTCCTCAGGTAAGAATGGCCACTCTAGGGCCTTTGTTTTCTGCTACTGCCTGTGGGGTTTCT
 TGAGTATTGTAGGTTGGTCCCTCGGGGCATGTTCCGAGGGGACCTGGGCGGACTGGCCAGGAGGGGACGGGCACTGGGGT
 GCCTTGAGGATCTGGGAGCCTCTGTGGATTTTCCGATGCCTTTGGAAAATGGGACTCAGGTTGGGTGCGTCTGATGGAG
 TAACTGAGCCTGGGGGCTTGGGGAGCCACATTTGGACGAGATGCCTGAACAAACCAGGGGTCTTAGTGATGGCTGAGGA
 ATGTGTCTCAGGAGCGGTGTCTGTAGGACTGCAAGATCGCTGCACAGCAGCGAATCGTGAAAATATTTTCTTTAGAGTTA
 TGAGGTGCGCTGTGTGTCAACCTGCATCTTAAATTCTTTATTGGCTGGAAAGAGAAGTGTGCGGAGTGGGTGAATCCAGC
 CAGGAGGGACGCGTAGCCCCGGTCTTGATGAGAGCAGGGTTGGGGCAGGGGTAGCCCAGAAACGGTGGCTGCCGTCTC
 GACAGGGG

Ly7 L-HVR

IGKV4-1, J1

AATGTTGCTGAGCAGGCATTGAAGAGTATCGATAAAAATTTATTGAGAATTTGTTTATTATGATTAACAGAGGTAAAAGC
 CAGTATATTACTGATTAATATAGGTAAGGCGAGTTAAGAAAATGGGAATGCTTTCTCTTCTGCTTTCTTCTACGATGC
 ACAAGGCGTTTTACATTTATGCCCCTATGAAAATTACTAGGCTGTCCTAGTCATTAGATCTTTCAGCAGTTTGTAGTTT
 TAGAGCTTCTAAGTTGACTTCTGTCTTTTCTATTTCATACAATTACACATTCTGTGATGATATTTTGGCTCTTGATTTA
CATTGGGTACTTTACAAACCCTGCTCATGAAATTTGCTTTTGTACTACTGGTTGTTTTTGCATAGGCCCTCCAGG
CCACGACCAGCTGTTTGGATTTTATAAACGGGCCGTTTGCATTGTGAAGTACTGAGCTACAACAGGCAGGCAGGGGCAGCAA
GATGGTGTTCAGACCCAGGCTTTCATTTCTCTGTTGCTCTGGATCTCTGGTGAGGAATTA AAAAGTGCCACAGTCTTT
 TCAGAGTAATATCTGTGTAGAAAATAAAAAAATTAAGATATAGTTGGAAATAATGACTATTTCCAATATGGATCCAATT
 ATCTGCTGACTTATAATACTACTAGAAAGCAAATTTAAATGACATATTTCAATTATATGTGAGACAGCGTGTATAAGTT
 TATGTATAATCATTGTCCATTACTGACTACAGTGCCTACGGGGACATCGTGATGACCCAGTCTCCAGACTCCCTGGCT
GTGCTCTGGGCGAGAGGGCCACCATCAACTGCAAGTCCAGCCAGACTGTTTTATACGGCTCCAACAATAAAAACACTACT
TAGCTTGGTACCAACAGAAACCAGGACAGCCTCCTAAGTTGCTCATTTACTGGGCATCTACCCGGGAATCCGGGGTCCC
TGACCGATTAGTGGCAGCGGGTCTGGGACAGATTTAGTCTCACCATCAGCAGCCTGCAGGCTGAAGATGTGGCAGTT
TATTACTGTAGCAATATTATAGTAACCCCTGGACGTTCCGGCAAGGGACCAAGGTGGAAATCAAACGTGAGTAGAATT
 TAACTTTGCTTCTCAGTTGTCTGTGTCTTCTGTTCCCTGTGTCTATGAAGTGATCTATAAGTCGACTCTGCAATCAG
 CCTCTGATATCCTTCAGGGAAAAGATAAAGATAAGTCTGTAGTCAAACCTCGAGAATTGATTGCACATTTTCTTTGAAGA
 GCAAGCAAGATTAGTCAATTGGGTGAGAATAACTTGTCTAAGGAATAGCTTCAGAAATGTCTGGGGAACAAAACATGT
 TCTGGACAGAGCCTTGGTCAATTGTGAGAAAGGGAGTTTTTGTCTAGGAGGGAACCTAAGAGGAACCATCGTGTGTACA
 CTTTTGGCCAGGGGACCAAGCTGGAGATCAAACGTTAGTACTTTTTTTTCACTGATTCTTCACTGTTTCCCTAATTAGTTTA
 CTTTGTGTTCCCTTGTGTGGATTTTCATTAGTCGGATGCCAGGGATCTAACAAAC

OCI-Ly19 H-HVR

IGHV3-48, D3-10, J4

GAGTATTGTCTCCTACAGAACATAGTTTACATGAATATTTAAAATGAAATAGGGTGATTAGTGCAAAGTGTTTATCACA
 GCACAATTTTATAATAAGACAGCATATTTTCCAAACGCAATCATTGCCAGCAAACCTCCACAGGGCACCGTCTCTTAT
 CTGGGTACAGCCTACTCCTCAAGGGTCCCACCCTAGAGCTTGGTTTATAGTAGGAGATTTGCAAGTAGGGCCCTCCCTC
 TACTGATGAAAGCCAACCCCAACCTGACCCTGCAGCTCTCAGAGAGGTGCCTTAGCCCTGGATTCCAAGGCATTTCCAC
TTGGTGATCAGCACTGAACACAGAGGACTCACCATGAAGTTGGGGCTGTGCTGGGTTTTCTTGTGGTATTTAGAAG
GTGATTTCATGGAAAAGTAGAGAGATTTAGTGTGTGGATATGAATGAGACAAACAGTGGATATGTGTGGCAGTTTCTG
 ATTTTGGTGTCTCTTTGTTTGCAGTGTGAGTTGAGTTGGTGGAGTCTGGGGGAGGGTTGGTACAGCCTGG
GGGGTCTTTGAGACTCTCCTGTGAAGTCTCTGGATTACCTTCAATACCTATACTATGAGCTGGGTCCGCCAGGCTCCA
GGTAAGGGGCTGGAGTGGGTTTCAAATATTAGTAGTAGTAGTAGTGCATATACTATGCAGGCTCTGTGAAGGGCCGAT
TCATCATCTCCAGAGACAATGCCAAAACCTATTATATCTGCAAATGAACAACCTGAGAGCCGAGGACACGGCTGTCTA
TTTCTGTGCGCGAGCGTCTTATGATTCGGGGACTTATTTCCACGACTACTGGGGCCAGGGAACCTGGTCAACCGTCTCC
TCAGGTGAGTCTCACAACGCTCATTACTTTAAGTCTGAAGCCTTTTTCTGTATTTTTGGGGGAAATACGGGTGCT
 GGGTCTCCTGCCTAGAGAGCCCCGGATCAGCCTGGGAGGCTCAGGAGGACGCCCTGAGGCAACACCGACCACAGGACG
 AGGGGCAAGGGCTCCAGATGTTCTTCTCGTGAGCCAGTAGTGCGGGTTTCTGTGTGGCCAGGGCCACCTAGGCCT
 CTGGGGTCCAATGTCTAACAAACACCCGGGCCCTCCCCGGG

Ly19 L-HVR

IGKV1-39, J1

AAAGACCATGTGACAATCACAGAGGTGTTGTTACTATAGCAAAAGGGATTGTTACTCTCACATCCCTTTAAGTAACTTG
 AAGGcCTGATAGACCCACCCTCTAAGACTTCATTAGACATTCCTACGAATGGTTATACTCTCCTGTATACTCCCAATA
 CAACTCTAAAATATATTATTCATATAGTCCCTAGGTTTGTATTAAGTTTACTTTTTTCTTCAAATATCTCTTGT
 CACAACAGCGGCTCTAGAGAGAAATACATTCCTCCAGGCAAATCTATGCTGCGTGGTCTGACCTGGGACCTGGGGA

CATTGCCCTGTGCTGAGTTACTAAGATGAGCCAGCCCTGCAGCTGTGCTCAGCCTGCCCCATGCCCTGCTGATTGATT
 TGCATGTTCCAGAGCACAGCCTCCTGCCCTGAAGACTTTTTTATGGGCTGGTCGCACCCTGTGCAGGAGTCAGTCTCAG
TCAGGACACAGCATCGACATGAGGGTCCCCGCTCAGCTCCTGGGGCTCCTGCTACTCTGGCTCCGAGGTAAGGATGGAG
 AACACTAGGAATTTACTCAGCCAGTGTACTCAGTACTGACCGGAACCTCAGGGAAAATCTCTGATAACATGATTAGTAG
 TAAAAATCTTTGTTTTTATGTTTTCACTTTCAGGTGCCAGATGTGACATCCAGATGACCCAGTCTCCCTCGTCCCTGTC
AGCATCTGTAGGAGACAGAGTCACATCACTTGCCGGGCAAGTCAGAATATTAGGACCAATTTAAATTGGTATCAACAA
AAACCAGGGAGGGCCCCCTAAGGTCCTGATCTATGCCGCTTCCAGTTTGCAAAGTGGAGTCCCATCAAGATTCAGTGGCA
GTGGATCTGGGACATATTTCACTCTCACCATTAGCAGTCTGCAGCCTGAGGATTTTGCAACTTTCTATTGTCAACAGAC
GTACAGTTTCGTCGTGGACGTTTCGGCCAAGGGACCAAGGTGGAAATCAGACGTGAGTGGGATTTACACTTTGTTTCTTCA
 CTTGTCTGTGCTTTTTGTTCCCTGTGTCTATGAAGTGATATATAAGGTTAGTCTAGAAGCAGTCTGTGACATCCTTCAG
 GGAAAAGGTTGATAAGTCTGGAATCAAACCTCGAAAATTGATTACACATTTTTTTGAGGAATAATCAACCTTCAGGCA
 TTGGGTGAGAATAAGTCGTCTACGTAATAATTTAGAGATGTCTGGGGAAACATAACATGTTCTGGACAGAACCTTGGTC
 AATTGTCACAAAGGGAATTTTTGCATAGGAGGCAAAGTAAGTGGAAACCAACGTGTATACACTTTTGGCCAGGGGACCAA
 GGTGGAGATCACACGTAAGTACTTTTGTCTACTGATTCTTCACTGTTCTTGTGAGTTTACTTTGTGTTCTGTGTG
 AATTTTCAAAGTCGGATGCCAGGGATCT

SUDHL4 H-HVR

IGHV4-59, D5-18, J4

CTCCACGGGTCACACATTGAGAAGGATGTAGATATGTCCCCTACCTTCTCCTGAGATCTCAGACAGAATCCCAAATTC
 AAAAGGACACAGAAGGACAGCTCTCAGGTGGTTTTAAAAAATGACCCACTTCCAGGGACAGGGAGCTTCCCTATAACCA
 TGGTGGATGTTCTGAACTACAATAAACATTGGATGGATCCAGGATTGTTTGAAGTCACTGTCATTATTACATTCAGCTG
 CTGTTTCAATGTTTCTGAAGTAGTAAATGACAATTTATATGACAAGTTATATGAATCTTCAAGGGTAGAACAATATTGA
 CCATATTTCCAAAATCTGTCTTGTATCCATGATCACACTCATCTCCAGACCAGGTCCTTCCAGCACGTCTATTTACCTGA
 AAGAAGAGGACTCTGGGCTTGGAGAGGGGAGACCCCAAGAAGACAACCTGAGTCTCAAAGGGCACAGCCAGCATCCTAC
 TCCAGGGCGAGCCCAAAGACTGGGGCCTCCCTCCTCCTTTTTCACCTCTCCAGACAAAGGCACCACCCACATGCAAA
TCCTCACTTAAGCACCCACAGGAAACCACCACACATTTCTTAAATTCAGGGTCCAGCTCACATGGGAAATACTTTCTG
AGAGTCTGGACCTCCTGTGCAAGAACAATGAAACATCTGTGGTTCTTCTTCTCGTGGTGGCAGCTCCAGATGTGAGT
 GTCTCAGGGATCCAGACATGGGGATATGGGAGGCGCCTCTGATCCAGGGCTCACTGTGGGTCTCTCTGTTCAAGGGG
TCCTGTCCAGATGCACCTGCAGGCGTCGGGCCGGGACTGCTGAAGCCTTCGGAGACCCTGTCCCTCACCTGCCTGT
CTCTGGTGGCTCCATCAGTAGTTACTCCTGGACTTGGATCCGGCAGCCCCAGGGAGGGGGCTAGAGTGGATTGGGAAT
ATCTCTTATAGTAAACCGACTACAATCCCTCCCTCAAGAGTCGAGTCACCATGTCACTGGACATGTCCAAGAATGAGT
TCTCCCTGAAGTTGGGCTCTGTGACCGCCGCTGACACGGCCATCTATTACTGCGCGAGACGGAGCCCTGATTACGGGCA
CAACTTTGACTTCTGGGGCCAGGGAACCCTGGTACCCTCTCCTCCGGTGAGTCCCCACAACCTATTCTCACTCTGAGGA
 TTTTGTGCTTTTTTTGGGGAAACATCAGTGTGCGGCTTCTCCTCCCAAGAGAGCCCCGGAGGAGCCTGGGGGACCCAGG
 AAAATGTCTGAGACAACAGCGCCACACAGTCGAGAGACAAGGGCTCCAGATGTTCCCCCTAATATCAGTGTGTCTG
 TGCCAGGGTCACCCTGGGCTCCTCCGGTCCAATGTCCGACAACCCCCGGGCCCTCTCCGGCCTCAGTCTGAGAGGCTC
 CCAGGGACTTAGGGGGTGACATTTTTGCCTGGGGTCTTGGCATTCTTGTACGATGTGACACCTGGTTCGACCCCCGG
 GGCCAGGGAGTCTGGTACGGTGAGTCTCACCACCCCTGTCTGACTCCACCTAGGAAGACTCAGGTTCTCGGGTC
 TCAGGGTCACAGTATTGGAGGCATTTTGGAGGTCAGGAAAAAACCTGGGGAGAGGGACCCCTCGATTGGCAACCCAGA
 CTGTCTTCCCAGGTCTGGCCAGAGATGTGACAGCGGGGGGGCTCCTTCGGCTGGTCTGGGGTGACCTCTCCCCGCT
 CACTGGAGCATCTCGGGGGCTGTCTGATGATTGCGGGGTGGGACTCTGCCCCAGTCCAAGGCACCCGCTCTCTGGG
 GCGGGTGCCCCCGGGGTTTTTGGACTCCTGGGGGTGACGTAGCAGCCGCTCTGGTTGCAGTTGGACTTCCCAGGCCGA
 CAGTGGTCAGGCTTCTGAGGGGTCAGGCCAGAAATGTGGGGTACGTGGGAGGCCAGCAGAGGGTTCCATGAGAAGGGCAG
 GACAGGGCCACGGACAGTCAGCTTCCATGTGACGTCCGGAGACAGAAGGTCTCTGGGTGGCTGGGTTTTTTGTGGGGTGA
 GGATGGACATTTGCCATTTGATTTCCACTACTTCTACTACATGGACGTCTGGGGCAAAGTGGGACTCAGGTTGGGGT
 CGTCTGATGGAGTAACTGAGCCTGGGGGCTTGGGGAGCCACATTTGGACGAGATGCCTGAACAAACCAGGGGTCTTGGT
 GATGGCTGAGGAATGTGTCTCAGGAGCGATGTCTGTAGGACTGCAAGATCGCTGCACAGCAGCGAATCGTGAAATATTT
 TCTTTATAATTATGAGGTGCGCTGTGTGTCAACCTGCATCTTAAATCTTTTATTGGCTGGAAAGAGAAGTGTGCGGAGTG
 GGTGAATCCAGCCAGGAGGGACGCTAGCCCCGCTTGTATGAGAGCAGGGTTGGGGGCAGGGGTAGCCAGAAACGGT
 GGCT

SUDHL-4 L-HVR

IGKV2-28, J4

CAGATACCAGACCACTCTTGAAGTGGCTCAAGACTATGTTTTATTTGTAGGCTGTCTGCTCATCAGTGTCTGTAGGAAA
 GGGTAAAGTTTTCTTTTTTATGATTAGCTGGGAGGGAGCCAAGAAGAATGGCATTCATCCATATTCATTCTAGACATATC
 TCTACATTTAGGGTTGTTATGCTTTCCTAGAGTTGCATATCCTATAACAATGGGACCTACCCAAGATCCAAACTGTCA

CAGTCAGATCCTTCCTCCCATTTTATATCACATTGCTCACAGGAGAGACATATCCCCTGCCCGCCTGCCCCATTGACTC
 TTTCCACACCCTGCATGCACCAGGGGATTTGCATATTGTCCACAGGGAGGACCTTCCCTTGTGAGTCTGAGATAAAA
 GCTCAGCTGTAACGTGCCTTGACT**GATCAGGACTCCTCAGTTCACCTTCTCACAATGAGGCTCCCTGCTCAGCTCCTG**
GGGCTGCTAATGCTCTGGGTCTCTGGTAAAGAAAAGAAGGAGATGAGGAAGGAGAATAGGGTGGGAGGGTGAGCTCTAGG
 GCTCCACAGCATCCCATGATCCCATGTTTAGTCTTACCCTGTGTTAGAGGAGCATCATCTGTGCTGTAGAAAAGGGAAC
 TTGATATTTTGTCTGTGAATAATTAGAAGCCTCATAACTAATATGACGTCTGGTGCTCTGATTAAGATCTTCAAATA
 TTTAGGTCTCTTATACTTAACAAAAAATTGAATTCATTTTATAGAGTGTGTATTTTAAAGGCATAAATCACTATTTTTATA
 ATTAAGTTTAAATAAATGACATAAGATGAATTATGAAAATTGCTCATTAGGTTTCTACATCACTTTGCAATTCATTATT
 TC**AGGCTCCGCTGGGACATTGTGCTGACTCAGTCTCCACTCTCCCTGTCCGTCAACCCTGGAGAGCCGGCCTCCATCT**
CCTGCAGGTCTAGTCAAGTCTCCTATATACTAGTGGACAGCATTATTTGAATTGGTACGTCCAGAAGCCAGGGCAGTC
TCCACAACCTCTTGATCTATTTGGTTTCTAATCGGGCCTCCGGGGTCCCTGACAGGTTCCGGTGGCAGTGGATCAGGCACA
GATTTTACACTAAAATCAGCAGAGTGGAGGCTGACGATGTTGGGGTTTATTACTGTATGCAAGCCGTACAACTCCTC
TCACTTTCGGCGGAGGGACCAAGGTGGAGATCAAACGTGAGTGCACCTTCATAATGTTTTTCTTATTAAGTTTACAT
 TTGGAGTGTGTGTGTGAGATATTAGTGCAGGTCAATTCGAAAAGTACCACGTTCTTTCAAAGTACATGAAT
 AGGGGGATAGAAAAATATTTCTTCTTGAGGAACAGGCAAGCGCTAGCCACTTAAATGAGGCATCCCAATTGCAAGATTC
 TTTCTGCATCGGTCAGGTCAAGTAAAGTAAACAGCGAAAAGAGAATTCTTTTAAAGAAGAAAAGAAATTAACCTTGACACTGT
 GGATCACCTTCGGCCAAGGGACACGACTGGAGATTATACGTAAATAATTTTCACTTTTGTCTTCTGAAATTTGCGTCT
 GATGGCCACTATTGACTTTTAGAGGCTTAAATAGGAGTTTGGTGAAGATTGATAAATGAGGGCATTGAGATTTGCCAT
 GGGTTGCAAAACTTAACTCAGCTTCAAAAATGGATTTGGGGAAAACAGATTAAATGCTCTAAATGAAATGACACAA
 AGTAAAAGAAAAAAGTGTGACTAAAAGGAACCCTTGTATTTCTAAGGAGCAAAAGTAAATTTATTTTTGTTCACTCTT
 GCCAAACATTGTATTGGTTGTTGGTGTCTTATGCATGATACGGAAAGTGGAAAAATATATTTTTTAGTCTTTCTCCCTTT
 TGTTTGATAAATATTTTTGTGCGACAACAATAAAAATCAGTAGCACGCCCTAAGAAAATCAGGGAAAAGTGAACATA
 CCTATTTGCTATGTAGAAGAGGCAGCATACTTAAAATCAGCAGCAGTGATGTTTTTAGAG

SUDHL6 H-HVR

IGHV3-48, D4-23, J4

TGGGTTTACTTCCACTTCTGTAATGGAGAAAATATTGTCTCCTACAGAACATAGTTTACATGAATATTTAAAATGAAA
 TAGGGTGATTAGTGCAAAGTGTATATCACAGCACAAATTCATAATAAGACAGCATATTTTCAAATGCAATCATTGCCA
 GCAAACCTTCTACAGGGCACCGTCTTATCTGGGTACAGCCTACTCCTCAAGGGTCCCACCCTAGAGCTTGCTATATA
 GTAGGAGATATGCAAATAGGGCCCTCCCTCTACTGATGAAAACCAACCAACCCTGACCCTGC**AGCTCTCAGAGAGGTG**
CCTTAGCCCTGGATTCCAAGGCATTTCCACTTGGTGATCAGCACTGAACACAGAGGACTCACCATGGAGTTGGGGCTGT
GCTGGGTTTTCTTGTGCTATTTTAGAAGGTGATTCATGGAAAAGTACAGAGATTTAGTGTGTGGATATGAGTGAG
 AGAAACAGTGGATATGTGTGGCAGTTTTCTGACCTTGGTGTCTCTTTGTTTGC**AGGTGTCCAGTGTGAAGTGCAGATGGT**
GGAATCTGGGGGAACCTTGGTACACCCGGGGGGTCCCTGAGACTCTCCTGTACAGCCTCAGAAATTAATTTAATTCC
TATACTATTAATTTGGGTCCGCTGCCTCCAGGGAAGGGCCTAGAGTGGATTGCAAATATAAGTAGTACTGGCAGTGACA
TATATTATGTAGACTCTTTGAAGGGCCGGTTCACCATCTCCAGAGACAATGCCAAGAATTCGGTATATCTCCAATGAC
TGGTCTGAAAGACGAGGACACGGCTGTCTACTATTGTGCGACGGGGGAACGGACTCCACCAGGGTCTTCTTTACTGG
GGCTGGGAACCTGGTACCGTCTCCTCGGGTGAGTCCGCACAACCTCAGTCCAACCTTAACTCTGAAAAATTTTTCT
 GTCTTTTTGGCACGAATAAGTCTTCTGCATCCCCTCTTAAAGAGAGACCCGGAGCCGCCTGGGGCCCTTAAAAGAATGG
 CCTGAGGCAACACCGACCAGACAGACGAAGGTCAAGGAATCCAGATGTTCTTCCGCCTGAGTCCATTAGGTGAGACT
 TTCTGTGGCCAGGGCCACCCTGGGCTCTGGGGTCCAACGTCCAGCAACCCCGGGCCCTCCCCG

SUDHL-6 L-HVR

IGKV1-5, J1

CCTGCCTGCATGGACCAACACGGTATCATCTTTGTATATCTGTAGTAAATTTGGTTGATCTAATACTAGTAAGAATAAAG
 GCACAACACCATTACTTAAAACCTTACAAATATATAGCATCATGGCGATACACTTTATTTTTTAAATTTTTTTTAGAAAGGA
 ACAATGTTAAACTCACAGAGATGTTGCAGGTATACCACAATTACCCCTTCCCTACCCGGAATCTTATGAGAGTCTTTT
 GAAGACTTGAGAATCCTACCATCTAACATTTTACTATGTGTTTCCCTACAAACAAGAATATTCTCCTAAATAATCTTGAT
 ACACCAATGAAAAACATTACTCTATCGGCTCCTGAGGAATATTTAAAATTTCTAAAAAATACTAAAATTTGTTTCTC
 TTAATAAAATAGTCCCCAGTAGAAACACATTTCTCTGCAGACAAAATTTGTGCTACCCTGGTCTTACCT**GGGACACCTGGG**
GACTGAGCTGGTGTGAGTTACTGAGATGAGCCAGCTCTGCAACTGTGCCAGCCTGCCCATCCCCTGCTCATTG
CATGTTCCCAGAGCACAACTCCTGCCCTGAAGCCTTATTAATAGGCTGGTCACTTTGTGCAGGAGTCAAGCCAGT
CAGGACACAGCATCGACATGAGGGTCCCCGCTCAGCTCCTGGGGCTCCTGCTGCTCTGGCTCCCAGGTAAAGGAAGGAGA
 AACTAGGAATTTACTCAGCCCAGTGTACTCAGTACTGCCTGGTTATTCAGGGAAGTCTTCTATAACATGATCAAAG
 TAACAAAATATGTGTCTCCATTTCCAATCTC**AGGTGCCAAATGTGACATCCAGATGACCCAGTCTCCTTCCACCCTGTC**
TGCATTTGTAGGAGACAGAATCACCATAACTTGGCGGGCCAGTCAGAGTATTTATAACTGGTTGGCCTGGTATCAACAA

AAACCAGGGAGAGCCCCAAAAGTCCTCGTCTATAAGGCGTCTAATTTACAAGGCGGCGTCCCATCAAGGTTTACGCGGCA
 GTGGATATGGGACAGAATTCAGTCTCACCATCAGCAGCCTGCAGCCTGAGGATTTTGAACATATTTACTGCCAACAGTA
 TCAGAGTTATTCGTGGACTTTTCGGCCAAGGGACCAAGGTGGAGATGAAACGTGAGTAGAATTCGGACTTTGCCTCCTCA
 ATTGTCTGTGTATTCGGTTCCCTGGGTCTGTGAAGTGATCTATAACGTGACTCGGCAATCGGCCTCTGATCTCCTTCAG
 GCAAAGATAAAAAATAAGTCTGTTGTCAAACTCGAGACTGGGTGCACATCTTCTTTGAAGAGCAGGCAAGGCAACATT
 CAGTCATTGGGTGAGAATACTTTGTCTAAGCATTGACTTCAGGAGTGTCTTGGGGAACATAACATGTTCTGGAGACAGT
 CTCGGGCAATTGTCAAAGGGGAATTTTTCTTTAGGAGGGAAGTTAAGAGGAACCCTTGTGTAAACACTTATGACCAGG
 GGACCAAGGTGGAGGTCAAAGGTAAGTACTTTTTTTCACTGATTCTTCATTGTTGGCAATTGTTTTACTCAGTATTCTT
 TTGTGTGGATTTTTACTAGTCGGATGCCA

TMD8 H-HVR

IGHV3-48, D1-26, J5

TTACTTCCACTTCTGTAAATGGAGAAAATATTGTCTCCTACAGAACATAGTTTACATGAATATTTAAAATGAAATAGGG
 TGATTAGTGCAAAGTGTATATCACAGCACAAATTCATAATAAGACAGCATATTTCCAAATGCAATCATTGCCAGCAA
 CTCTACAGGGCACCCTCGTCTTATCTGGGTACAGCCTACTCCTCAAGGGTCCCACCCTAGAGCTTGCTATATAGTAGG
 AGATATGCAAATAGGGCCCTCCCTCTACTGATGAAAACCAACCCAACCCTGACCCTGCAGCTCTCAGAGAGGTGCCTTA
 GCCCTGGATTCCAAGGCATTTCCACTTGGTGATCAGCACTGAACACAGAGGCCCTCACCATGGATTTGGGGCTGTGCTGG
 GTTTTCCTTGTGCTATTTTAGAAGGTGATTCAATGTAACACTGGAGAGACTTAGTCTGTGTGGATAGGAGTGAGAAAA
 GAGAGGATATGTGCGGCAGTTTGTGACCTTGGTGTCTTTTTCTTTACAGGTGGCCAGTGTAGAGTGCAACTGGTGGAGT
 CTGGGGGAGACCTGGTACAGTCGGGGGGTCCCTGAGACTCTCCTGTGTAGCCTCTGGATTACCTTTAGTTCTTACAG
 TATGAAGTGGGTCGGCCAGGCTCCAGGAAAGGGACTGGACTGGGTCTCATATATTAGTGGTACTAGTGGAACCATATAC
 TACACAGACTCTGTGAAGGGCCGATTCATCATCTCCAGAGACAATGCGAAGAAGTTCGCTATATTTACAAATGAACAGCC
 TGAGAGATGATGACACGGCTGTCTATTATTGTGTGAGAGATCGGGTGGGGGTAACCCATGGGGCCGCGGAACCCTGGT
 CACCGTCTCCTCAGCTGAGTCTTCAACCTCTTTGTTGTTTTTCTCCGAGGCACTTTGTTCTTTTTTGGGGGAGA
 TGAGGCTTCTGAGTCTCCCGCAAAGAGAACCCCGGAGCGCCCTGGGAGATTACGACGATGCCCTCTCAGACAGACGAG
 GGGCAAGGACTCCTCATACTCTTTCATGTTGACCCCTCCAGTCTGGGTCTCTTTGTGGCCAGGGCCACCCTAGGCCTCT
 GGGTCCAATGTCCAATAACCTCCGGGCCCGCCCCGGGGTCAGTTTGCAGTGTCTCGGGGCGTCGCGGGGCGCCAGT
 GCTTGCCTGGGGTCTTGACATGATTGCCACAGTGTGACACCTAATTCGACCCCTGGGGCCAGGGGACCCTGGTCATCGT
 CTCTCAGGTGAGTCTTACCACCCCTCTCTGAGTCCACTTGGGGAGACTCCACTTGCCTGGGTCTCAGGGTCAAAT
 CTTGGAGACATTGTGGACCCACCAAACACAGGTGTGCAGAGGGACCCTTCGAACGGGAGCCAGCCTGTCTCCCCAA
 CTCCGGCCACACATGTCGTCAGTTGGGGGGTCTTTCGGCTGGTCTGGGGTGACCTCTCTCCCCTTACCTGGAGCATT
 GTCAGG

TMD8 L-HVR

IGkV2-30, J1

ATGTGCCTGGGAGAGTACTATGAAACAAGAAATCTGTTAGGGAAGACAGAAGAAATACTTAAATTTCTCCAACATAGA
 CAGCATAGATTTTATGCCTATTCGTTTCCCTCCAACAGAGAAGATATTTAAGTCATTTTGTCTACAAGAGAGGCTCCT
 ACCCTCCCCTTGGCTCTTTCCACCCCACTGCACCCACCAGGTTATTTGCATATTATCCCTTAGTGAGGACTTTCTTGT
 GAGTCTGAGATAAGAGCTCAGCTTACCCTTGCCTTGACTGATCAGGACTCCTCAGTTCACCTTCTCACATGAGGCTC
 CCTGCTCAGCTCCTGGGGCTGCTAATGCTCTGGGTCCCAGTAAGGGTAGAAGGGAGATGAGGGAGGAGAATGGCATGG
 AGCGGTGACTTCTGGGGCCCCACTGCCTCTAACAAACAGTCATCTCTGGGGGTCTCACTACACTCCTATGTGTGTTCTT
 TTCTATATTGGACATGTACATGTTGTCTCCAAAACAAAGATCTGTGTGTGGGGAAGACTGATACTAAAACGGGATGA
 TGTGGGGTCTTCTGGGGACCCCTTTGAGGCTTGGATCCCTTGGATTGCACTTTGAAACTGTGTTTTTTTGGAGACATGGA
 TAGATATGTGTGTAGCCTGAAATAAAGAAGAGATCCAAGTTTATGAAAATTACAGATGAGCTTTATACATAGGCTTCTT
 ATTCTTTCCAATTATTGTAGGATCCAGTGGGAATGTGGTGATGACTCAGTCTCCTCCTCCTCCGTACCCCTAGGA
 CAGCCGGCCTCCATCTCCTGCATGTCTAGTCGAAGTCTCGTACACAGTGATGGAACACTTATTTGAATTGGTTTCATC
 AGAGGCCAGGCCAATCTCCGAGGCGCTAATTTATAAAGTTTCTAACCGGGACTCTGGGGTCCCAGACAGATTGAGTGG
 CAGTGGGTGAGGCACCGATTTACACTGAAGATCAGCAGGGTGGAGGCTGAGGATATTGGGGTTTATTATTGTATGCAA
 GCTACACACTGGCCTCCGTGGACGTTTCGGCCAAGGGACCAAGGTGGAAATTCACAGTACAAATTAATGTGTCTT
 CTGTTGCCTGTGTGATGAGGTGATCTCTAAGGTGACTCCACAATCAGTCTCTGATATCGTTTAGGGAAAACATAAAGA
 TAGGTCTGTAGTCAAAGTCGGGAATTGATTGCACAGTGTCTTTGAAGAGTATAACAAGGGTCACTATTGAGTGAAAATA
 TCTTTTCTAAATAATATGTTTGAATGTCTTGGGGAACAAAACATGTTCTAGACAGAGCCTTGGTCAATTGTCAGAAA
 GGGAGTTTTTGTATAGGAGGGAAGTTAAGAGGAACCAATGTGTGCACACTTTTGGCCAGGGGACCAAGCTGGAGATCAA
 ACGCAAGTACGTTTTTCCACTGATTCTTTATTATTGTTAATTCGTTTACTTTGTATTCTTTGTGCGGTTTTTTCATTAG
 TCGAATGCCAGGGATCTAACAACTTCAATCCCATGTAAGGTACTGAGGAGGGGAATTTGTTCCACAGGAAGTTACCTT

GTGACTAATTTTTAAGAATTCTAAATCAAAACAACCTTCCTTGGGGGAAAGAGGCTTGCTGCAATTTTCAGGGACCTTTTT
GTAAAGGGAAAAGTCAAGACGACTCACTGTGATTCACTTTTCGGCCCTGGGACCAAGGTAGATGTCAAACGT

U2932 H-HVR

IGHV4-39, D3-22, J4

TGACTATTTAGATGGCCTGGGTGTGTGGTTGGTTTTATATGAATCTTTAAGGGTTGAACAGTACTGACCCTATTCCAAA
ATCTGTCCTTGATCCAGGATCACACTCATCTCTCAGACCAGCTCCTTCAGCACATCTCTTTACCTGGAAGAAGAGGACT
CTGGGCTTGAGAGGGGGAGGCCCAAGAAGAGAAGTGAATTTCTCAAAGGGCACAGCCAGCATTCTCCTCCCAGGGTGAG
CTCAAAGACTGGCGCCTCTCTCATCCCTTTTCACTGCTCCGTACAAACGCACCACCCCATGCAAATCCTCACTTAGG
CGCCACAGGAAGCCACCACACATTTCTTAAATTCAGGTCCAACCTATAAGGAAATGCTTCTGAGAGTCATGGATC
TCATGTGCAAGAAAATGAAGCACCTGTGGTTCTTCTCCTGCTGGTGGCGGCTCCCAGATGTGAGTGTTTCTAGGATGC
AGACATGGAGATATGGGAGACTGCCTCTGATCCCAGGGCTCACTGTGGGTTTTTCTGTTAC**AGGGTCTGTCC**CAGC
TGCAGCTGCAGGAGTCGGGCCAGGACTGGTGAAGCCTTCGGAGACCCTGTCCCTCACCTGCACTGTCTCTCGTGTCTC
CATCAGCAGTAGTAATTACTACTGGGGCTGGATCCGCCAGCCCCAGGGAAGGGGCTGGAATGGATTGGGAGTGACTAT
TATGGTGGCAGTACCTCCTACAACCCGTCCCTCAAGGTCGAGTCATTATATCCGTAGACACGTCCAAGAACCATTCT
CCCTGAAACTGACCTCTGTGACCGCCGACACAGGCTCTATATTACTGTGCGAGAGCGCTGTCTTACTATGATACTGG
TGGTTTCAGGTACTTCTTTGACTACTGGGGCCAGGGAACCCCTGGTCACCGTCTCCTCAGGTGAGTCCTCACGACCTCTC
TCCTGCTTTAACTCTTAAGGATTTTGTCTGCATTTTTGGGGGGAAATAAGCGTGCTGGGTCTCCTGCCAAGAGAGCCCCG
GGCTGGGTCTCCTGCCAAGAGAGCCCCGGAGCAGCCTGGGGCTCAGGAGGATGCCCTGAGGCAACAGCGGCCACACAGA
CGAGGGGCAAAGGCTCCAGATGTTCCCTCCTCCTGAGCCCAGCAGCACGGGTCTCTCTGTGGCCAGGGCCACCCTGGGC
CTCTGGGGTCCAATGTCCAACAACCCCCGGGCCCTCCCCGGGCTCAGTCTGAGAGGGTCCCAGAGACTTAACGGGGTGC
CAGTTCCTTGCCCTGGGGTCTGGCATTGTTGTACAATGTGACACCTGGTTCGCCCCCTGGGGCCAGGGACCCCTGGTCA
CCGTCTCCTCAGGTGAGTCTCACCGCCCCCTCTCTGAGTCCACTTAGGGAGACTCAGCTTGCCAGGGTCTCAGGGTCA
GAGTCTTGAGGCATTTTGGAGGTGAGAAAGAAAGCTGGGGAGAGGGACCCCTTCAATGGGAACCCAGCCTGTCTCC
CCAAGTCCGGCCACAGATGTCGGCAGCTGGGGGGCTCCTTCGGCTGGTCTGGGGTGACCTCTCTCCGCTTACCTGGAG
CATTCTCAGGGCTGTCTGATGATTGCGTGGTGGGACTCTGTC

U2932 L-HVR

IGKV3-20, J1

AGAATGAGACAGCTTCTGGACCCTCAGGAAAGATCACTAACAAGTAAATACAAGTATATCCGGAAGATAAAGTTGTAAT
AGACTCTTCCCTTCAACCTGATCCATCATGCATTTAGGGAGCTGACTGGGCACAAGTTGGAGCAGAAAGAGAAAAATGA
AACCACAGCCTTCTATTTTGTCTTCTAACAGACTTGTACCAACATTCTGTGGCTCAATCTAGGTGATGGTGAGACAAGA
GGACACAGGGGTAAATTTCTGTGGCCGAGGGGAGAAGTTCTACCCTCAGACTGAGCCAACGGCCTTTTTCTGGCCTGAT
CACCTGGGCATGGGCTGCTGAGAGCAGAAAGGGGAGGCAGATTGTCTCTGCAGCTGCAAGCCAGCACCCGCCCCAGCT
GCTTTCATGTCCCTCCAGCCGCCCTGCAGTCCAG**AGCCATATCAATGCCCTGGGT**CAGAGCTCTGGAGAAGAGCTGC
TCAGTTAGGACCCAGAGGGAACCATGGAAACCCAGCGCAGCTTCTCTTCTCCTGCTACTCTGGCTCCCAGGTGAGGG
GAACATGGGATGGTTTTGCATGTCAGTGAAAACCCCTCTCAAGTCCTGTTACCTGGCAACTCTGCTCAGTCAATCAATA
ATTAAAGCTCAATATAAAGCAATAATTCTGGCTCTTCTGGGGAGACAATGGGTTTGATTTAGATTACATGGGTGACTTT
TCTGTTTTATTTCCAATCTC**AGATAACCACCGGA**GAATTGTGTTGACGCAGTCTCAGGCACCCGTCTTTGTCTCCAG
GGAAAGAGCCACCCCTCCTGCAGGGCCAGTCAGAGTGTAGCAGCAGCTACTTAACCTGGTACCAGCAGAAACCTGG
CCAGGCTCCCAGGCTCCTCATCTATGGTGGTCCAACAGGGCCACTGGCATCCAGACAGGTTCAGTGGCAGTGGGTCT
GGGACAGACTTCACTCTCACCATCAGCAGACTGGAGCCTGAAGATTTTGCAGTGTATTACTGTCAGCAGTATCGTAGCT
CACCTCCGACGTGGACGTTCCGGCCAAGGGACCAAGGTGGAGATCAACGTGAGTAGAATTTAAAGTTTGCTTCTCAGT
TGTCTGTGCTTCTGCTCCCTGTGTCTATGAAGTGATCTATAAACTGACTCTGCAATCAGCCTCTGATATCCTTCAGGG
AAAAGAAAAAGATAAGTCTGTAGTCAAACCTCGAGAATTGATTGCACATTTTTCTTTGAAGAGCAAGCAAGATTGATCAT
TGGGTGAGAATAACTTGTCTAAGTAATAGCTTCAGAAATGTCCTGGGGAAACATAACATGTTCTGGACAGAGCCTTGGTC
AATTGTCAGAAAGGGAGTTTTTGTATAGGAGGGAAGTTAAGAGGAACCATTGTGTGTACACTTTTGGCCAGGGGACCAA
GCTGGAGATCAAACGTAAGTACTTTTTTCCACTGATTCTTCACTGTTGCTAATTAGTTTACTTTGTGTTCCCTTGTGTG
GATTTTCATTAGTCGGATGCCAGGATCTAACAACTTCATTCCAGGTTAGGTACAGAGGAGGGGAAATTGTTCCACA
GGAAGCTAGCTTGTGGCTAATTTTTAAGATTTCTAAATCAAAATAACTTCATTGGGGGAAAGAGGCTTGCTGAGCTTTC
AGGGAGGTTTTTGTAAAGGGAAAAGTTAAGACGAATCACTGTGATCCTTTCGGCCCTGGGACCAAGTGGATATCAA
ACGTAAGTACATCT

Homology arms for H-HVR replacement with inserted GFP and F2A sequences

Fragments of DNA as inserted in the into pSC-B-amp/kan plasmid (Agilent Technologies) and used for ligation mediated assembly of repair template plasmids for H-HVR and L-HVR replacement.

The sequences are marked as follows:

Introns: GTTATAT

Exons in bold: **CCTTAAA**

GFP: **ATGGTGA**

F2A: **GTGACAG**

Splice donor and acceptor sites: **GT AG**

Silent changes to prevent re-targeting of repair template plasmid and modified genomic locus: **A**CTG**C**

BsmBI restriction cassette: GGAGACGCCCTCGTCTCC

BsmBI restriction sites: GAGACG and CGTCTC

BbsI restriction sites: GAAGAC and GTCTTC

Cas9/sgRNA sites: underlined

HBL-1_H_HA_GFP_F2A

AACTGTATTCCAAAATCTGTCTTTGATCCATGATCACACTTGTCTCCCAGACCAGCTCCTTCAGCACATTTCTACCTG
 GAAGAAGAGGACTCTGGGTTTGGTGAGGGGAGGCCACAGGAAGAGAAGTCTCAGAGGGCACAGCCAGCATAAC
 CTCCCAGGGTGAGCCCAAAGACTGGGGCCTCCCTCATCCCTTTTTACCTATCCATACAAAGGCACCACCCACATGCAA
 ATCCTCACTTAGGCACCCACAGGAAATGACTACACATTTCTTAAATTCAGGGTCCAGCTCACATGGGAAGTGCTTTCT
 GAGAGTCT**CTGAAACTTCTGCACAAGAACATGGTGAGCAAGGGCGAGGAGCTGTTACCCGGGTGGTGCCCATCCTGGTC**
GAGCTGGACGGCGACGTAAACGGCCACAAGTTCAGCGTGTCCGGCGAGGGCGAGGGCGATGCCACCTACGGCAAGCTGA
CCCTGAAGTTCATCTGCACCACCGGCAAGCTGCCCGTGCCTGGCCACCCTCGTGACCACCTTCACCTACGGCGTGCA
GTGCTTCGCCCCTACCCCGACCACATGAAGCAGCAGACTTCTTCAAGTCCGCCATGCCCGAAGGCTACGTCCAGGAG
CGCACCATCTTCTTCAAGGACGACGGCAACTACAAGACCCGCGCCGAGGTGAAGTTCGAGGGCGACACCCTGGTGAACC
GCATCGAGCTGAAGGGCATCGACTTCAAGGAGGACGGCAACATCCTGGGGCACAAGCTGGAGTACAACATAACAGCCA
CAAGGTCTATATCACCGCCGACAAGCAGAAGAAGCCATCAAGGTGAAGTTCAGACCCGCCACAACATCGAGGACGGC
AGCGTGCAGCTCGCCGACCCTACCAGCAGAACACCCCATCGGCGACGGCCCCGTGCTGCTGCCCGACAACCCTACC
TGAGCACCCAGTCCGCCCTGAGCAAAGACCCCAACGAGAAGCGCGATCACATGGTCTGCTGGAGTTCGTGACCGCCCGC
CGGGATCACTCTCGGCATGGACGAGCTGTACAAGGTGACAGAGTTGCTGTACAGGATGAAGCGGGCCGAGACCTACTGT
 CCAAGGCCTCTGCTGGCAATTCACCCAACGGAGGCTCGGCATAAGCAAAGATTTGTGGCCCTGTCAAGCAGACTCTGA
 ACTTCGATTTGCTCAAACCTGGCCGGCGATGTGGAGTCCAATCCGGGACCCGGAGACGCCCTCGTCTCCAGGTGAGTCTT
GAGAACGTCTCTCCTGGTTTAACTCTGACGGTTTTTATTGTATTATTGGGGGAAGTTCGGGTGTTGGGTCTCCTGCCA
 GGAGAACCCCGGAGCAGTCTGGGTGACTCAAGAGGATGCCCTGAGGCAACCGCACCACACAGACGAGGGGCAAGGGCT
 CCAGATGTTCTTCTCCTGAGCCCAACAATACTAATCTCTCTGTGGCCAGGGCCACCCTAGGCCTCTGGGGTCCAATG
 CCCGACAATCCCCGGGCCCTCCCCGACTCAGTCTGAGAGGGTCCAGGGACGTCACGGGGCGCCACTTCTTGCCAGGG
 GTCTTGGCATTGTTGTACAATGTGACAACACTAGTT

OCI-Ly7_H_HA_GFP_F2A

GTCAGAGACAACAATGGTCCCAAAAAACCAGGTAATCTTTAGGCCAATAAAAATGTGGGTTCACAGTGAGGAGTGCA
 TCCTGGGGTTGGGGTTTGTCTGCAGCGGGAAGAGCGCTGTGCACAGAAAGCTTAGAAATGGGGCAAGAGATGCTTTTC
 CTCAGGCAGGATTTAGGGCTTGGTCTCTCAGCATCCACACTTGTACAGCTGATGTGGCATCTGTGTTTTCTTCTCAT
 CGTAGATCAGGCTTTGAGCTGTGAAATACCCTGCCTCATGCATATGCAAATAACCTGAGGTCTTCTGAGATAAATATAG
 ATATATTGGTGCCCTGAG**AGCATCACATAACAACCACATTCTACCTAAAGAAGCCCCTGGGAGCAAGGTGCATCACC**
ATGGTGAGCAAGGGCGAGGAGCTGTTACCCGGGTGGTGCCCATCCTGGTTCGAGCTGGACGGCGACGTAAACGGCCACA
AGTTCAGCGTGTCCGGCGAGGGCGAGGGCGATGCCACCTACGGCAAGCTGACCCTGAAGTTCATCTGCACCACCGGCAA
GCTGCCCGTGCCTGGCCACCCTCGTGACCACCTTCACCTACGGCGTGCAGTGCTTCGCCCCTACCCCGACCACATG
AAGCAGCAGACTTCTTCAAGTCCGCCATGCCCGAAGGCTACGTCCAGGAGCGCACCATCTTCTTCAAGGACGACGGCA
ACTACAAGACCCGCGCCGAGGTGAAGTTCGAGGGCGACACCCTGGTGAACCGCATCGAGCTGAAGGGCATCGACTTCAA
GGAGGACGGCAACATCCTGGGGCACAAGCTGGAGTACAACATAACAGCCACAAGGTCTATATCACCGCCGACAAGCAG
AAGAACGGCATCAAGGTGAAGTTCAGACCCGCCACAACATCGAGGACGGCAGCGTGCAGCTCGCCGACCCTACCAGC
AGAACACCCCATCGGCGACGGCCCCGTGCTGCTGCCCGACAACCCTACCTGAGCACCCAGTCCGCCCTGAGCAAAGA

CCCCAACGAGAAGCGCGATCACATGGTCCTGCTGGAGTTTCGTGACCGCCGCGGGATCACTCTCGGCATGGACGAGCTG
 TACAAGGTGACAGAGTTGCTGTACAGGATGAAGCGGGCCGAGACCTACTGTCCAAGGCCTCTGCTGGCAATTCACCCAA
 CGGAGGCTCGGCATAAGCAAAAAGATTGTGGCCCTGTCAAGCAGACTCTGAACTTCGATTTGCTCAAACCTGGCCGGCGA
 TGTGGAGTCCAATCCGGGACCCGGAGACGCCCTCGTCTCCAGGTGAGTCCTCATAATCTATCATACTGCAGTATTTTGC
 TGCCTTTTTGGGGGAAATAAGGGTCTGCTGGTCTCCTGCCAAGAAAGACCCGGAGCAGCCGGGGGGGGCTCAGGAGGAT
 GCCCTGGGGCAACAGCGGACACGCAGACGAGGGTCAAGGGCTCCAGAAGCCCTTCTCCTGAGGCCGACAGCGCGGGT
 CTCTCTGTGGCCAGGGCCACCTAGGCCTCTGGGGTCCAATGCCAACAAACCCCGGGCCCTCCCCGGGTTCACTCTGA
 GAGGTCCCAGGGACGTGGCGGGGCGCCAGTTCTTGCTGGGTCTTGACATTGTTGTCACAATGTGACAACCTGGTTCC
 ACCCTGGGGCCAGGGAACCTGG

OCI-Ly19_H_HA_GFP_F2A

TTAGTGCAAAGTGTTTATCACAGCACAATTTATAATAAGACAGCATATTTTCCAAACGCAATCATTGCCAGCAAACCTT
 CCACAGGGCACCCTCGTCTTATCTGGGTACAGCCTACTCCTCAAGGGTCCCACCCTAGAGCTTGGTTTATAGTAGGAGA
 TTTGCAAGTAGGGCCCTCCCTCTACTGATGAAAGCCAACCCAACCTGACCCTGCAGCTCTCAGAGAGGTGCCTTAGCC
 CTGGATTCCAAGGCATTTCCACTTGGTGATCAGCACTGAACACAGAGGACTCACCATGGGTGAGCAAGGGCGAGGAGCTG
 TTCACCGGGGTGGTGCCCATCCTGGTTCGAGCTGGACGGCGACGTAAACGGCCACAAGTTCAGCGTGTCCGGCGAGGGCG
 AGGGCGATGCCACCTACGGCAAGCTGACCCTGAAGTTCATCTGCACCACCGGCAAGCTGCCCGTGCCTGGCCACCCT
 CGTGACCACCTTACCTACGGCGTGCAGTGCTTCGCCCGCTACCCCGACCACATGAAGCAGCAGACTTCTTCAAGTCC
 GCCATGCCCCAAGGCTACGTCCAGGAGCGCACCATCTTCTTCAAGGACGACGGCAACTACAAGACCCGCGCCGAGGTGA
 AGTTCGAGGGCGACACCCTGGTGAACCGCATCGAGCTGAAGGGCATCGACTTCAAGGAGGACGGCAACATCCTGGGGCA
 CAAGCTGGAGTACAACACAACAGCCACAAGGTCTATATCACCGCCGACAAGCAGAAGAACGGCATCAAGGTGAACCTC
 AAGACCCGCCACAACATCGAGGACGGCAGCGTGCAGCTCGCCGACCCTACCAGCAGAACACCCCATCGGCGACGGCC
 CCGTGCTGCTGCCGACAACCACTACCTGAGCACCCAGTCCGCCCTGAGCAAAGACCCCAACGAGAAGCGCGATCACAT
 GGTCCTGCTGGAGTTCGTGACCGCCGCGGGATCACTCTCGGCATGGACGAGCTGTACAAGGTGACAGAGTTGCTGTAC
 AGGATGAAGCGGGCCGAGACCTACTGTCCAAGGCCTCTGCTGGCAATTCACCCAACGGAGGCTCGGCATAAGCAAAAAGA
 TTGTGGCCCTGTCAAGCAGACTCTGAACTTCGATTTGCTCAAACCTGGCCGGCGATGTGGAGTCCAATCCGGGACCCGG
 AGACGCCCTCGTCTCCAGGTGAGTCCTGACAAAGTCTCATTACTTTAAGTCTGAAGCCTTTTCTGTATTTTGGGGG
 GAAATACGGGTGCTGGGTCTCCTGCCTAGAGAGCCCCGGATCAGCCTGGGAGGCTCAGGAGGACGCCCTGAGGCAACAC
 CGACCACACGGACGAGGGGCAAGGGCTCCAGATGTTCTTCTCGTGAGCCAGTAGTGCGGGTTTCTCTGTGGCCAGG
 GCCACCCTAGGCCTCTGGGGTCCAATGTCTAACAAACACCCGGGCATATCAAGCTTATCGATACCGTGCACCTCGAGGGG
 GGGCCCGGTACCCAGCTTTTGTTC

SUDHL-4_H_HA_GFP_F2A

GGGACAATTTATATGACAAGTTATATGAATCTTCAAGGGTAGAACAATATTGACCATATTCCAAAATCTGTCTTTGATC
 CATGATCACACTCATCTCCAGACCAGGTCTTTCAGCACGTCTATTTACCTGAAAGAAGAGGACTCTGGGCTTGGAGAG
 GGGAGACCCCAAGAAGACAACCTGAGTCTCAAGGGCACAGCCAGCATCCTACTCCAGGGCGAGCCAAAAGACTGGG
 GCCTCCCTCCTCTTTTTACCTCTCCAGACAAAGGCACCACCACATGCAAAATCTTGCTTAAGCACCCACAGGAAAC
 CACCACATTTCTTAAATTCAGGGTCCAGCTCACATGGGAAATACTTTCTGAGAGTCTTGACCTCCTGTGCAAGAA
 CATGGGTGAGCAAGGGCGAGGAGCTGTTACCGGGGTGGTGCCATCCTGGTTCGAGCTGGACGGCGACGTAAACGGCCAC
 AAGTTCAGCGTGTCCGGCGAGGGCGAGGGCGATGCCACCTACGGCAAGCTGACCCTGAAGTTCATCTGCACCACCGGCA
 AGCTGCCCGTGCCTGGCCACCCTCGTGACCACCTTACCTACGGCGTGCAGTGCTTCGCCCGCTACCCCGACCACAT
 GAAGCAGCAGACTTCTTCAAGTCCGCCATGCCCGAAGGCTACGTCCAGGAGCGCACCATCTTCTTCAAGGACGACGGC
 AACTACAAGACCCGCGCCGAGGTGAAGTTCGAGGGCGACACCCTGGTGAACCGCATCGAGCTGAAGGGCATCGACTTCA
 AGGAGGACGGCAACATCCTGGGGCACAAGCTGGAGTACAACACAACAGCCACAAGGTCTATATCACCGCCGACAAGCA
 GAAGAACGGCATCAAGGTGAACCTCAAGACCCGCCACAACATCGAGGACGGCAGCGTGCAGCTCGCCGACCCTACCAG
 CAGAACACCCCATCGGCGACGGCCCGTGTGCTGCTGCCGACAACCACTACCTGAGCACCCAGTCCGCCCTGAGCAAAG
 ACCCAACGAGAAGCGCGATCACATGGTCTGCTGGAGTTCGTGACCGCCGCGGGATCACTCTCGGCATGGACGAGCT
 GTACAAGGTGACAGAGTTGCTGTACAGGATGAAGCGGGCCGAGACCTACTGTCCAAGGCCTCTGCTGGCAATTCACCCA
 ACGGAGGCTCGGCATAAGCAAAAAGATTGTGGCCCTGTCAAGCAGACTCTGAACTTCGATTTGCTCAAACCTGGCCGGCG
 ATGTGGAGTCCAATCCGGGACCCGGAGACGCCCTCGTCTCCAGGTGAGTCCTCACAACCTATTCTCACCTAGTATTTT
 GTCGCTTTTTTGGGGAAACATCAGTGTGCGGCTTCTCCTCCCAAGAGAGCCCCGGAGGAGCCTGGGGGACCCAGGAAAA
 TGTCCTGAGACAACAGCGCCACACAGTGCAGAGACAAGGGCTCCAGATGTTCCCCCTAATATCAGTGTGTCTGTGCC
 CAGGGTACCCCTGGGCTCTCCGGTCCAATGTCCGACAACCCCGGGCCCTCTCCGGCCTCAGTCTGAGAGGCTCCCAG
 GGACTTAGGGGGGTGACATTTTTGCCTGGGGTCTTGGCATTCTTGTACAGATGTGACACCTGGTTCGACCCCGGGGCC
 AGGGAGTCTGGTACGGTGGAGTCTCACCACCCCTGTCTGACTCCACC

SUDHL-6_H_HA_GFP_F2A

GGGTTTACTTCCACTTCTGTAAATGGAGAAAATATTGTCTCTACAGAACATAGTTTACATGAATATTTAAAATGAAAT
 AGGGTGATTAGTGCAAAGTGTTTATCACAGCACAATTTTATAATAAGACAGCATATTTTCCAAATGCAATCATTGCCAG
 CAACTTCTACAGGGCACCGTCGTCTTATCTGGGTACAGCCTACTCCTCAAGGGTCCCACCCTAGAGCTTGCTATATAG
 TAGGAGATATGCAAATAGGGCCCTCCCTCTACTGATGAAAACCAACCCAACCTGACCCTGC**AGCTCTCAGAGAGGTGC**
CTTAGACCAGATTCCAAGGCATTTCCACTTGGTGATCAGCACTGAACACAGAGGACTCACCATGGTGAGCAAGGGCGA
 GGAGCTGTTACCGGGGTGGTGCCCATCCTGGTCGAGCTGGACGGCGACGTAAACGGCCACAAGTTCAGCGTGTCCGGC
 GAGGGCGAGGGCGATGCCACCTACGGCAAGCTGACCCTGAAGTTCATCTGCACCACCGGCAAGCTGCCCGTGCCCTGGC
 CCACCCTCGTGACCACCTTACCTACGGCGTGCAGTGCTTCGCCCGCTACCCCGACCACATGAAGCAGCAGACTTCTT
 CAAGTCCGCCATGCCGAAGGCTACGTCCAGGAGCGACCATCTTCTTCAAGGACGACGGCAACTACAAGACCCGCGCC
 GAGGTGAAGTTCGAGGGCGACACCCTGGTGAACCGCATCGAGCTGAAGGGCATCGACTTCAAGGAGGACGGCAACATCC
 TGGGGCACAAGCTGGAGTACAAC TACAACAGCCACAAGGTCTATATCACCGCCGACAAGCAGAAGAACGGCATCAAGGT
 GAACTTCAAGACCCGCCACAACATCGAGGACGGCAGCGTGCAGCTCGCCGACCACTACCAGCAGAACACCCCCATCGGC
 GACGGCCCCGTGCTGCTGCCCGACAACCACTACCTGAGCACCCAGTCCGCCCTGAGCAAAGACCCCAACGAGAAGCGCG
ATCACATGGTCTGCTGGAGTTCGTGACCGCCGCGGGATCACTCTCGGCATGGACGAGCTGTACAAGGTGACAGAGTT
 GCTGTACAGGATGAAGCGGGCCGAGACCTACTGTCCAAGGCCTCTGCTGGCAATTCACCCAACGGAGGCTCGGCATAAG
 CAAAAGATTGTGGCCCCTGTCAAGCAGACTCTGAACTTCGATTTGCTCAAACCTGGCCGGCGATGTGGAGTCCAATCCGG
 GACCCGGAGACGCCCTCGTCTCC**AGGT**GAGTCCGCACAA**CTGA**ATCCAACCTTAACTCTGAAAAATTTTTCTGTCTTT
 TTGGCACGAAATAAGTCTTCTGCATCCCCTCTTAAGAGAGACCCGGAGCCGCTGGGGGCTTAAAGAATGGCCTGAG
 GCAACACCGACCAGACAGACGAAGGTCAAGGAATCCAGATGTTCTTCCGCTGAGTCCATTAGGTTCGAGACTTTCTGT
 GCCAGGGCCACCCTGGGCCTCTGGGGTCCAACGTCCAGCAACCCCCGGGCCCTCCCC

U2932_H_HA_GFP_F2A

GGGTTGAACAGTACTGACCCTATTCCAAAATCTGTCTTGGATCCAGGATCACACTCATCTCTCAGACCAGCTCCTTCAG
 CACATCTCTTTACCTGGAAGAAGAGGACTCTGGGCTTGAGAGGGGAGGCCCAAGAAGAGAAGTGAAGTCTCAAAGGG
 CACAGCCAGCATTTCTCCTCCAGGGTGAGCTCAAAGACTGGCGCCTCTCTCATCCCTTTTCACTGCTCCGTACAAACG
 CACCACCCCATGCAAATCCTCACTTAGGCGCCACAGGAAGCCACCACAC**ATTTCTTAAATTCAGGTCCAACTCATA**
AGGGAAATGCTTTCTGAGAGCATGATCTCATGTGCAAGAAAATGGTGAGCAAGGGCGAGGAGCTGTTACCGGGGTG
 GTGCCATCCTGGTCGAGCTGGACGGCGACGTAAACGGCCACAAGTTCAGCGTGTCCGGCGAGGGCGAGGGCGATGCCA
 CCTACGGCAAGCTGACCCTGAAGTTCATCTGCACCACCGGCAAGCTGCCCGTGCCCTGGCCCACCCTCGTGACCACCTT
 CACCTACGGCGTGCAGTGCTTCGCCCGCTACCCCGACCACATGAAGCAGCAGACTTCTTCAAGTCCGCCATGCCCGAA
 GGCTACGTCCAGGAGCGCACCATCTTCTTCAAGGACGACGGCAACTACAAGACCCGCGCCGAGGTGAAGTTCGAGGGCG
 ACACCCTGGTGAACCGCATCGAGCTGAAGGGCATCGACTTCAAGGAGGACGGCAACATCCTGGGGCACAAGCTGGAGTA
 CAACTACAACAGCCACAAGGTCTATATCACCGCCGACAAGCAGAAGAACGGCATCAAGGTGAAC TCAAGACCCGCCAC
 AACATCGAGGACGGCAGCGTGCAGCTCGCCGACCACTACCAGCAGAACACCCCCATCGGCGACGGCCCCGTGCTGCTGC
 CCGACAACCACTACCTGAGCACCCAGTCCGCCCTGAGCAAAGACCCCAACGAGAAGCGCGATCACATGGTCTGCTGGA
GTTCGTGACCGCCGCGGGATCACTCTCGGCATGGACGAGCTGTACAAGGTGACAGAGTTGCTGTACAGGATGAAGCGG
 GCCGAGACCTACTGTCCAAGGCCTCTGCTGGCAATTCACCCAACGGAGGCTCGGCATAAGCAAAGATTGTGGCCCCTG
 TCAAGCAGACTCTGAACCTCGATTTGCTCAAACCTGGCCGGCGATGTGGAGTCCAATCCGGGACCCGGAGACGCCCTCGT
 CTGGGTCTCCTGCCAAGAGAGCCTCGGGCTGGGTCTCCTGCCATGAGAGCCCCGGAGCAGCTGGGGCTCAGGAGGATG
 CCCTGAGGCAACAGCGGCCACACAGACGAGGGGCAAAGGCTCCAGATGTTCTTCTCCTGAGCCCAGCAGCAGGGTCT
 TCTCTGTGGCCAGGGCCACCCTGGGCCTCTGGGGTCCAATGTCCAACAACCCCCGGGCCCTCCCCGGGCTCAGTCTGAG
 AGGGTCCCAGAGACTTAACGGGGTGCCAGTTCTTGCTGGGGTCTCTC

Homology arms for L-HVR replacement with inserted mTurquoise2 and F2A

Fragments of DNA as inserted in the into pSC-B-amp/kan plasmid (Agilent Technologies) and used for ligation mediated assembly of repair template plasmids for H-HVR and L-HVR replacement.

The sequences are marked as follows:

Introns: GTTATAT
 Exons in bold: **CCTTAAA**
 mTurquoise2: **ATGGTGA**
 F2A: **GTGACAG**
 Splice donor and acceptor sites: **GT AG**
 Silent changes to prevent re-targeting of repair template plasmid and modified genomic locus: **A**CTG**C**
 BsmBI restriction cassette: GGAGACGCCCTCGTCTCC
 BsmBI restriction sites: GAGACG and CGTCTC
 BbsI restriction sites: GAAGAC and GTCTTC
 Cas9/sgRNA sites: underlined

HBL-1_L_HA_mTurquoise2_F2A

CCATCATGCATTTAGGGAGCTGACTGGGCACAAGTTGGAGCAGAAAGAGAAAAATGAAACCACAGCCTTCTATTTTGT
 TCTAACAGACTTGTACCAACATTCTGTGGCTCAATCTAGGTGATGGTGAGACAAGAGGACACAGGGGTTAAATTCTGT
 GGCCGCAGGGGAGAAGTTCTACCCCTCAGACTGAGCCAACGGCCTTTTCTGGCCTGATCACCTGGGCATGGGCTGCTGAG
 AGCAGAAAGGGGAGGCAGATTGTCTCTGCAGCTGCAAGCCAGCACCCGCCCCAGCTGCTTTGCATGTCCCTCCAGCC
 GCCCTGCAGTCCAGAGCCCATATCAATG**CCTGGGT**CAGAGCT**C**GGAGAAGAGCTGCTC**GGT****AGT****ACCCAGAGGGAAC**
CATGGTGAGCAAGGGCGAGGAGCTGTTACCGGGGTGGTGCCCATCCTGGTCGAGCTGGACGGCGACGTAAACGGCCAC
AAGTTCAGCGTGTCCGGCGAGGGCGAGGGCGATGCCACCTACGGCAAGCTGACCCTGAAGTTCATCTGCACCACCGGCA
AGCTGCCCCTGCCCTGGCCCACCTCGTGACCACCTGTCTGGGGCGTGCAGTGCTTCGCCCGCTACCCCGACCACAT
GAAGCAGCAGACTTCTTCAAGTCCGCCATGCCGAAGGCTACGTCCAGGAGCGCACCATCTTCTTCAAGGACGACGGC
AACTACAAGACCCGCGCCGAGGTGAAGTTCGAGGGCGACACCCTGGTGAACCGCATCGAGCTGAAGGGCATCGACTTCA
AGGAGGACGGCAACATCCTGGGGCACAAGCTGGAGTACAATACTTTAGCGACAACGTCTATATCACCGCCGACAAGCA
GAAGAACGGCATCAAGGCCAACTTCAAGATCCGCCACAACATCGAGGACGGCGGCGTGCAGCTCGCCGACCACTACCAG
CAGAACACCCCATCGGGCAGCGCCCGTGTCTGCTGCCGACAACCACTACCTGAGCACCCAGTCCAAGCTGAGCAAAG
ACCCCAACGAGAAGCGCGATCACATGGTCTCTGCTGGAGTTCGTGACCGCCGCCGGGATCACTCTCGGCATGGACGAGCT
GTACAAGGTGACAGAGTTGCTGTACAGGATGAAGCGGGCCGAGACCTACTGTCCAAGGCCTCTGCTGGCAATTACCCA
ACGGAGGCTCGGCATAAGCAAAAGATTGTGGCCCTGTCAAGCAGACTCTGAACTTCGATTTGCTCAAACCTGGCCGGCG
ATGTGGAGTCCAATCCGGGACCCGGAGACGCCCTCGTCTCC**ACGT**AAGTACATCTGTCTCAATTATTCGTGAGATTTTA
GTG**CA**CTG**A**ATCATTTGTGCAAATTTGTGATATTTTGGTTGAATAAACCTGGTGACCCAGAAGTAAATAGCAGGACA
CCAGAAAATGAACTTAAAAATCTGAGCAAATAGACGAATCATTTGGTTTGGAGGAGAATAGGATTCATGGGGAAATG
GGGAAGAAATAGCTAGATTTTCTCTGAACAAGCAGCCTATCTCGTATGATTGGCTTCAAGAGAAGTTTTTGTGAGGG
GAAAGGTGAGATCCCTCACTGTGACTCACTTTCGGCGGAGGGACCAAGGTGGAGATCAAACATAAGTGCATTTTCTTA
ATGCTTTTTCTTATAAGGTTTTAAATTTGGAGCATTTTTTGTGTTTGGAGATATTAGCTCAGG

OCI-Ly7_L_HA_mTurquoise2_F2A

GTATATTACTGATTAATATAGGTAAGAGGCGAGTTAAGAAATTGGGAATGCTTTCTCTTCTGCTTTCTTCTACGATGCAC
 AAGGCGTTTTACATTTATGCCCTATGAAAATTACTAGGCTGTCTAGTCATTAGATCTTTCAGCAGTTTGTAGTTTTTA
 GAGCTTCTAAGTTGACTTCTGTCTTTTCTATTTCATACAATTACACATTCTGTGATGATATTT**TTGGCTCTTGATTTACA**
TTGGGTACTTTTACAACC**CACTGCTCATGAAATTTGCTTTTGTACTCACTGGTTGTTTTTGCATAGGCCCTCCAGGCC**
ACGACCAGCTGTTTGGATTTTATAAACGGCCGTTTGCATTGTGA**ACTGAGCTACAACAGGC****GG****AGT****GGCAGCAAGA**
TGGTGAGCAAGGGCGAGGAGCTGTTACCGGGGTGGTGCCCATCCTGGTCGAGCTGGACGGCGACGTAAACGGCCACAA
GTTTCAGCGTGTCCGGCGAGGGCGAGGGCGATGCCACCTACGGCAAGCTGACCCTGAAGTTCATCTGCACCACCGGCAAG
CTGCCCGTGCCCTGGCCCACCTCGTGACCACCTGTCTGGGGCGTGCAGTGCTTCGCCCGCTACCCCGACCACATGA
AGCAGCAGACTTCTTCAAGTCCGCCATGCCGAAGGCTACGTCCAGGAGCGCACCATCTTCTTCAAGGACGACGGCAA
CTACAAGACCCGCGCCGAGGTGAAGTTCGAGGGCGACACCCTGGTGAACCGCATCGAGCTGAAGGGCATCGACTTCAAG
GAGGACGGCAACATCCTGGGGCACAAGCTGGAGTACAATACTTTAGCGACAACGTCTATATCACCGCCGACAAGCAGA

AGAACGGCATCAAGGCCAACTTCAAGATCCGCCACAACATCGAGGACGGCGGCGTGCAGCTCGCCGACCACTACCAGCA
 GAACACCCCATCGGCGACGGCCCCGTGCTGCTGCCCGACAACCACTACCTGAGCACCAGTCCAAGCTGAGCAAAGAC
 CCCAACGAGAAGCGCGATCACATGGTCCTGCTGGAGTTCGTGACCGCCGCCGGGATCACTCTCGGCATGGACGAGCTGT
 ACAAGGTGACAGAGTTGCTGTACAGGATGAAGCGGGCCGAGACCTACTGTCCAAGGCCTCTGCTGGCAATTCACCCAAC
 GGAGGCTCGGCATAAGCAAAAGATTGTGGCCCTGTCAAGCAGACTCTGAACTTCGATTTGCTCAAACCTGGCCGGCGAT
 GTGGAGTCCAATCCGGGACCCGGAGACGCCCTCGTCTCCACGTGAGTAGAATTTAAACTTTGCTTACTTAGCTGTCTGT
 GTCTTCTGTTCTCTAGCTATGAAGTGATCTATAAGTCGACTCTGCAATCAGCCTCTGATATCCTTCAGGGAAAAGAT
 AAAGATAAGTCTGTAGTCAAACCTCGAGAATTGATTGCACATTTTCTTTGAAGAGCAAGCAAGATTTCAGTCATTGGGTGA
 GAATAACTTGTCTAAGGAATAGCTTCAGAAATGTCCTGGGGAACAAAACATGTTCTGGACAGAGCCTTGGTCAATTGTC
 AGAAAGGGAGTTTTTGTCTAGGAGGGAACCTAAGAGGAACCATCGTGTGTACACTTTTGGCCAGGGGACCAAGCTGGAG
 ATCAAACGTTAGTACTTTTTTCTACTGATTCTTCACTGTTCC

OCI-Ly19_L_HA_mTruquoise2_F2A

CCCACCCTCTAAGACTTCATTAGACATTCCCTACGAATGGTTATACTCTCCTGTATACTCCCAATACAACCTCTAAAATA
 TATTATTCCATATAGTCTTAGGTTTGTATTAAAGTTTGACTTTTTTCCTTCAAATATCTCTTGTACACAACAGCGGCT
 CTAGAGAGAAAATACATTCCCTCCAGGCAAATCTATGCTGCGCTGGTCTGACCTGGGACCCTGGGGACATTGCCCTGTG
 CTGAGTTACTAAGATGAGCCAGCCCTGCAGCTGTGCTCAGCCTGCCCATGCCCTGCTGATTGATTGTCATGTTCCAGA
 GCACAGCCTCCTGCCCTGAAGACTTTTTTATGGGCTGGTGCACCCTGTGCAGGAGTCAGTCTCAGTCAGGACACAGCA
 TGGTGAGCAAGGGCGAGGAGCTGTTACCCGGGTGGTGCCCATCCTGGTTCGAGCTGGACGGCGACGTAAACGGCCACAA
 GTTCAGCGTGTCCGGCGAGGGCGAGGGCGATGCCACCTACGGCAAGCTGACCCTGAAGTTTCATCTGCACCACCGGCAAG
 CTGCCCGTGCCTGGCCACCCTCGTGACCACCCTGTCTGGGGCGTGCAGTGCTTCGCCCGCTACCCCGACCACATGA
 AGCAGCAGACTTCTTCAAGTCGCCATGCCCGAAGGCTACGTCCAGGAGCGCACCATCTTCTTCAAGGACGACGGCAA
 CTACAAGACCCGCGCCGAGGTGAAGTTCGAGGGCGACACCCTGGTGAACCGCATCGAGCTGAAGGGCATCGACTTCAAG
 GAGGACGGCAACATCCTGGGGCACAAGCTGGAGTACAATACTTTAGCGACAACGTCTATATCACCGCCGACAAGCAGA
 AGAACGGCATCAAGGCCAACTTCAAGATCCGCCACAACATCGAGGACGGCGGCGTGCAGCTCGCCGACCACTACCAGCA
 GAACACCCCATCGGCGACGGCCCCGTGCTGCTGCCCGACAACCACTACCTGAGCACCAGTCCAAGCTGAGCAAAGAC
 CCCAACGAGAAGCGCGATCACATGGTCCTGCTGGAGTTCGTGACCGCCGCCGGGATCACTCTCGGCATGGACGAGCTGT
 ACAAGGTGACAGAGTTGCTGTACAGGATGAAGCGGGCCGAGACCTACTGTCCAAGGCCTCTGCTGGCAATTCACCCAAC
 GGAGGCTCGGCATAAGCAAAAGATTGTGGCCCTGTCAAGCAGACTCTGAACTTCGATTTGCTCAAACCTGGCCGGCGAT
 GTGGAGTCCAATCCGGGACCCGGAGACGCCCTCGTCTCCACGTGAGTGGGATTTACACTTTGTTTCTTCACTTGTCTGT
 GTCTTTTGTTCCTGCTGATGAAGTGATATATAAGGTTAGTCTAGAAGCAGTCTGTGACATCCTTCAGGGAAAAGG
 TTGATAAGTCTGGAATCAAACCTCGAAAATTGATTACACATTTTTTTTTGAGGAATAATCAACCTTCAGGCATTGGGTGAG
 AATAAGTCGTCTACGTAATAATTTAGAGATGTCGTGGGGAACATAACATGTTCTGGACAGAACCCTGGTCAATTGTCAC
 AAAGGGAATTTTTGCATAGGAGGCAAAGTAAGTGAACCAACGTGTATAACTTTTTGGCCAGGGGACCAAG

SUDHL-4_L_HA_mTruquoise2_F2A

GGCTGTCTGCTCATCAGTGCTTGTAGGAAAGGGTAACGTTTCTTTTTTAGATTAGCTGGGAGGGAGCCAAGAAGAATG
 GCATTCATCCATATTCATTCTAGACATATCTCTACATTGTTAGGGTTGTTATGCTTTCCTAGAGTTGCATATCCTATAC
 AATGGGACCTACCCAAGATCCAACTGTCACAGTCAGATCCTTCCCTCCATTTTATATCACATTGCTCACAGGAGAGAC
 ATATCCCCTGCCCGCTGCCCATTTGACTCTTCCACACCACTGCATGCACCAGGGGATTTGCATATTGTCCCACAGGG
 AGGACCTTCCCTTGTGAGTCTGAGATAAAAGCTCAGCTGTAACCTGTGCCTTGACTGATCAGGACTCCTCAGTTCACCTT
 CTCACAATGGTGAGCAAGGGCGAGGAGCTGTTACCCGGGTGGTGCCCATCCTGGTTCGAGCTGGACGGCGACGTAAACG
 GCCACAAGTTTACGCTGTCCGGCGAGGGCGAGGGCGATGCCACCTACGGCAAGCTGACCCTGAAGTTTCATCTGCACCAC
 CGGCAAGCTGCCCGTGCCTGGCCACCCTCGTGACCACCCTGTCTGGGGCGTGCAGTGCTTCGCCCGCTACCCCGAC
 CACATGAAGCAGCAGACTTCTTCAAGTCCGCCATGCCCGAAGGCTACGTCCAGGAGCGCACCATCTTCTTCAAGGACG
 ACGGCAACTACAAGACCCGCGCCGAGGTGAAGTTCGAGGGCGACACCCTGGTGAACCGCATCGAGCTGAAGGGCATCGA
 CTTCAAGGAGGACGGCAACATCCTGGGGCACAAGCTGGAGTACAATACTTTAGCGACAACGTCTATATCACCGCCGAC
 AAGCAGAAGAACGGCATCAAGGCCAACTTCAAGATCCGCCACAACATCGAGGACGGCGGCGTGCAGCTCGCCGACCACT
 ACCAGCAGAACACCCCATCGGCGACGGCCCCGTGCTGCTGCCCGACAACCACTACCTGAGCACCAGTCCAAGCTGAG
 CAAAGACCCCAACGAGAAGCGCGATCACATGGTCCTGCTGGAGTTCGTGACCGCCGCCGGGATCACTCTCGGCATGGAC
 GAGCTGTACAAGGTGACAGAGTTGCTGTACAGGATGAAGCGGGCCGAGACCTACTGTCCAAGGCCTCTGCTGGCAATTC
 ACCCAACGGAGGCTCGGCATAAGCAAAAGATTGTGGCCCTGTCAAGCAGACTCTGAACTTCGATTTGCTCAAACCTGGC
 CGGCGATGTGGAGTCCAATCCGGGACCCGGAGACGCCCTCGTCTCCACGTGAGTGGGATTTACACTTTGTTTCTTCACTTGTCTGT
 TAAGTTTTACATTTGGAGTGTTTTTGTGTTTGGAGATATTAGTGCAGGTCAATTCGAAAAAGTACCACGTTCTTTCAAAA
 AGTCACATGAATAGGGGATAGAAAAATATTTCTTCTTGGAGAACAGGCAAGCGCTAGCCACTTAAATGAGGCATCCCA
 ATTGCAAGATTCTTCTGCATCGGTCAGGTCAGTGAAGTAACAGCGAAAAGAGAATCTTTTAAAGAAGAAAGAAATTA

ACTTGACACTGTGGATCACCTTCGGCCAAGGGACACGACTGGAGATTATACGTAAATAATTCTTCACTTTTGTCTTCTG
AAATTTGCGTCTGATGGCCACTATTGACTTTTAGAGGCTTAAATAGGAGTTTGGTGAAG

SUDHL-6_L_HA_mTruquoise2_F2A

CCTACCATCTAACATTTTACTATGTGTTTCTTACAAACAAGAATATTCTCCTAAATAATCTTGATACACCAATGAAAA
CATTACTCTATCGGCTCCTGAGGAATATTTAAAATTCTCAAAAAATACCTAAAAATTGTTTCTCTTAATAAAATAGTC
CCCAGTAGAAACACATTCTCTGCAGACAAATTTGTGCTACCTGGTCTTACCTGGGACACCTGGGGACACTGAGCTGGT
GCTGAGTTACTGAGATGAGCCAGCTCTGCAACTGTGCCAGCCTGCCCATCCCTGCTCATTTGCATGTTCCAGAGC
ACAACCTCCTGCCCTGAAGCCTTATTAATAGGCTGGTCACACTTTGCGAAGTAGTCAGACCCAGTCAGGACACAGCATG
GTGAGCAAGGGCGAGGAGCTGTTACCCGGGGTGGTGCCATCCTGGTCGAGCTGGACGGCGACGTAAACGGCCACAAGT
TCAGCGTGTCCGGCGAGGGCGAGGGCGATGCCACCTACGGCAAGCTGACCCTGAAGTTCATCTGCACCACCGCAAGCT
GCCCCTGCCCTGGCCACCCTCGTGACCACCCTGTCTGGGGCGTGCAGTGCTTCGCCCCTACCCCGACCACATGAAG
CAGCAGACTTCTTCAAGTCCGCCATGCCGAAGGCTACGTCCAGGAGCGCACCATCTTCTTCAAGGACGACGGCAACT
ACAAGACCCGCGCGAGGTGAAGTTCGAGGGCGACACCCTGGTGAACCGCATCGAGCTGAAGGGCATCGACTTCAAGGA
GGACGGCAACATCCTGGGGCACAAGCTGGAGTACAATACTTTAGCGACAACGTCTATATCACCGCCGACAAGCAGAAG
AACGGCATCAAGGCCAACTTCAAGATCCGCCACAACATCGAGGACGGCGGGCTGCAGCTCGCCGACCACTACCAGCAGA
ACACCCCATCGGCGACGGCCCCGTGCTGCTGCCGACAACCACTACCTGAGCACCCAGTCCAAGCTGAGCAAAGACCC
CAACGAGAAGCGCGATCACATGGTCTGCTGGAGTTCGTGACCGCCGCGGGATCACTCTCGGCATGGACGAGCTGTAC
AAGGTGACAGAGTTGCTGTACAGGATGAAGCGGGCCGAGACCTACTGTCCAAGGCCTCTGCTGGCAATTCACCCAACGG
AGGCTCGGCATAAGCAAAGATTGTGGCCCTGTCAAGCAGACTCTGAACTTCGATTTGCTCAAACCTGGCCGGCGATGT
GGAGTCCAATCCGGGACCCGGAGACGCCCTCGTCTCCACGTGAGTAGAATTCGGACTTTGCCTACTGACTTGTCTGTGT
ATTCGGTTCACTAGGTCTGTGAAGTGATCTATAACGTGACTCGGCAATCGGCCTCTGATCTCCTTCAGGCAAAGATAA
AAATAAGTCTGTGTCAAACCTCGAGACTGGGTGCACATCTTCTTTGAAGAGCAGGCAAGGCAACATTCAGTCATTGGG
TGAGAATACTTTGTCTAAGCATTGACTTCAGGAGTGTCTGGGGAACATAACATGTTCTGGAGACAGTCTCGGGCAATT
GTCAAAGGGGAATTTTCTTTAGGAGGGAAGTTAAGAGGAACCCTTGTGTAAACACTTATGACCAGGGGACCAAGGTG
GAGTCAAAGGTAAGTACTTTTTTCACTGATTCTTCATGG

U2932_L_HA_mTruquoise2_F2A

CCATCATGCATTTAGGGAGCTGACTGGGCACAAGTTGGAGCAGAAAGAGAAAAATGAAACCACAGCCTTCTATTTTGT
TCTAACAGACTTGTACCAAACATTTCTGTGGCTCAATCTAGGTGATGGTGAGACAAGAGGACACAGGGGTTAAATTTCTGT
GGCCGAGGGGAGAAGTTCTACCCTCAGACTGAGCCAACGGCCTTTTCTGGCCTGATCACCTGGGCATGGGCTGCTGAG
AGCAGAAAGGGGAGGAGATTGTCTCTGCAGCTGCAAGCCAGCACCCGCCCCAGCTGCTTTGCATGTCCCTCCCAGCC
GCCCTGCAGTCCAGAGCCATATCAATGCCTGGGTGAGAGCTCTGGAGAAGAGCTGCTCAGTAGTACCTACCCG
CATGGTGAGCAAGGGCGAGGAGCTGTTACCCGGGGTGGTGCCATCCTGGTCGAGCTGGACGGCGACGTAAACGGCCAC
AAGTTCAGCGTGTCCGGCGAGGGCGAGGGCGATGCCACCTACGGCAAGCTGACCCTGAAGTTCATCTGCACCACCGGCA
AGCTGCCCGTGCCCTGGCCACCCTCGTGACCACCCTGTCTGGGGCGTGCAGTGCTTCGCCCCTACCCCGACCACAT
GAAGCAGCAGACTTCTTCAAGTCCGCCATGCCGAAGGCTACGTCCAGGAGCGCACCATCTTCTTCAAGGACGACGGC
AACTACAAGACCCGCGCGAGGTGAAGTTCGAGGGCGACACCCTGGTGAACCGCATCGAGCTGAAGGGCATCGACTTCA
AGGAGGACGGCAACATCCTGGGGCACAAGCTGGAGTACAATACTTTAGCGACAACGTCTATATCACCGCCGACAAGCA
GAAGAACGGCATCAAGGCCAACTTCAAGATCCGCCACAACATCGAGGACGGCGGGCTGCAGCTCGCCGACCACTACCAG
CAGAACACCCCATCGGCGACGGCCCCGTGCTGCTGCCGACAACCACTACCTGAGCACCCAGTCCAAGCTGAGCAAAG
ACCCCAACGAGAAGCGCGATCACATGGTCTGCTGGAGTTCGTGACCGCCGCGGGATCACTCTCGGCATGGACGAGCT
GTACAAGGTGACAGAGTTGCTGTACAGGATGAAGCGGGCCGAGACCTACTGTCCAAGGCCTCTGCTGGCAATTCACCCA
ACGGAGGCTCGGCATAAGCAAAGATTGTGGCCCTGTCAAGCAGACTCTGAACTTCGATTTGCTCAAACCTGGCCGGCG
ATGTGGAGTCCAATCCGGGACCCGGAGACGCCCTCGTCTCCACGTGAGTAGAATTTAAAGTTGCTTACTTAGTTGTCT
GTGCTTTCTGCTCCGGTGTCTATGAAGTGATCTATAAACTGACTCTGCAATCAGCCTCTGATATCCTTCAGGAAAAG
AAAAAGATAAGTCTGTAGTCAAACCTCGAGAATTGATTGCACATTTTCTTTGAAGAGCAAGCAAGATTTCAGTCATTGGGT
GAGAATAACTTGTCTAAGTAATAGCTTCAGAAATGTCCTGGGGAACATAACATGTTCTGGACAGAGCCTTGGTCAATTG
TCAGAAAGGGAGTTTTTGTATAGGAGGGAAGTTAAGAGGAACCATTGTGTGTACTTTTTGGCCAGGGGACCAAGCTGG
AGATCAAACGTAAGTACTTTTTTCACTGATTCTTCACTGTTGCTA

H-HVR fragments

Fragments of DNA as inserted in the into pSC-B-amp/kan plasmid (Agilent Technologies) and used for ligation mediated assembly of repair template plasmids for H-HVR replacement.

The sequences are marked as follows:

Introns: GTTATAT

Exons in bold: **CCTTAAA**

F2A: GTGACAG

Splice donor and acceptor sites: **GT AG**

Silent changes to prevent re-targeting of repair template plasmid and modified genomic locus: **ACTGC**

Silent mutations to disrupt restriction enzyme site: **T**

BsmBI restriction sites: GAGACG and CGTCTC

BbsI restriction sites: GAAGAC and GTCTTC

Cas9/sgRNA sites: underlined

HBL-1_H-HVR

GGACACTGA**GAAGACCT**ACCC**AAACACCTGTGGTTCTTCTCCTCCTGGTGGCAGCTCCCGGAT****GT**GAGTGTCTCAGGA
 ATGCGGATATGAAGATATGAGATGCTGCCTCTGATCCCAGGACTACTGTGGGTTTCTCTGTTCCAC**AG**GGGTCCTGTCC
 CAGGTGCAGCTACAGCAGTGGGGCGCAGGACTGTTGAAGCCTTCGGAGACCCTGTCCCTCACTTGC**CGCTGTCTATGGTG**
GGTCCTTCACTGATTACTACTGGACCTGGATCCGTCAGTCCCAGGAAAGGGGCTGGAGTGGATTGGGGAAATCAATCG
TAGTGGAAAGTACCGACTACAACCCGTCCTCAAGAGTCGAGTCACCATATCACTAGACACGTCCAAGAACCAATTCTCC
CTGCATCTGACCTCTGTGACCGCCGCGGACACGGCTCTATATTACTGTGCGGGGGGACAAGACTACGGTACTATGTTA
GGGGGGTAGTACTACTGGGGCCAGGAAACCTGGTCACCGTCTCCTCAG**GTGGGTCTTC**GACC

OCI-Ly7_H-HVR

GGAA**CGTCTCC**ACCC**GACTGGACCTGGAGGTTCTCTTTGTGGTGGCAGCAGCTACAG****GT**AAGGGGCTTCTAGTCCTA
 AGGCTGAGGAAGGGATCCTGGTTTAGTTAAAGAGGATTTTATTCACCCCTGTGTCCTCTCCAC**AG**GTGTCCAGTCCCAG
 GTACAGTTGGTGCAGTCTGGGGCTGAGGTGAAGAAGCCTGGGTCCTCGGTGAATGTCTCCTGCAAGACTTCTAGAGACA
 CCTTCAGCAGCTATGCTATCAACTGGGTGCGACAGGCCCTGGACAAGGGTTTGGAGTGGATGGGAGGGATCATCCCTAT
 CGTTGGTACAGCAA**ACTACACACAGAAGTTC**CAGGGCAGAGTCACGATTACCGCGGACGAATCCACGAGCACAA**CTAC**
ATGGAACTGAGCAGCCTGACATATGAAGACACGGCCGTTTATTACTGTGTGACCGGCCCGGGGGCTGTTTGGAG**CG**
CTGGGGACAGGGAAT**ACTGGTCA**AGT**TCCTCAG****GTGGAGACGAAACC**

OCI-Ly19_H-HVR

GGATGT**CGTCTCC**ACCC**AAGTTGGGGCTGTGCTGGGTTTCTTGTGGTATTTTAGAAG****GT**GATTCATGGAAA**ACTAG**
 AGAGATTTAGTGTGTGGATATGAATGAGACAAACAGTGGATATGTGTGGCAGTTTCTGATTTTGGTGTCTCTTTGTT
 TGC**AG**GTGTCCAGTGTGAAGTTGAGTTGGTGGAGTCTGGGGGAGGGTTGGTACAGCCTGGGGGGTCTT**GAGACTCTCC**
TGTGAAGTCTCTGGATTACCTTCAATACCTATACTATGAGCTGGGTCCGCCAGGCTCCAGGTAAGGGGCTGGAGTGGG
TTTCAAATATTAGTAGTAGTAGTAGTGCATATACTATGCAGGCTCTGTGAAGGGCCGATTATCATCTCCAGAGACAA
TGCCAAAAACTCATTATATCTGCAAATGAACAACCTGAGAGCCGAGGACACGGCTGTCTATTTCTGTGCGCGAGCGTCT****
TATGATTCGGGACTTATTTCCACGACTACTGGGGCCAGGGAAC**ACT**CGTCA**AGT**CTCTCCTCAG**GT**GGAGACGACC****

SUDHL-4_H-HVR

GGAC**GAAGACCT**ACCC**AAACATCTGTGGTTCTTCTCCT****GTCTGGT****GTGGCAGCTCCCAGAT****GT**GAGTGTCTCAGGGATCCA
 GACATGGGGATATGGGAGGCGCCTCTGATCCCAGGGCTCACTGTGGGTCTCTCTGTTCCAC**AG**GGGTCCTGTCCAGATG
 CACCTGCAGGCGTGGGGCCGGACTGCTGAAGCCTTCGGAGACCCTGTCCCTCACCTGC**ACTGTCTCTGGTGGCTCCA**
TCAGTAGTTACTCTGGACTTGGATCCGGCAGCCCCAGGGAGGGGGCTAGAGTGGATTGGGAATATCTCTTATAGTGA
AACCGACTACAATCCCTCCCTCAAGAGTCGAGTCACCATGTCACTGGACATGTCCAAGAATGAGTTCTCCCTGAAGTTG
GGCTCTGTGACCGCCGCTGACACGGCCATCTATTACTGCGCGAGACGGAGCCCTGAC**CTATGG****CACA**ACTTTGACTTCT****
GGGGCCAGGGAACCTGGTCACCGTCTCCTCAG**GTGGGTCTTC**GACC

SUDHL6-H-HVR

GGACGAAGACCTACCCGAGTTGGGGCTGTGCTGGGTTTTCTTGTTGCTATTTTAGAAGGTGATTCATGGAAAACCTAGAGAGATTTAGTGTGTGTGGATATGAGTGAGAGAAACAGTGGATATGTGTGGCAGTTTCTGACCTTGGTGTCTCTTTGTTTGCAGGTGTCCAGTGTGAAGTGCAGATGGTGGAACTCTGGGGGAACCTTGGTACACCCGGGGGGTCCCTGAGACTCTCCTGTACAGCCTCAGAATTTAATTTAATTCCTATACTATTAATTGGGTCCGCTGCCTCCAGGGAAGGGCCTAGAGTGGATTGCAAATATAAGTAGTACTGGCAGTGACATATATTATGTAGACTCTTTGAAGGGCCGGTTCACCATCTCCAGAGACAATGCCAAGAATTCGGTATATCTCCAAATGACTGGTCTGAAAGACGAGGACACGGCTGTCTACTATTGTGCGACGGGGGGAACTGGACTCCACCAGGGGTCTTCTTTACTGGGGCTGGGAACCTGGTACAGTCTCCTCAGGTGGTCTTCGACC

TMD8_H-HVR

GGAAACGTCCTCCACCCGATTTGGGGCTGTGCTGGGTTTTCTTGTTGCTATTTTAGAAGGTGATTCATGTAACACTGGAGAGACTTAGTCTGTGTGGATAGGAGTGAGAAAAAGAGAGGATATGTGCGGCAGTTTGTGACCTTGGTGTCTTTTTCTTTACAGGTGGCCAGTGTAGAGTGCAACTGGTGGAGTCTGGGGGAGACCTGGTACAGTCGGGGGGTCCCTGAGACTCTCCTGTAGCCTCTGGATTCACCTTTAGTTCTTACAGTATGAACTGGGTCCGCCAGGCTCCAGGAAAGGGACTGGACTGGGTCATATATATTAGTGGTACTAGTGGAACCATATACTACACAGACTCTGTGAAGGGCCGATTATCATCTCCAGAGACAATGCGAAGAATTCGCTATATTTACAAATGAACAGCCTGAGAGATGATGACACGGCTGTCTATTATTGTGTGAGAGATCGGGTGGGGGTAACCCATGGGGCCGCGGAACCTGGTACCCTGTCCCTCAGGTGGAGACGAAACC

U2932_H-HVR

GGACGAAGACCTACCCAAGCACCTGTGGTTCTTCTCCTGCTGGTGGCGGCTCCAGATGTGAGTGTCTTAGGATGCAGACATGGAGATATGGGAGACTGCCTCTGATCCCAGGGCTCACTGTGGGTTTTCTGTTCACAGGGTCTGTCCAGCTGCAGCTGCAGGAGTCGGGCCAGGACTGGTGAAGCCTTCGGAGACCCTGTCCCTCACCTGCAGTGTCTCTCGTGTCTCCATCAGCAGTAGTAATTACTACTGGGGCTGGATCCGCCAGCCCCAGGGAAGGGGCTGGAATGGATTGGGAGTGACTATTATGGTGGCAGTACCTCCTACAACCCGTCCCTCAAGGGTCGAGTCATTATATCCGTAGACACGTCCAAGAACCATTCTCCCTGAAACTGACCTCTGTGACCGCCGACACAGGCTCTATATTACTGTGCGAGAGCGCTGTCTTACTATGATACTGGTGGTTTCAGGTACTTCTTCGATTAATGGGGCCAGGGAACCTGGTACAGTCTCCTCAGGTGGTCTTCGACC

L-HVR fragments

Fragments of DNA as inserted in the into pSC-B-amp/kan plasmid (Agilent Technologies) and used for ligation mediated assembly of repair template plasmids for L-HVR replacement.

The sequences are marked as follows:

Introns: GTTATAT

Exons in bold: **CCTTAAA**

F2A: GTGACAG

Splice donor and acceptor sites: **GT AG**

Silent changes to prevent re-targeting of repair template plasmid and modified genomic locus: **ACTGC**

BsmBI restriction sites: GAGACG and CGTCTC

Cas9/sgRNA sites: underlined

HBL-1_L-HVR

GGAA**CGTCTCC**ACCC**GAGAC**CC**GCGCAGCTTCTCTTCTCCTGCTACTCTGGCTCCCAG****GT**GAGGGGAACATGGGAT
GGTTTTGCATGTCAGTGAAAACCCCTCTCAAGTCCTGTTACCTGGCAACTCTGCTCAGTCAATACAATAATTAAAGCTCT
GTATAAAGCAATAATTCTGGCTCTTCTGGGAAGACAATGGGTTTATTGATTACATGGGTGACTTTTTCTGTTTTATT
TCCAATCTC**AG**ATACCACCGGAGAAATTGTGTTGACGCAGTCTCCAGGCACCC**TGTCTTTGTCTCCAGGGGAAAGAGCC**
ACCCTCTCCTGCAGGGCCAGTCAGAGTATTAGCAGCAACTACTTAGCCTGGTTCCAGCTGAAAGGTGGCCAGGCTCCCA
GGCTCCTCATCTTTGGTGCATCCAACAGGGCCACTGGCATCCAGACAGGTTCCAGTGGCAGTGGGTCTGGGACAGACTT
CACTCTCACCATCAGCAGACTGGAGCCTGAAGATTTTGCAGTGTATTACTGTCAGCAGTATGGTAGCTCACCGATCACT
TTCGGCCCTGG**ACA****AAG****GTGGATATCAAAC****GT**GGAGACGAAACC

OCI-Ly7_L-HVR

GGAA**CGTCTCC**ACCC**GTGTTGCAGAC****A****CAGGCTTTCATTTCTCTGTTGCTCTGGATCTCTG****GT**GAGGAATTAAAAAGTG
CCACAGTCTTTTTCAGAGTAATATCTGTGTAGAAATAAAAAAATTAAGATATAGTTGGAAATAATGACTATTTCCAATA
TGGATCCAATTATCTGCTGACTTATAATACTACTAGAAAGCAAATTTAAATGACATATTTCAATTATATGTGAGACAGC
GTGTATAAGTTTATGTATAATCATTGTCCACTACTGACTAC**AG****GTGCCTACGGGGACATCGTGTATGACCCAGTCTCCAG**
ACTCCCTGGCTGTGTCTCTGGGCGAGAGGGCCACCATCAACTGCAAGTCCAGCCAGACTGTTTTATACGGCTCCAACAA
TAAAACTACTTAGCTTGGTACCAACAGAAACCAGGACAGCCTCCTAAGTTGCTCATTTACTGGGCATCTACCCGGGAA
TCCGGGGTCCCTGACCGATTTCAGTGGCAGCGGGTCTGGGACAGATTTTCAGTCTCACCATCAGCAGCCTGCAGGCTGAAG
ATGTGGCAGTTTATTACTGTCAGCAATATTATAGTAA**CCCCCTGGAC****CTT****GG****CAAGGGACCAAGGTGGAAATCAA****AC**
TGGAGACGAAACC

OCI-Ly19_L-HVR

GGAA**CGTCTCC**ACCC**GACATGAGGGTCCCCGCTCAGCTCCTGGGGCTCCTGCTACTCTGGCTCCGAG****GT**AAGGATGGAG
AACACTAGGAATTTACTCAGCCAGTGTACTCAGTACTGA**TCGA****AC**CTTCAGGGAAAATCTCTGATAACATGATTAGTAG
TAAAAATCTTTGTTTTTATGTTTTCACTTTC**AG****GTGCCAGATGTGACATCCAGATGACCCAGTCTCCCTCGTCCCTGTC**
AGCATCTGTAGGAGACAGAGTCACTATCACTTGCCGGGCAAGTCAGAATATTAGGACCAATTTAAATTGGTATCAACAA
AAACCAGGGAGGGCCCCTAAGGTCCTGATCTATGCCGCTTCCAGTTTGCAAAGTGGAGTCCCATCAAGATTCAGTGGCA
GTGGATCTGGGACATATTTCACTCTCACCATTAGCAGTCTGCAGCCTGAGGATTTTGCAACTTTCTATTGTCAACAGAC
GTACAGTTTCGTCTGGACGTTCCGGCCAAGG**ACA****AA****AGTGGAAATCAGAC****GT**GGAGACGAAACC

SUDHL-4_L-HVR

GGAA**CGTCTCC**ACCC**AGGCTCCCTGCTCAGCTCCTGGGGCTGCTAATGCTCTGGGTCTCTG****GT**AAGAAAAGAAGGAGAT
GAGGAAGGAGAATAGGGTGGGAGGGTGGAGCTCTAGGGCTCCACAGCATCCCATGATCCCATGTTTGTAGTCTTAC**ACTGG**
TTAGAGGAGCATCATCTGTGCTGTAGAAAAGGGAACTTGATATTTTGTCTCTGTGAATAATTAGAAGCCTCATACTAAT
ATGACGTATG**TT**GTCTCTGATTAAGATCTTCAAAAATATTTAGGTCTCTTATACTTAACAAAAATGAATTCATTTTAGAG
TGTGTATTTTAAAGGCATAAATCACTATTTTTTATAATTAAGTTTAAATAAATGACATAAGATGAATTATGAAAATTGC
TCATTAGGTTTCTACATCACTTTGCAATTCATTATTT**AG****GCTCCGCTGGGGACATTGTGCTGACTCAGTCTCCACTCT**
CCCTGTCCGTACCCCTGGAGAGCCGGCCTCCATCTCCTGCAGGCTAGTCAGAGTCTCCTATATACTAGTGGACAGCA
TTATTTGAATTGGTACGTCCAGAAGCCAGGGCAGTCTCCACAACCTTTGATCTATTTGGTTTCTAATCGGGCTCCGGG

GTCCCTGACAGGTTCCGGTGGCAGTGGATCAGGCACAGATTTTACACTAAAAATCAGCAGAGTGGAGGCTGACGATGTTG
 GGGTTTATTACTGTATGCAAGCCGTACAACTCCTCTCACCTTGGAGGAGGGACAAAAGTCGAGATCAAACGTGGAGA
 CGAAACC

SUDHL-6_L-HVR

GGAACGTCTCCACCCGACATGAGGGTCCCCGCTCAGCTCCTGGGGCTCCTGCTGCTCTGGCTCCAGGTAAAGGAAGGAG
 AACACTAGGAATTTACTCAGCTCACTGTACTCAGTACTGCCTGGTTATTTCAGGGAAGTCTTCCTATAACATGATCAAAA
 GTAACAAAATATGTGTCTCCATTTCCAATCTCAGGTGCCAAATGTGACATCCAGATGACCCAGTCTCCTTCCACCCTGT
 CTGCATTTGTAGGAGACAGAATCACCATAACTTGCCGGGCCAGTCAGAGTATTTATAACTGGTTGGCCTGGTATCAACA
 AAAACCAGGGAGAGCCCCAAAAGTCCTCGTCTATAAGGCGTCTAATTTACAAGGCGGCGTCCCATCAAGGTTTCAGCGGC
 AGTGGATATGGGACAGAATTCAGTCTCACCATCAGCAGCCTGCAGCCTGAGGATTTTGCAACATATTACTGCCAACAGT
 ATCAGAGTTATTCGTGGACTTTCGGCCAAGGGACCAAGGTGGAGATGAAACGTGGAGACGAAACC

TMD8-L-HVR

GGAACGTCTCCACCCAGGCTCCCTGCTCAGCTCCTGGGGCTGCTAATGCTCTGGGTCCAGGTAAAGGGTAGAAGGGAGA
 TGAGGGAGGAGAAATGGCATGGAGCGGTGACTTCTGGGGCCCCACTGCCTCTAACAACAGTCATCTCTGGGGGTCTCACT
 AACTCCTATGTGTGTTTCTTTCTATATTGGACATGTACATGTTGTCTCCAAAAACAAAGATCTGTGTGTGGGGAAG
 ACTGATACTAAAACGGGATGATGTGGGGTCTTCTGGGGACCCCTTTGAGGCTTGGATCCCTTGAGTTGCACTTTGAAAC
 TGTGTTTTTTTTGAGACATGGATAGATATGTGTGTAGCCTGAAATAAAGAAGAGATCCAAGTTTATGAAAATTACAGATG
 AGCTTTATACATAGGCTTCTTATTCTTTCCAATTATTGTAGATCCAGTGGGAATGTGGTGTGACTCAGTCTCCACTC
 TCCCTCTCCGTCACCCTAGGACAGCCGGCCTCCATCTCCTGCATGTCTAGTCGAAGTCTCGTACACAGTGATGGAACA
 CTTATTTGAATTGGTTTTCATCAGAGGCCAGGCCAATCTCCGAGGCGCCTAATTTATAAAGTTTCTAACCGGGACTCTGG
 GGTCACAGACAGATTCAGTGGCAGTGGGTGAGCACCATTTCACACTGAAGATCAGCAGGGTGGAGGCTGAGGATATT
 GGGTTTATTATTGTATGCAAGCTACACACTGGCCTCCGTGGACGTTTCGGCCAAGGGACCAAGGTGGAAATTCACCTG
 GAGACGAAACC

U2932_L-HVR

GGAACGTCTCCACCCGAAACCCAGCGCAGCTTCTCTTCTCCTGCTACTCTGGCTCCAGGTGAGGGGAACATGGGAT
 GGTTTTGCATGTCAGTGAAAACCTCTCAAGTCTGTTACCTGGCAACTCTGCTCAGTCAATTCATAAATTAAGCTCA
 ATATAAAGCAATAATTCTGGCTCTTCTGGGGAGACAATGGGTTTGATTTAGATTACATGGGTGACTTTTCTGTTTTATT
 TCCAATCTCAGATACCACCGGAGAAATTGTGTTGACGCAGTCTCCAGGCACCCGTCTTTGTCTCCAGGGGAAAGAGCC
 ACCCTCTCCTGCAGGGCCAGTCAGAGTGTAGCAGCAGCTACTTAACCTGGTACCAGCAGAAACCTGGCCAGGCTCCCA
 GGCTCCTCATCTATGGTTCGTTCCAACAGGGCCACTGGCATCCAGACAGGTTTCAGTGGCAGTGGGTCTGGGACAGACTT
 CACTCTCACCATCAGCAGACTGGAGCCTGAAGATTTTGAGTGTATTACTGTCAGCAGTATCGTAGCTCACCTCCGACG
 TGGACGTTTCGGCCAAGGGACAAAAGTCGAGATCAAACGTGGAGACGAAACC

U2932 somatic hypermutation reverted HVR fragments

Fragments of DNA as inserted in the into pSC-B-amp/kan plasmid (Agilent Technologies) and used for ligation mediated assembly of repair template plasmids for L-HVR and H-HVR replacement.

The sequences are marked as follows:

Introns: GTTATAT

Exons in bold: **CCTTAAA**

F2A: GTGACAG

Splice donor and acceptor sites: **GT AG**

Silent changes to prevent re-targeting of repair template plasmid and modified genomic locus: **ACTGC**

BsmBI restriction sites: GAGACG and CGTCTC

BbsI restriction sites: GAAGAC and GTCTTC

U2932_H-HVR_reveted

GGAC**GAAGACCT**ACCC**AAGCACCTGTGGTTCTTCCTCCTGCTGGTGGCGGCTCCCAGAT****GT**GAGTGTTTCTAGGATGCA
 GACATGGAGATATGGGAGGCTGCCTCTGATCCCAGGGCTCACTGTGGGTTTTTCTGTTCAC**AG**GGGTCTGTCCCAGCT
GCAGCTGCAGGAGTCGGGCCAGGACTGGTGAAGCCTTCGGAGACCCTGTCCCTCACCTGCACCTGTCTCTGGTGGCTCC
ATCAGCAGTAGTAGTTACTACTGGGGCTGGATCCGCCAGCCCCAGGGAAGGGGCTGGAGTGGATTGGGAGTATCTATT
ATAGTGGGAGCACCTACTACAACCCGTCCCTCAAGAGTCGAGTCACCATATCCGTAGACACGTCCAAGAACCAGTTCTC
CCTGAAGCTGAGCTCTGTGACCGCCGAGACACGGCTGTGTATTACTGTGCGAGAGCGCTGTATTACTATGATAGTAGT
GGTTTCAGGTACTACTTTGACTACTGGGGCCAGGGAACCCTGGTCACCGTCTCCTCAG**GT**GGTCTTCGACC

U2932_L-HVR_reverted

GGAACGTCTCCACCC**GAAACCCAGCGCAGCTTCTCTTCCTCCTGCTACTCTGGCTCCCAG****GT**GAGGGGAACATGGG
 ATGGTTTTGCATGTCAGTGAAAACCCCTCTCAAGTCCTGTTACCTGGCAACTCTGCTCAGTCAATACAATAAT
 TAAAGCTCAATATAAAGCAATAATTCTGGCTCTTCTGGGAAGACAATGGGTTTGATTAGATTACATGGGTG
 ACTTTTCTGTTTTATTTCCAATCTC**AG**ATACCACCGAGAAATTGTGTTGACGCAGTCTCCAGGCACCCTGTCTTT
GTCTCCAGGGGAAAGAGCCACCCTCTCCTGCAGGGCCAGTCAGAGTGTTAGCAGCAGCTACTTAGCCTGGTACCAGCAG
AAACCTGGCCAGGCTCCCAGGCTCCTCATCTATGGTGCATCCAGCAGGGCCACTGGCATCCCAGACAGGTTTCAGTGGCA
GTGGGTCTGGGACAGACTTCACTCTCACCATCAGCAGACTGGAGCCTGAAGATTTTGCAGTGTATTACTGTCAGCAGTA
TGGTAGCTCACCTCCGACGTGGACGTTCCGCCAAGGGAC**AAA****GT****C**GAAATCAAAC**GT**GGAGACGAAACC

Tetanus Toxoid recognizing HVR fragments

Fragments of DNA as inserted in the into pSC-B-amp/kan plasmid (Agilent Technologies) and used for ligation mediated assembly of repair template plasmids for L-HVR and H-HVR replacement.

The sequences are marked as follows:

Introns: GTTATAT

Exons in bold: **CCTTAAA**

F2A: GTGACAG

Splice donor and acceptor sites: **GT AG**

Silent changes to prevent re-targeting of repair template plasmid and modified genomic locus: **ACTGC**

BsmBI restriction sites: GAGACG and CGTCTC

TET-H-3-HVR

GGAA**CGTCTCC**ACCC**GACTGGACCTGGAGGATCCTCTTTTTGGTGGCAGCAGCCACAG**GTAAAGGGCTGCCAAATCCCA
GTGAGGAGGAAGGGATCGAGGCCAGTCAAGGGGAATTCCATCCACTCCTGTGTCTTCTCTAC**AGGTGCCACTCCAGG**
TCCAGCTGGTACAGTCTGGAGCTGAGGTGAAGAAGCCTGGGGCCTCAGTGAGGGTCTCCTGCAAGGCTTCTGGATACAC
CTTCACTAGGTATGCTATGCATTGGGTGCGCCAGGCCCCCGGACAAAGGCTGAGTGGATGGGCTGGATCAACGTTGAC
AATGGAAACACAGAATATTCACAGAAATTCAGGGCAGACTCACCATTACCAGGGACACATCCGCGAGCACAGCCTACA
TGGAGCTGAGCAGCCTGACCTCTGACGACACGGCTGTATATTACTGTGCGAAAGATCGGGTCCGCGTAGTACAAGCTGC
GACCACCCTTGACTTCTGGGGCCAGGGAAC**ACTGGTCACAGTCTCCTCAG**GTGGAGACGAAACC

TET-L-3-HVR

GGAA**CGTCTCC**ACCC**GAAACCCAGCGCAGCTTCTCTTCTCCTGCTACTCTGGCTCCAG**GTGAGGGGAACATGGGAT
GGTTTTGCATGTCAGTGAAAACCCCTCTCAAGTCCCTGTTACCTGGCAACTCTGCTCAGTCAATAACAATAATTAAAGCTCA
ATATAAAGCAATAATTCTGGCTCTTCTGGGAAGACAATGGGTTGATTTAGATTACATGGGTGACTTTTCTGTTTTATT
TCCAATCTC**AGATACCACCGGAGAAATTGTATTGACACAGTCTCCAGGCACCCTGTCTTTGTCTCCAGGGGAAAGAGCC**
ACCCTCTCATGTAGGGCCAGTCAGACTATTTCCAGCAAGTACTTAGGCTGGTACCAGCAGAAACTTGGCCAGGCCTCCCA
GGCTCCTCATCTATGGTGCATCCAGCAGGGCCACTGGCATCCAGACAGGTTTCAAGTGGCAGTGGGTCTGGGACAGACTT
CACTCTCACCATCAGCAGACTGGAGCCTGAAGATTTTGCAGTGTATTACTGTGTCAGCAGTATGGTAGTTTATCAGCGATC
ACCTTCGGCCAAGGGACACGACTGGAGATTAACGTGGAGACGAAACC

TET-H-6-HVR

GGAA**CGTCTCC**ACCC**GACTGGACCTGGAGCATCCTTTTTCTTGGTGGCAGCAGCAACAG**GTAAACGGACTCCCCAGTCCCA
GGGCTGAGAGAGAAACCAGGCCAGTCAATGTGAGACTTCACCCACTCCTGTGTCTTCTCCAC**AGGTGCCACTCCAGGT**
GCAGCTGGTGAATCTGGAAGCGAGGTGCGGAAGCCTGGGGCCTCAGTGAAGTCTCCTGCAAGGCTCTGGTTACACC
TTTTCCCGCTACGGCCTCACCTGGGTGCGACAGGCCCTGGACAAGGACTTGAATGGATGGGATGGATCAGCGGTTACA
ATAGCAACACAACTATGCGCCGAAGTTCAGGGCAGAGTCACCATGACGACAGACACATCCACGAATACAGCCTACTT
GGAAGTGGAGGCTCAGATCTAACGACACGGCCGTTTTATTACTGTGCGAGAGATTACTTTTCATTCGGGGAGTCAATAT
TTTTTTGACTACTGGGGCCAGGGAAG**ACTTGTACAGTCTCGTCAG**GTGGAGACGAAACC

TET-L-6-HVR

GGAA**CGTCTCC**ACCC**GACATGAGGGTCCCCGCTCAGCTCCTGGGGCTCCTGCTACTCTGGCTCCGAG**GTAAAGGATGGA
GAACACTAGGAATTTACTCAGCCAGTGTGCTCAGTACTGACTGGAACCTCAGGGAAAGTTCTCTGATAACATG
ATTAATAGTAAGAATATTTGTTTTTATGTTTCCAATCTC**AGGTGCCAGATGTGACATCCGGTTGACCCAGTCTCC**
ATCCTCCCTATCTGCATCTGTGGGAGACAGAGTCACCATCACTTGCCGGTCAAGTCAAGCATTAGCACCTATTTAAAT
TGGTATCAGCAGAAACCAGGGGAAGCCCTAAGATTCTAATCTATGCTGCATCCAGTCTGCACACTGGGGTCCCATCAA
GGTTCAGTGGCAGTGGATCTGGGACAGATTTCACTCTCACCATAACCAGTCTGCAACCTGAAGATTTTGAATTTACCA
CTGTCAACAGAGTTACAGTACCCCGTACACTTTTGGCCAGGGGAC**AAAGTCTGAAATCAAAC**GTGGAGACGAAACC

Ovalbumin (OVA) recognizing HVR fragments

Fragments of DNA as inserted in the into pSC-B-amp/kan plasmid (Agilent Technologies) and used for ligation mediated assembly of repair template plasmids for L-HVR and H-HVR replacement.

The sequences are marked as follows:

Introns: GTTATAT

Exons in bold: **CCTTAAA**

F2A: GTGACAG

Published sequence that used to re-create the HVR underlined **GGCTGT**

Splice donor and acceptor sites: **GT AG**

Changes to disrupt low GC window for better gBlock Synthesis **C**

BsmBI restriction sites: GAGACG and CGTCTC

OVA-H-HVR

GGAACGTCTCCACCC**GGATGGAGCTGTATCATCCTCTTTTTGGTAGCAACAGCTACAG****GT**AAGGGGCTCACAGTAGCA
 GGCTTGAGATCTGGCAATACACTTGGGTGACAATGACATCCACTCTCTCTTTCTCTCCAT**AG**GTGTCCACTCCAGGT
CCAACTGCAGCAGCCTGGGGCTGTGTTGGTGAGGCCTGGGGCTTCAGTGAAGCTGTCCTGTAGAGCCTTCTGGCTACATC
TTCACCAGTTACTGGATGAATTGGGTGAAACAGAGGCCTGGACAAGGCCTTGAATGGATTGGTATGATTGATTGTTTCAG
ACAGAAAACTCACTACAATCAAATGTTCAAAGACAAGGCCACATTGACTGTTGACAAGTCTCCAATATAGCCTACAT
TCAGCTCATCAGTCTGACATCTGAGGACTCTGCGGTCTATTACTGTTCAAGGGGAGTAAATCTGGGGCCAAGGGACT
CTGGTCACTGTCTCTTCAG**GT**GGAGACGAAACC

OVA-L-HVR_01

GGAACGTCTCCACCC**ATGAGTCCTGCCAGTTCCTGTTTCTGTTAGTGCTCTGGATTCCGGG****GT**AAGGAGTTCTGGAAT
 GGGAGGGATGAGAATGGGGATGGAGGGTGATCTCTGGATGCCATATGTGTGCTGTTTATTTGTGGTGGGGCAGGTCATAT
 CTCTAGGATGTGAGGTTTTGTTACATCCTAATGAGATATTCCAGATGGAACAGTAGCTGTACTAAGATCAATATTCTG
 ACATAGATTGGATGGAGTGGTATAGACTCTGATGTTTAGAACCTTCAACATTTGTTTTATGACAA**C**ATATTTGATATAT
CATAT**C**TTTTAAATCTGAAAAACTGCTAGGATCTTACTTCAAAGGAATAGCATTTTCAAGTAAGATTTCAAGTAGATTTT
 CAAGTAGATTTCAAAAGGTTGCTCAGGACCTTGCACATGATTTTCCACTATTGTATTGTAATTT**AG**AAACCAACG
GTGATGTTGTGATGACCCAGACTCCACTCACTTTGTGCGTTACCATTGGACAACCAGCCTCCATCTCTTGCAAGTCAAG
TCAGAGCCTCTTAGATAGTGATGGAAAGACATATTTGAATTGGTTGTTACAGAGGCCAGGCCAGTCTCCAAAGCGCCTA
ATCTATCTGGTGTCTAAACTGGACTCTGGAGTCCCTGACAGGTTTCAGTGGCAGTGGGTCTGGAACGGATTTCACTGA
AAATCAGCAGAGTGGAGGCTGAGGATTTGGGAGTTTATTATTGCTGGCAAGCTACACATTTTCCTCAGACGTTCCGGTGG
AGGTACCAAGTTGAAATCAAAC**GT**GGAGACGAAACC

TACTATGAGCTGGGTCCGCCAGGCTCCAGGTAAGGGGCTGGAGTGGGTTTCAAATATTAGTAGTAGTAGTAGTGCCATA
TACTATGCAGGCTCTGTGAAGGGCCGATTCATCATCTCCAGAGACAATGCCAAAACTCATTATATCTGCAAATGAACA
ACCTGAGAGCCGAGGACACGGCTGTCTATTTCTGTGCG

CD79A modification repair template plasmids

Fragments of DNA as inserted in the into pSC-B-amp/kan plasmid (Agilent Technologies).

The sequences are marked as follows:

Introns: GTTATA
 Exons in bold: **CCTTAA**
 Hinge: GGAGGA
 GFP: ATGGTG
 3xFLAG: GACTAT
 bGH polyA signal site: CTTCTA
 Y to F mutations: TAT to TTC

Silent changes to prevent re-targeting of repair template plasmid and modified genomic locus: **T**

wtCD79A-hinge-GFP

GAAGGAAGGAAGGAAGGAAGGAAGGAAGGAAGGAAGGAAGGAAGGAGAACACTGGTTGTAGACTCAGAGAGAAGTCTGTTA
 CATAACCAGTATGTGGCCTTGGGGACATCTCTTACCCTTTCTGGAAAAGTACTTCCTGGCATCCAGGAGGGTCTGAAAG
 ATATTCACCTCCCCCTGCTCACTGAGGCACCCACCCACCCCTACAG**AAACGATGGCAGAACGAGAAGCTCGGGT**
TGGATGCCGGGGATGAATATGAAGATGAAAATCTTTACGAAGGCCTGAACCTGGACGACTGCTCTATGTACGAAGACAT
CTCCGGGGCCTCCAGGGCACCTACCAGGATGTGGGCAGCCTCAACATAGGAGATGTCCAGCTGGAGAAGCCGGAGGA
GGCAGCGGTGGTGGAAAGTGGAGTGAGCAAGGGCGAGGAGCTGTTACCGGGGTGGTGCCCATCCTGGTTCGAGCTGGACG
 GCGACGTAAACGGCCACAAGTTCAGCGTGTCCGGCGAGGGCGAGGGCGATGCCACCTACGGCAAGCTGACCCTGAAGTT
 CATCTGCACCACCGCAAGCTGCCCGTGCCTTGCCACCCCTCGTGACCACCTTCACCTACGGCGTGCAGTGTCTCGCC
 CGCTACCCCGACCACATGAAGCAGCAGACTTCTTCAAGTCCGCCATGCCCGAAGGCTACGTCCAGGAGCGCACCATCT
 TCTTCAAGGACGACGGCAACTACAAGACCCGCGCCGAGGTGAAGTTCGAGGGCGACACCCTGGTGAACCGCATCGAGCT
 GAAGGGCATCGACTTCAAGGAGGACGGCAACATCCTGGGGACAAGCTGGAGTACAACAGCCACAAGGTCTAT
 ATCACCGCCGACAAGCAGAAGAACGGCATCAAGGTGAACCTCAAGACCCGCCACAACATCGAGGACGGCAGCGTGCAGC
 TCGCCGACCACTACCAGCAGAACACCCCATCGGGCAGCGCCCGTGTCTGCTGCCGACAACCACTACCTGAGCACCCA
 GTCCGCCCTGAGCAAAGACCCCAACGAGAAGCGCGATCACATGGTCTGCTGGAGTTCGTGACCGCCGCCGGGATCACT
 CTCGGCATGGACGAGCTGTACAAG**TAA**GATCAGCCTCGACTGTGCCTTCTAGTTGCCAGCCATCTGTTGTTTGCCCTC
 CCCCCTGCCTTCCCTGACCCTGGAAGGTGCCACTCCCACTGTCCCTTCCCTAATAAAATGAGGAAATTGCATCGCATTGT
 CTGAGTAGGTGTCTATTCTATTCTGGGGGGTGGGGTGGGGCAGGACAGCAAGGGGGAGGATTGGGAAGACAATAGCAGGC
ATGCTGGGGA**GAA****GACATCTCCCGGGCCTCCAGGGCACCTACCAGGATGTGGGCAGCCTCAACATAGGAGATGTCCAG**
CTGGAGAAGCCG**TGA****CACCCCTACTCCTGCCAGGCTGCCCCCGCCTGCTGTGCACCCAGCTCCAGTGTCTCAGCTCACT**
TCCCTGGGACATTTCTCCTTTACGCCCTTCTGGGGGCTTCCCTTAGTCATATTCCCCCAGTGGGGGGTGGGAGGGTAACCT
CACTCTTCTCCAGGCCAGGCCTCCTTGACTCCCCTGGGGGTGTCCCACTCTTCTTCCCTCTAAACTGCCCCACCTCCT
AACCTAATCCCCCGCCCCGCTGCCTTTCCAGGCTCCCTCACCCAGCGGGTAATGAGCC

wtCD79A-hinge-flag

GAAGGAAGGAAGGAAGGAAGGAAGGAAGGAAGGAAGGAAGGAAGGAGAACACTGGTTGTAGACTCAGAGAGAAGTCTGTTA
 CATAACCAGTATGTGGCCTTGGGGACATCTCTTACCCTTTCTGGAAAAGTACTTCCTGGCATCCAGGAGGGTCTGAAAG
 ATATTCACCTCCCCCTGCTCACTGAGGCACCCACCCACCCCTACAG**AAACGATGGCAGAACGAGAAGCTCGGGT**
TGGATGCCGGGGATGAATATGAAGATGAAAATCTTTACGAAGGCCTGAACCTGGACGACTGCTCTATGTACGAAGACAT
CTCCGGGGCCTCCAGGGCACCTACCAGGATGTGGGCAGCCTCAACATAGGAGATGTCCAGCTGGAGAAGCCGGAGGA
GGCAGCGGTGGTGGAAAGTGGAGTGACTATAAAGACGACGACGACAAAGACTATAAGGACGACGATGACAAGGATTACAAGG
 ACGACGACGATAAG**TAA**GATCAGCCTCGACTGTGCCTTCTAGTTGCCAGCCATCTGTTGTTTGCCCTCCCCCTGCCT
 TCCTTGACCCTGGAAGGTGCCACTCCCACTGTCCCTTCCCTAATAAAATGAGGAAATTGCATCGCATTGTCTGAGTAGGT
 GTCATTCTATTCTGGGGGGTGGGGTGGGGCAGGACAGCAAGGGGGAGGATTGGGAAGACAATAGCAGGCATGCTGGGGA
GAA**GACATCTCCCGGGCCTCCAGGGCACCTACCAGGATGTGGGCAGCCTCAACATAGGAGATGTCCAGCTGGAGAAGC**
CGTGA**CACCCCTACTCCTGCCAGGCTGCCCCCGCCTGCTGTGCACCCAGCTCCAGTGTCTCAGCTCACTTCCCTGGGAC**
ATTCCTTTTACGCCCTTCTGGGGGCTTCCCTTAGTCATATTCCCCCAGTGGGGGGTGGGAGGGTAACCTCACTCTTCTC
CAGGCCAGGCCTCCTTGACTCCCCTGGGGGTGTCCCACTCTTCTTCCCTCTAAACTGCCCCACCTCCTAACCTAATCC
CCCCGCCCGCTGCCTTTCCAGGCTCCCTCACCCAGCGGGTAATGAGCC

CCCCGTGCCTTCCTTGACCCTGGAAGGTGCCACTCCCCTGTCTTTCCCTAATAAAAATGAGGAAATTGCATCGCATTGT
 CTGAGTAGGTGTCATTCTATTCTGGGGGGTGGGGTGGGGCAGGACAGCAAGGGGGAGGATTGGGAAGACAATAGCAGGC
 ATGCTGGGGA **GAA**GACATCTCCCGGGGCTCCAGGGCACCTACCAGGATGTGGGCAGCCTCAACATAGGAGATGTCCAG
 CTGGAGAAGCCG **TGA**CACCCCTACTCCTGCCAGGCTGCCCCGCCTGCTGTGCACCCAGCTCCAGTGTCTCAGCTCACT
 TCCCTGGGACATTCCTTTTTCAGCCCTTCTGGGGGCTTCTTAGTCATATTCCCCCAGTGGGGGGTGGGAGGGTAACCT
 CACTCTTCTCCAGGCCAGGCTCCTTGGACTCCCCTGGGGGTGTCCCCTCTTCTTCCCTCTAAACTGCCCCACCTCCT
 AACCTAATCCCCCGCCCCGCTGCCTTTCCAGGCTCCCCTCACCCAGCGGGTAATGAGCC

Y199F CD79A-hinge-GFP

GAAGGAAGGAAGGAAGGAAGGAAGGAAGGAAGGAAGGAAGGAGAACACTGGTTGTAGACTCAGAGAGAACTGTTA
 CATAACCAGTATGTGGCCTTGGGGACATCTCTTACCCTTTCTGGAAAAGTACTTCCTGGCATCCAGGAGGGTCTGAAAG
 ATATTCACCTCCCCCTGCTCACTGAGGCACCCACCCACCCCTACAG **AAACGATGGCAGAACGAGAAGCTCGGGT**
TGGATGCCGGGGATGAATATGAAGATGAAAA **CTTTA** **C**GAAGGCCTGAACCTGGACGACTGCTC **TATGTT** **GA** **GACAT**
CTCCCGGGGCTCCAGGGCACCTACCAGGATGTGGGCAGCCTCAACATAGGAGATGTCCAGCTGGAGAAGCCG **GGAGGA**
GGCAGCGGTGGTGGAAGTGGA **GTGAGCAAGGGCGAGGAGCTGTT** **CACCGGGTGGTGCCCATCCTGGT** **CGAGCTGGACG**
GCGACGTAAACGGCCACAAGTTCAGCGTGTCCGGCGAGGGCGAGGGCGATGCCACCTACGGCAAGCTGACCCCTGAAGTT
CATCTGCACCACCGCAAGCTGCCCGTGCCCTGGCCACCCCTCGTGACCACCTTACCTACGGCGTGCAGTGTTCGCC
CGTACCCCGACCACATGAAGCAGCAGACTTCTTCAAGTCCGCCATGCCCGAAGGCTACGTCCAGGAGCGCACCATCT
TCTTCAAGGACGACGGCAACTACAAGACCCGCGCCGAGGTGAAGTTCGAGGGCGACACCCTGGTGAACCGCATCGAGCT
GAAGGGCATCGACTTCAAGGAGGACGGCAACATCCTGGGGCACAAGCTGGAGTACAACAGCCACAAGGTCTAT
ATCACCGCCGACAAGCAGAAGAACGGCATCAAGGTGAACCTCAAGACCCGCCACAACATCGAGGACGGCAGCGTGCAGC
TCGCCGACCACTACCAGCAGAACACCCCATCGGCGACGGCCCGTGTCTGCTGCCGACAACCACTACCTGAGCACCA
GTCCGCCCTGAGCAAAGACCCCAACGAGAAGCGCGATCACATGGTCTGCTGGAGTTCGTGACCGCCGCCGGGATCACT
CTCGGCATGGACGAGCTGTACAAG **TAA**GATCAGCCTCGACTGTGC **CTTCTAGTTGCCAGCCATCTGTTGTTT** **GCCCCTC**
CCCCGTGCCTTCCTTGACCCTGGAAGGTGCCACTCCCCTGTCTTTCCCTAATAAAAATGAGGAAATTGCATCGCATTGT
CTGAGTAGGTGTCATTCTATTCTGGGGGGTGGGGTGGGGCAGGACAGCAAGGGGGAGGATTGGGAAGACAATAGCAGGC
ATGCTGGGGA **GAA**GACATCTCCCGGGGCTCCAGGGCACCTACCAGGATGTGGGCAGCCTCAACATAGGAGATGTCCAG
CTGGAGAAGCCG **TGA**CACCCCTACTCCTGCCAGGCTGCCCCGCCTGCTGTGCACCCAGCTCCAGTGTCTCAGCTCACT
TCCCTGGGACATTCCTTTTTCAGCCCTTCTGGGGGCTTCTTAGTCATATTCCCCCAGTGGGGGGTGGGAGGGTAACCT
CACTCTTCTCCAGGCCAGGCTCCTTGGACTCCCCTGGGGGTGTCCCCTCTTCTTCCCTCTAAACTGCCCCACCTCCT
AACCTAATCCCCCGCCCCGCTGCCTTTCCAGGCTCCCCTCACCCAGCGGGTAATGAGCC

HT BCR re-expression repair template plasmid

Fragment of DNA as inserted in the into pSC-B-amp/kan plasmid (Agilent Technologies).

The sequences are marked as follows:

Introns:

GTTATA

Exons in bold:

CCTTAA

Splice donor and acceptor sites: **GT AG**

Used Cas9/sgRNA sites:

Codon with predicted deletion repaired by A insertion **TAC**

Silent changes to prevent re-targeting of repair template plasmid and modified genomic locus: **T**

HT_HA_1

ATATGTGTGGCTCTTTCTAACCAATGTCTCTGTGTTTGC**AG**GTGTCCAGTCTGGGGTGCAGTTGGTGGAGACTGGAGGA
GGCTTGTTCAGCCGGGGGAGTCCCTGAGACTCTCCTGTGCAACCTCTGACTTCACCGTCAGTAACAACACTACATGGCCT
GGGTCCGCCAGGCTCCAGGGAAGGGACTGAATTGGGTCTCACTTATCTCTGCCGCTGGTGTACATTCTACGCAGACTC
CGTGAAGGGCCGATTCTCCATTTCCCGAGACAACCTCCAAGAACAACACTATATCTTCAAATGACA**AG**TCT**CAGAGCCGAG**
GACACGGCCATGTATTACTGTGCGAGAGCATCTTTTGCAACAACTACT**TACTTTGACTCCTGGAG**CAA**GGAA**ATC****
TC**GTCACCGTCTCCTCAG**GT**GAGTCCTCAGAACCTCTCTCGGGGTCTGCTTCTGAAGGATATTGCTACATTTTCGGGGA**
AAATTAAGGATGCTGGGTACCTGGCCAGACAGACGCGGACCACCCTGGGGTCTCAGGAGGAGGCCCTGAGGCAACAG
CGGCCGCACAGACGAGGTACAAGGACTCCAGATGTCCCTTCTCCAGAGCCCAAACCACGGGTCTCTCTGTGCCTAGG
ACCACCCTAGGCCTCTGGGGTCCAATGTCCCACAAGTCCCGGGCCCTCCCCGGCCTCAGTCTTAGAGGGTCCCAGGGAC
GTGGCGG

AKT activity FRET reporter and control plasmids

DNA coding for the AKT activity reporter and control constructs as inserted in the sleeping beauty donor plasmid pSBbi-Pur between SfiI restriction sites.

The sequences are marked as follows:

SfiI restriction sites: **ggcctctgagGCC** and **ggcctgtcaggcc**

Lyn tag: **GGGTGC**

Cerulean3: **gtgagc**

Sequence surrounding Thr-24 of FOXO1 CCTCGT

cpVenus[E172] **ggcggcg**

Valine instead of Threonine in catalytically dead Lyn-AKT-AR2: **GTC**

TRAF2 spacer: **TGCGAG**

Lyn-AKT-AR2

aagct**ggcctctgagGCC**ACC**ATGGGTGCATTAAGTCTAAGCGGAAGGACAAA**AAGGATCCC**atg**gtgagcaagggcg
aggagctgttcaccggggtggtgcccatcctggtcgagctggacggcgacgtaaacggccacaggttcagcgtgtccgg
cgagggcgagggcgatgccacctacggcaagctgacctgaagttcatctgcaccaccggcaagctgcccgtgccctgg
cccaccctcgtgaccaccctgAGCtggggcgtgcagtgttcgcccgtaccccgaccacatgaagcagcagcacttct
tcaagtccgccatgccgaaggctacgtccaggagcgtaccatcttcttcaaggacgacggcaactacaagaccgcg
cgaggtgaagttcgagggcgacaccctggtgaaccgcatcgagctgaagggcatcgacttcaaggaggacggcaacatc
ctggggcacaagctggagtacaacgccatCACGGCaagctctatatcaccgccgacaagcagaagaacggcatcaagg
ccAACTtcGGCCTCAACTGCaacatcgaggacggcagcgtgcagctcgccgaccactaccagcagaacacccccatcgg
cgacggccccgtgctgctgcccgacaaccactacctgagcaccagtcgcccctgagcaaagaccccacgagaagcgc
gatcacatggtcctgctggagttcgtgaccgcccgggatcactctcgccatggacgagctgtacaagcgcatgcata
agttttctcaagaacagatcggcgaaaacattgtgtgcagggtcatttgtaccacgggtcaaattcccacccgagattt
gtcagctgatatttcacaagtgttaaggaaaaacgatccataaagaaagtttggacatttggtagaaaccagcctgt
gactatcatttaggaacatttcaagactgtcaaataagcatttccaaataactactaggagaagacggtaaacctttat
tgaatgacatttccactaatgggacctggttaaagggcaaaaagtcgagaagaacagcaatcagttactgtctcaagg
tgatgaaataaccgttgggtgtaggctggaatcagatattttatctctgggtcattttcataaacgacaaaatttaagcag
tgccctcgagcagaacaaagttgatcgtctgcaggtgaagccagggcagcggcgagggcgagcaccaggcctggctgacC
CTCGTCCGCGCTCGTGCACCTGGCCGGACCCAGGCCGGAGTTTGGAGGTACCGGCGGCAGCgagctcatg**ggcggcg**
gcagctcgccgaccactaccagcagaacacccccatcggcgacggccccgtgctgctgcccgacaaccactacctgagc
taccagtccaagctgagcaaagaccccacgagaagcgcgatcacatggtcctgctggagttcgtgaccgcccggga
tactctcgccatggacgagctgtacaag**ggaggtaccgggtgatctatg**gtgagcaagggcgaggagctgttcaccgg
ggtggtgcccatcctggctcgagctggacggcgacgtaaacggccacaagttcagcgtgtccggcgagggcgagggcgat
gccacctacggcaagctgacctgaagctgatctgcaccaccggcaagctgcccgtgcccaccctcgtgacca
cctgggctacggccttcagtgttcgcccgtaccccgaccacatgaagcagcagcacttcttcaagtccgccatgcc
cgaaggctacgtccaggagcgcaccatcttcttcaaggacgacggcaactacaagaccgcccggaggtgaagttcgag
ggcgacaccctggtgaaccgcatcgagctgaagggcatcgacttcaaggaggacggcaacatcctggggcacaagctgg
agtacaactacaacagccacaacgtctatatcaccgccgacaagcagaagaacggcatcaaggccaacttcaagatccg
ccacaacatcgag**taaggcctgtcaggcca**aag

Dead-Lyn-AKT-AR2

aagct**ggcctctgagGCC**ACC**ATGGGTGCATTAAGTCTAAGCGGAAGGACAAA**AAGGATCCC**atg**gtgagcaagggcg
aggagctgttcaccggggtggtgcccatcctggtcgagctggacggcgacgtaaacggccacaggttcagcgtgtccgg
cgagggcgagggcgatgccacctacggcaagctgacctgaagttcatctgcaccaccggcaagctgcccgtgccctgg
cccaccctcgtgaccaccctgAGCtggggcgtgcagtgttcgcccgtaccccgaccacatgaagcagcagcacttct
tcaagtccgccatgccgaaggctacgtccaggagcgtaccatcttcttcaaggacgacggcaactacaagaccgcg
cgaggtgaagttcgagggcgacaccctggtgaaccgcatcgagctgaagggcatcgacttcaaggaggacggcaacatc
ctggggcacaagctggagtacaacgccatCACGGCaagctctatatcaccgccgacaagcagaagaacggcatcaagg
ccAACTtcGGCCTCAACTGCaacatcgaggacggcagcgtgcagctcgccgaccactaccagcagaacacccccatcgg
cgacggccccgtgctgctgcccgacaaccactacctgagcaccagtcgcccctgagcaaagaccccacgagaagcgc
gatcacatggtcctgctggagttcgtgaccgcccgggatcactctcgccatggacgagctgtacaagcgcatgcata
agttttctcaagaacagatcggcgaaaacattgtgtgcagggtcatttgtaccacgggtcaaattcccacccgagattt
gtcagctgatatttcacaagtgttaaggaaaaacgatccataaagaaagtttggacatttggtagaaaccagcctgt

gactatcatttaggaaacatttcaagactgtcaataagcatttccaaatactactaggagaagacggtaaccttttat
 tgaatgacatttccactaatgggacctggttaaaggggcaaaaagtcgagaagaacagcaatcagttactgtctcaagg
 tgatgaaataaccgttgggtgtaggcgtggaatcagatattttatctctgggtcattttcataaacgacaaatttaagcag
 tgacctgagcagaacaaagttgatcgctctgcaggttaagccaggcagcggcgaggcgagcaccaggcctggctgacC
 CTCGTCCGCGCTCGTGC**GTG**TGGCCGGACCCAGGCCGGAGTTGGAGGTACCGGCCGAGCgagctcatg**ggcggcgt**
gcagctcgccgaccactaccagcagaacacccccatcgccgacggccccgtgctgctgcccgacaaccactacctgagc
taccagtccaagctgagcaaaagacccccaacgagaagcgcgatcacatggctcctgctggagttcgtgaccgcccggga
 tcactctcgcatggacgagctgtacaag**ggaggtaccgggtgatct****atg**gtgagcaagggcgaggagctgttcaccgg
 ggtggtgcccacctcctggctgagctggacggcgacgtaaacggccacaagttcagcgtgtccggcgagggcgagggcgat
 gccacctacggcaagctgacctgaagctgatctgcaccaccggcaagctgcccgtgcccctggcccacctcgtgacca
 cctggggctacggccttcagtgcttcgcccgtaccaccgaccacatgaagcagcagcacttcttcaagtcggccatgcc
 cgaaggctacgtccaggagcgcaccatcttcttcaaggacgacggcaactacaagaccgcgcccagggtgaagttcgag
 ggcgacaccctggtgaaccgcatcgagctgaagggcatcgacttcaaggaggacggcaacatcctggggcacaagctgg
 agtacaactacaacagccacaacgtctatatcaccgcccgaacgagaagaacggcatcaaggccaacttcaagatccg
 ccacaacatcgag**taaggcctgtcaggccaag**

Ceruean3

aagct**ggcctctgagGCCACC****ATG**GTGCGGGTTCTCATCATCATCATCATCATGGTATGGCTAGCATGACTGGTGGAC
 AGCAAATGGGTCTGGGATCTGTACGACGATGACGATAAGGATCCC**atg**gtgagcaagggcgaggagctgttcaccggggt
 ggtgcccacctcctggctgagctggacggcgacgtaaacggccacaggttcagcgtgtccggcgagggcgagggcgatgcc
 acctacggcaagctgacctgaagttcatctgcaccaccggcaagctgcccgtgcccctggcccacctcgtgaccacce
 tgAGCTggggcgtgagctgcttcgcccgtaccaccgaccacatgaagcagcagcacttcttcaagtcggccatgccga
 aggctacgtccaggagcgtaccatcttcttcaaggacgacggcaactacaagaccgcgcccagggtgaagttcgagggc
 gacaccctggtgaaccgcatcgagctgaagggcatcgacttcaaggaggacggcaacatcctggggcacaagctggagt
 acaacgccatcCAGGCCaacgtctatatcaccgcccgaacgagaagaacggcatcaaggccaACTtccGGCCTCAACTG
 Caacatcgaggacggcagcgtgcagctcgccgaccactaccagcagaacacccccatcgccgacggccccgtgctgctg
 cccgacaaccactacctgagcaccagtcgcccctgagcaaaagacccaacgagaagcgcgatcacatggctcctgctgg
 agttcgtgaccgcccgggatcactctcggcatggacgagctgtacaag**cg**catgcataagttttctcaagaacagat
 cggcgaaaacattgtgtgcag**taaggcctgtcaggccaag**

cpVenus [E172]

aagct**ggcctctgagGCCACC****ATG**GTGCGGGTTCTCATCATCATCATCATCATGACgaaaaacattgtgtgcagggtca
 tttgtaccacgggtcaaatccactccgagatttgtcagctgatatttcacaagtgcttaaggaaaaacgatccataaa
 gaaagtttggacatttggtagaaaccagcctgtgactatcatttaggaaacatttcaagactgtcaataagcatttc
 caaatactactaggagaagacggtaaccttttattgaatgacatttccactaatgggacctggttaaagggcaaaaag
 tcgagaagaacagcaatcagttactgtctcaaggtgatgaaataaccgttgggtgtaggcgtggaatcagatattttatc
 tctgggtcattttcataaacgacaaatttaagcagtgctcgcagcagaacaaagttgatcgctctgcaggttaagccaggc
 agcggcgagggcgagcaccaggcctggctgac**CCTCGTCCGCGCTCGTGACCTGGCCGGACCCAGGCCGGAGTTG**
GAGGTACCGGCCGAGCgagctcatg**ggcggcgtg**cagctcgccgaccactaccagcagaacacccccatcgccgacgg
ccccgtgctgctgcccgacaaccactacctgagctaccagttcaagctgagcaaaagacccaacgagaagcgcgatcac
atggtcctgctggagttcgtgaccgcccgggatcactctcggcatggacgagctgtacaag**ggaggtaccgggtggat**
ct**atg**gtgagcaagggcgaggagctgttcaccggggtggtgcccacctcctggctgagctggacggcgacgtaaacggcca
 caagttcagcgtgtccggcgagggcgagggcgatgccacctacggcaagctgacctgaagctgatctgcaccaccggc
 aagctgcccgtgcccctggcccacctcgtgaccacctgggctacggccttcagtgcttcgcccgtaccaccgaccaca
 tgaagcagcagcacttcttcaagtcggccatgccgaaggctacgtccaggagcgcaccatcttcttcaaggacgacgg
 caactacaagaccgcgcccagggtgaagttcgagggcgacaccctggtgaaccgcatcgagctgaagggcatcgacttc
 aaggaggacggcaacatcctggggcacaagctggagtacaactacaacagccacaacgtctatatcaccgcccgaacg
 agaagaacggcatcaaggccaacttcaagatccgccacaacatcgag**taaggcctgtcaggccaag**

C3-cpV

aagct**ggcctctgagGCCACC****ATG**GTGCGGGTTCTCATCATCATCATCATCATGGTATGGCTAGCATGACTGGTGGAC
 AGCAAATGGGTCTGGGATCTGTACGACGATGACGATAAGGATCCC**atg**gtgagcaagggcgaggagctgttcaccggggt
 ggtgcccacctcctggctgagctggacggcgacgtaaacggccacaggttcagcgtgtccggcgagggcgagggcgatgcc
 acctacggcaagctgacctgaagttcatctgcaccaccggcaagctgcccgtgcccctggcccacctcgtgaccacce
 tgAGCTggggcgtgagctgcttcgcccgtaccaccgaccacatgaagcagcagcacttcttcaagtcggccatgccga
 aggctacgtccaggagcgtaccatcttcttcaaggacgacggcaactacaagaccgcgcccagggtgaagttcgagggc

gacaccctggtgaaccgcatcgagctgaagggcatcgacttcaaggaggacggcaacatcctggggcacaagctggagt
 acaacgccatcCACGGCaacgtctatatcaccgccgacaagcagaagaacggcatcaaggccAACTtcGGCCTCAACTG
 Caacatcgaggacggcagcgtgcagctcgccgaccactaccagcagaacacccccatcgggcgacggccccgtgctgctg
 cccgacaaccactacctgagcaccagtcgccctgagcaagaccccaacgagaagcgcgatcacatggtcctgctggtg
 agttcgtgaccgccgcccgggatcactctcgccatggacgagctgtacaagTCCGGACTCAGATCTatgggcgcgctgca
 gctcgccgaccactaccagcagaacacccccatcgggcgacggccccgtgctgctgcccgacaaccactacctgagctac
 cagtccaagctgagcaagaccccaacgagaagcgcgatcacatggtcctgctggagttcgtgaccgccgcccgggatca
 ctctcgccatggacgagctgtacaagggaggtaccgggtggatctatgggtgagcaagggcgaggagctgttcaccggggt
 ggtgcccatcctggtcgagctggacggcgacgtaaacggccacaagttcagcgtgtccggcgagggcgagggcgatgcc
 acctacggcaagctgaccctgaagctgatctgcaccaccggcaagctgcccgtgccctggcccaccctcgtgaccacce
 tgggctacggccttcagtgtctcgcccgtacccccgaccacatgaagcagcagcacttcttcaagtccgccatgcccga
 aggtacgtccaggagcgcaccatcttcttcaaggacgacggcaactacaagaccgcgcccaggtgaagttcgagggc
 gacaccctggtgaaccgcatcgagctgaagggcatcgacttcaaggaggacggcaacatcctggggcacaagctggagt
 acaactacaacagccacaacgtctatatcaccgccgacaagcagaagaacggcatcaaggccaacttcaagatccgcca
 caacatcgagtaaggcctgtcaggccaag

C3-spacer-cpV

aagctggcctctgagGCCACCATG GTGCGGGGTTCTCATCATCATCATCATCATGGTATGGCTAGCATGACTGGTGGAC
 AGCAAATGGGTCGGGATCTGTACGACGATGACGATAAGGATCCC atgggtgagcaagggcgaggagctgttcaccggggt
 ggtgcccatcctggtcgagctggacggcgacgtaaacggccacaggttcagcgtgtccggcgagggcgagggcgatgcc
 acctacggcaagctgaccctgaagttcatctgcaccaccggcaagctgcccgtgccctggcccaccctcgtgaccacce
 tgAGCTggggcgctgcagtgcttcgcccgtacccccgaccacatgaagcagcagcacttcttcaagtccgccatgcccga
 aggtacgtccaggagcgtaccatcttcttcaaggacgacggcaactacaagaccgcgcccaggtgaagttcgagggc
 gacaccctggtgaaccgcatcgagctgaagggcatcgacttcaaggaggacggcaacatcctggggcacaagctggagt
 acaacgccatcCACGGCaacgtctatatcaccgccgacaagcagaagaacggcatcaaggccAACTtcGGCCTCAACTG
 Caacatcgaggacggcagcgtgcagctcgccgaccactaccagcagaacacccccatcgggcgacggccccgtgctgctg
 cccgacaaccactacctgagcaccagtcgccctgagcaagaccccaacgagaagcgcgatcacatggtcctgctggtg
 agttcgtgaccgccgcccgggatcactctcgccatggacgagctgtacaagcgcatgcataagttttctcaagaacagat
 cggcgaaaacattgtgtgcaggggtcatttgtaccacgggtcaaattcccacccagatttgtcagctgatatttcaaa
 gtgcttaaggaaaaacgatccataaagaaagtttgacatttggtagaaaaccagcctgtgactatcatttaggaaca
 tttcaagactgtcaataagcatttccaaataactactaggagaagacggtaaccttttattgaatgacatttccactaa
 tgggacctggttaaatgggcaaaaagtcgagaagaacagcaatcagttactgtctcaaggatgaataaccgttgggt
 gtaggcgtggaatcagatattttatctctggtcattttcataaacgacaaaatttaagcagtgccctcgagcagaacaaag
 ttgatcgtctctgcaggtgaagccagcagcggcgagggcagcaccgaagggcctggtcgacCCTCGTTGCGAGAGCCTGGA
 GAAGAAGACGGCCACTTTTGAGAACATTGTCTGCGTCTGAACCGGGAGGTGGAGAGGGTGGCCATGACTGCCGAGGCC
 TGCAGCCGGCAGCACCGGCTGGACCAAGACAAGATTGAAGCCCTGAGTAGCAAGGTGCAGCAGCTGGAGAGGAGCATTG
 GCCTCAAGGACCTGGCGATGGCTGACTTGGAGCAGAAGGTCTTGGAGATGGAGGCATCCACCTACGATGGGGTCTTCAT
 CTGGAAGATCTCAGACTTCGCCAGGAAGCGCCAGGAAGCTGTGGCTGGCCGCATACCCGCCATCTTCTCCCCAGCCTTC
 TACACCAGCAGGTACGGCTACAAGATGTGTCTGCGTATCTACCTGAACGGCGACGGCACCGGGCGAGGAACACACCTGT
 CCTCTTCTTTGTGGTGATGAAGGGCCCGAATGACGCCCTGTGCGGTGGCCCTTCAACCAGAAGGTGACCTTAATGCT
 GCTCGACCAGAATAACCGGGAGCACGTGATTGACGCCTTACGGCCCGACGTGACTTCATCCTCTTTTCAGAGGCCAGTC
 AACGACATGAACATCGCAAGCGGCTGCCCCCTCTTCTGCCCGTCTCCAAGATGGAGGCAAAGAATTCCTACGTGCGGG
 ACGATGCCATCTTCATCAAGGCCATTGTGGACCTGACAGGGGCTCCCGAGTTTGGAGGTACCGGGCGGCAGCgagctcat
 gggcgcgctgcagctcgccgaccactaccagcagaacacccccatcgggcgacggccccgtgctgctgcccgacaaccac
 tacctgagctaccagttcaagctgagcaaaagaccccaacgagaagcgcgatcacatggtcctgctggagttcgtgaccg
 ccgcccgggatcactctcgccatggacgagctgtacaagggaggtaccgggtggatctatgggtgagcaagggcgaggagct
 gttcaccggggtggtgcccatcctggtcgagctggacggcgacgtaaacggccacaagttcagcgtgtccggcgagggc
 gagggcgatgccacctacggcaagctgaccctgaagctgatctgcaccaccggcaagctgcccgtgccctggcccacc
 tctgaccaccctgggctacggccttcagtgtctcgcccgtacccccgaccacatgaagcagcagcacttcttcaagtc
 cgccatgcccgaaggctacgtccaggagcgcaccatcttcttcaaggacgacggcaactacaagaccgcgcccaggtg
 aagttcgagggcgacaccctggtgaaccgcatcgagctgaagggcatcgacttcaaggaggacggcaacatcctggggc
 caaagctggagtacaactacaacagccacaacgtctatatcaccgccgacaagcagaagaacggcatcaaggccaactt
 caagatccgccacaacatcgagtaaggcctgtcaggccaag

SUPPLEMENTAL REFERENCES

1. Tiller T, Meffre E, Yurasov S, Tsuiji M, Nussenzweig MC, Wardemann H. Efficient generation of monoclonal antibodies from single human B cells by single cell RT-PCR and expression vector cloning. *J Immunol Methods*. 2008;329(1-2):112-124.
2. Doenecke A, Winnacker EL, Hallek M. Rapid amplification of cDNA ends (RACE) improves the PCR-based isolation of immunoglobulin variable region genes from murine and human lymphoma cells and cell lines. *Leukemia*. 1997;11(10):1787-1792.
3. Brochet X, Lefranc MP, Giudicelli V. IMGT/V-QUEST: the highly customized and integrated system for IG and TR standardized V-J and V-D-J sequence analysis. *Nucleic Acids Res*. 2008;36(Web Server issue):W503-508.
4. Giudicelli V, Brochet X, Lefranc MP. IMGT/V-QUEST: IMGT standardized analysis of the immunoglobulin (IG) and T cell receptor (TR) nucleotide sequences. *Cold Spring Harb Protoc*. 2011;2011(6):695-715.
5. Cong L, Ran FA, Cox D, et al. Multiplex genome engineering using CRISPR/Cas systems. *Science*. 2013;339(6121):819-823.
6. Ran FA, Hsu PD, Wright J, Agarwala V, Scott DA, Zhang F. Genome engineering using the CRISPR-Cas9 system. *Nat Protoc*. 2013;8(11):2281-2308.
7. Hsu PD, Scott DA, Weinstein JA, et al. DNA targeting specificity of RNA-guided Cas9 nucleases. *Nat Biotechnol*. 2013;31(9):827-832.
8. Covassin LD, Siekmann AF, Kacergis MC, et al. A genetic screen for vascular mutants in zebrafish reveals dynamic roles for Vegf/Plcg1 signaling during artery development. *Dev Biol*. 2009;329(2):212-226.
9. Minskaia E, Nicholson J, Ryan MD. Optimisation of the foot-and-mouth disease virus 2A co-expression system for biomedical applications. *BMC Biotechnol*. 2013;13:67.
10. Goedhart J, von Stetten D, Noirclerc-Savoie M, et al. Structure-guided evolution of cyan fluorescent proteins towards a quantum yield of 93%. *Nat Commun*. 2012;3:751.
11. DeKosky BJ, Ippolito GC, Deschner RP, et al. High-throughput sequencing of the paired human immunoglobulin heavy and light chain repertoire. *Nat Biotechnol*. 2013;31(2):166-169.
12. Dougan SK, Ogata S, Hu CC, et al. IgG1+ ovalbumin-specific B-cell transnuclear mice show class switch recombination in rare allelically included B cells. *Proc Natl Acad Sci U S A*. 2012;109(34):13739-13744.
13. Ran FA, Hsu PD, Lin CY, et al. Double nicking by RNA-guided CRISPR Cas9 for enhanced genome editing specificity. *Cell*. 2013;154(6):1380-1389.
14. Kowarz E, Loscher D, Marschalek R. Optimized Sleeping Beauty transposons rapidly generate stable transgenic cell lines. *Biotechnology journal*. 2015;10(4):647-653.
15. Beum PV, Lindorfer MA, Hall BE, et al. Quantitative analysis of protein co-localization on B cells opsonized with rituximab and complement using the ImageStream multispectral imaging flow cytometer. *J Immunol Methods*. 2006;317(1-2):90-99.
16. Davis RE, Brown KD, Siebenlist U, Staudt LM. Constitutive nuclear factor kappaB activity is required for survival of activated B cell-like diffuse large B cell lymphoma cells. *J Exp Med*. 2001;194(12):1861-1874.
17. Avalos AM, Bilate AM, Witte MD, et al. Monovalent engagement of the BCR activates ovalbumin-specific transnuclear B cells. *J Exp Med*. 2014;211(2):365-379.
18. Honczarenko M, Le Y, Glodek AM, et al. CCR5-binding chemokines modulate CXCL12 (SDF-1)-induced responses of progenitor B cells in human bone marrow through heterologous desensitization of the CXCR4 chemokine receptor. *Blood*. 2002;100(7):2321-2329.
19. Zhou X, Clister TL, Lowry PR, Seldin MM, Wong GW, Zhang J. Dynamic Visualization of mTORC1 Activity in Living Cells. *Cell Rep*. 2015.
20. Gao X, Zhang J. Spatiotemporal analysis of differential Akt regulation in plasma membrane microdomains. *Mol Biol Cell*. 2008;19(10):4366-4373.
21. He L, Wu X, Simone J, Hewgill D, Lipsky PE. Determination of tumor necrosis factor receptor-associated factor trimerization in living cells by CFP->YFP->mRFP FRET detected by flow cytometry. *Nucleic Acids Res*. 2005;33(6):e61.
22. Komatsu N, Aoki K, Yamada M, et al. Development of an optimized backbone of FRET biosensors for kinases and GTPases. *Mol Biol Cell*. 2011;22(23):4647-4656.

23. Mates L, Chuah MK, Belay E, et al. Molecular evolution of a novel hyperactive Sleeping Beauty transposase enables robust stable gene transfer in vertebrates. *Nat Genet.* 2009;41(6):753-761.
24. Zal T, Gascoigne NR. Photobleaching-corrected FRET efficiency imaging of live cells. *Biophys J.* 2004;86(6):3923-3939.
25. Chen H, Puhl HL, 3rd, Koushik SV, Vogel SS, Ikeda SR. Measurement of FRET efficiency and ratio of donor to acceptor concentration in living cells. *Biophys J.* 2006;91(5):L39-41.
26. Ma W, Wang M, Wang ZQ, et al. Effect of Long-Term Storage in Trizol on Microarray-Based Gene Expression Profiling. *Cancer Epidemiol Biomarkers Prev.* 2010;19(10):2445-2452.
27. Subramanian A, Tamayo P, Mootha VK, et al. Gene set enrichment analysis: a knowledge-based approach for interpreting genome-wide expression profiles. *Proc Natl Acad Sci U S A.* 2005;102(43):15545-15550.
28. Heberle H, Meirelles GV, da Silva FR, Telles GP, Minghim R. InteractiVenn: a web-based tool for the analysis of sets through Venn diagrams. *BMC Bioinformatics.* 2015;16:169.
29. Spurgeon SE, Coffey G, Fletcher LB, et al. The selective SYK inhibitor P505-15 (PRT062607) inhibits B cell signaling and function in vitro and in vivo and augments the activity of fludarabine in chronic lymphocytic leukemia. *J Pharmacol Exp Ther.* 2013;344(2):378-387.
30. Somoza JR, Koditek D, Villasenor AG, et al. Structural, biochemical, and biophysical characterization of idelalisib binding to phosphoinositide 3-kinase delta. *J Biol Chem.* 2015;290(13):8439-8446.
31. Furlong MT, Mahrenholz AM, Kim KH, Ashendel CL, Harrison ML, Geahlen RL. Identification of the major sites of autophosphorylation of the murine protein-tyrosine kinase Syk. *Biochim Biophys Acta.* 1997;1355(2):177-190.